

MYELOID CELLS INDUCE NEUROFIBROMATOSIS TYPE 1 ANEURYSM  
FORMATION THROUGH INFLAMMATION AND OXIDATIVE STRESS

Brandon David Downing

Submitted to the faculty of the University Graduate School  
in partial fulfillment of the requirements  
for the degree  
Doctor of Philosophy  
in the Department of Biochemistry and Molecular Biology,  
Indiana University

June 2014

Accepted by the Graduate Faculty, of Indiana University, in partial fulfillment of the requirements for the degree of Doctor of Philosophy.

---

David A. Ingram Jr., M.D., Chair

---

Reuben Kapur, Ph.D.

Doctoral Committee

---

Mervin C. Yoder, M.D.

April 30, 2014

---

Simon J. Conway, Ph.D.

## ACKNOWLEDGEMENTS

I would first like to acknowledge my mentor, Dr. David Ingram. Thank you for allowing me to train within your laboratory on a productive and exciting thesis project. Thank you for spending countless hours training me to become a competent researcher, scientific writer and future clinician-scientist. Your mentorship will be the cornerstone of my career and I thank you. I would also like to thank all the members of the Ingram lab, past and present, who patiently shared their time and knowledge to ensure my success in the lab. Each of you were instrumental in my scientific training and overall enjoyment of my time in the lab. Attack on.

I would like to thank the members of my committee, Drs. Simon J. Conway, Cynthia M. Hingtgen, Reuben Kapur, and Mervin C. Yoder. Thank you for your time, support, and training throughout this process. Each of you contributed individually and as a group to my proper training and future success as a scientist.

To the directors and staff of the medical scientist training program, thank you for the opportunity to be part of the MSTP family. Drs. Chan, Clapp, Harrington, and Mirmira, thank you for promoting a great environment allowing for my success as a student and future clinician-scientist. To Jan Receveur, thank you for your daily programmatic guidance allowing for successful navigation throughout my time as a graduate student. Without your guidance I would not be writing this dissertation.

To the faculty and staff of the biochemistry and molecular biology department, thank for your assistance and patience throughout the graduate school process. Your knowledge and willingness to assist allowed for a pleasant and successful graduate experience. To the faculty and staff of the University Graduate School, thank you for your patience, guidance and assistance in navigating the logistics and challenges of graduate school.

Finally, to my family and friends, thank you for your encouragement and support throughout this process. To my parents, Al and Sue, and sister, Jodi, thank you for believing in me and supporting me through everything I have pursued. Finally, to my wife, Jeni, thank you the most for being incredibly patient and exceedingly supportive over the last 8 years. Without your emotional support and caring ways this process would have been nearly impossible. Thank you for supporting me everyday and keeping me focused and grounded.

Brandon David Downing

MYELOID CELLS INDUCE NEUROFIBROMATOSIS TYPE 1 ANEURYSM  
FORMATION THROUGH INFLAMMATION AND OXIDATIVE STRESS

Neurofibromatosis Type 1 (NF1) is a genetic disorder resulting from mutations in the NF1 tumor suppressor gene. Neurofibromin is the protein product of NF1 and functions as a negative regulator of Ras activity in both hematopoietic and vascular wall cells, which are critical for maintaining blood vessel homeostasis. NF1 patients are predisposed to chronic inflammation and premature cardiovascular disease, including development of large arterial aneurysms, which may result in sudden death secondary to their rupture. However, the molecular pathogenesis of NF1 aneurysm formation is completely unknown. Utilizing a novel model of *Nf1* murine aneurysm formation, we demonstrate that heterozygous inactivation of *Nf1* (*Nf1*<sup>+/-</sup>) results in enhanced aneurysm formation with myeloid cell infiltration and increased reactive oxygen species in the vessel wall. Using cell lineage-restricted transgenic mice, we show that loss of a single *Nf1* allele in myeloid cells is sufficient to recapitulate the *Nf1*<sup>+/-</sup> aneurysm phenotype *in vivo*. Additionally, oral administration of simvastatin, a statin with antioxidant and anti-inflammatory effects, significantly reduced aneurysm formation in *Nf1*<sup>+/-</sup> mice. Finally, the antioxidant apocynin was administered orally and also resulted in a significant reduction of *Nf1*<sup>+/-</sup> aneurysms. These data provide genetic and pharmacologic evidence that neurofibromin-deficient myeloid cells are the central cellular triggers for aneurysm formation in a novel model of NF1 vascular disease, implicated

oxidative stress as the key biochemical mechanisms of NF1 aneurysm formation and provide a potential therapeutic target for NF1 vasculopathy.

David A. Ingram Jr., M.D., Chair

## TABLE OF CONTENTS

List of Figures .....	ix
Abbreviations .....	xi
Chapter One: Development of two novel <i>Nf1</i> heterozygous aneurysm models and identification of myeloid cells as the primary effectors of <i>Nf1</i> <sup>+/-</sup> aneurysm formation.....	1
Introduction	
Neurofibromatosis Type 1 .....	2
Neurofibromatosis Type 1 and Cardiovascular Disease .....	3
Neurofibromin .....	5
Aneurysm Pathogenesis .....	6
Murine Models of Aneurysm Formation .....	9
Materials and Methods	
Animals.....	12
Angiotensin II Infusion Abdominal Aortic Aneurysm Model.....	13
Classification and Quantification of Abdominal Aortic Aneurysms .....	13
Histopathology and Immunohistochemistry.....	14
Murine Blood Pressure Measurements .....	15
Matrix Metalloproteinase Activity Analysis.....	16
<i>In situ</i> Superoxide Detection .....	17
Statistical Analysis.....	17
Results	
Heterozygous inactivation of <i>Nf1</i> amplifies the incidence and severity of aneurysm formation within <i>ApoE</i> <sup>-/-</sup> mice .....	18
Heterozygous inactivation of <i>Nf1</i> amplifies the incidence and severity of aneurysm formation in angiotensin II-infused mice.....	26
<i>Nf1</i> <sup>+/-</sup> aneurysms are characterized by inflammatory cell infiltration, vascular smooth muscle cell expansion, and reactive oxygen species production .....	33
Heterozygous inactivation of <i>Nf1</i> in myeloid cells alone is sufficient to recapitulate <i>Nf1</i> <sup>+/-</sup> aneurysm formation .....	46
Discussion.....	56

Chapter Two: Identification of excessive inflammation and oxidative stress as critical biochemical processes leading to <i>Nf1</i> <sup>+/-</sup> aneurysm formation .....	62
Introduction	
Cardiovascular Disease and Oxidative Stress .....	63
HMG-CoA Reductase Inhibitors and Cardiovascular Disease .....	66
Apocynin and Cardiovascular Disease.....	68
Materials and Methods	
Patient Recruitment.....	70
Comet Assay .....	70
Simvastatin Administration .....	70
Apocynin Administration.....	71
Results	
NF1 patients have evidence of oxidative stress in white blood cells .....	72
Simvastatin attenuates Ang II-induced AAA formation in <i>Nf1</i> <sup>+/-</sup> mice .....	75
Apocynin attenuates Ang II-induced AAA formation in <i>Nf1</i> <sup>+/-</sup> mice .....	83
Discussion.....	90
References.....	93
Curriculum Vitae	



## LIST OF FIGURES

Figure 1.	<i>ApoE</i> <sup>-/-</sup> ; <i>Nf1</i> <sup>+/-</sup> mice fed a high fat diet have augmented aneurysm formation. ....	22
Figure 2.	<i>ApoE</i> <sup>-/-</sup> ; <i>Nf1</i> <sup>+/-</sup> mice fed a high fat diet have augmented histological aneurysm formation. ....	24
Figure 3.	<i>Nf1</i> <sup>+/-</sup> mice have increased Ang II-induced abdominal aortic aneurysm formation .....	27
Figure 4.	<i>Nf1</i> <sup>+/-</sup> mice have larger Ang II-induced abdominal aortic aneurysms.....	29
Figure 5.	<i>Nf1</i> <sup>+/-</sup> mice display increased severity of Ang II-induced abdominal aortic aneurysms .....	31
Figure 6.	<i>Nf1</i> <sup>+/-</sup> mice have increased Mac3+ macrophage infiltration in abdominal aortic aneurysms .....	36
Figure 7.	<i>Nf1</i> <sup>+/-</sup> mice have increased vascular smooth muscle cells in abdominal aortic aneurysms .....	38
Figure 8.	Relative location of macrophages and VSMCs in abdominal aortic aneurysms .....	40
Figure 9.	<i>Nf1</i> <sup>+/-</sup> mice have increased MMP activity and increased MMP-2 and MMP-9 expression in abdominal aortic aneurysms.....	42
Figure 10.	<i>Nf1</i> <sup>+/-</sup> mice have increased superoxide formation in abdominal aortic aneurysms .....	44
Figure 11.	<i>Nf1</i> <sup>fl/+</sup> ; <i>LysM</i> <sup>cre</sup> mice display efficient recombination .....	48
Figure 12.	Heterozygous inactivation of <i>Nf1</i> in myeloid cells alone is sufficient to recapitulate <i>Nf1</i> abdominal aortic aneurysm formation .....	50
Figure 13.	<i>Nf1</i> <sup>fl/+</sup> ; <i>LysM</i> <sup>cre</sup> mice have enlarged and more severe abdominal aortic aneurysms similar to <i>Nf1</i> <sup>+/-</sup> mice.....	52
Figure 14.	<i>Nf1</i> <sup>fl/+</sup> ; <i>LysM</i> <sup>cre</sup> aneurysms contain increased macrophage infiltration, MMP activity and superoxide levels in <i>Nf1</i> <sup>+/-</sup> mice .....	54

Figure 15.	NF1 patients have increased DNA damage.....	73
Figure 16.	Simvastatin reduces Ang II-induced <i>Nf1</i> <sup>+/-</sup> abdominal aortic aneurysms.....	77
Figure 17.	Simvastatin reduces Ang II-induced <i>Nf1</i> <sup>+/-</sup> abdominal aortic aneurysms and macrophage infiltration .....	79
Figure 18.	Simvastatin attenuates Ang II-induced <i>Nf1</i> <sup>+/-</sup> MMP expression and activation and superoxide production .....	81
Figure 19.	Apocynin reduces Ang II-induced <i>Nf1</i> <sup>+/-</sup> abdominal aortic aneurysms.....	84
Figure 20.	Apocynin prevents Ang II-induced AAA formation in <i>Nf1</i> <sup>+/-</sup> mice .....	86
Figure 21.	Apocynin reduces Ang II-induced superoxide formation in <i>Nf1</i> <sup>+/-</sup> mice.....	88

## LIST OF ABBREVIATIONS

AAA	Abdominal Aortic Aneurysm
ApoE	Apolipoprotein E
$\alpha$ -SMA	Alpha-Smooth Muscle Actin
Ang II	Angiotensin II
ANOVA	Analysis of Variance
CAD	Coronary Artery Disease
CD	Cluster of Differentiation
CGD	Chronic Granulomatous Disease
CVD	Cardiovascular Disease
DHE	Dihydroethidium
DUOX	Dual Oxidase
ECM	Extracellular Matrix
FPG	Formamidopyrimidine DNA Glycosylase
GAP	GTPase Activating Protein
H&E	Hematoxylin and Eosin
HMG-CoA	3-hydroxy-3-methyl-glutaryl-coenzyme A
HPF	High Power Field
IHC	Immunohistochemistry
LDLr	Low-density Lipoprotein receptor
LOH	Loss of Heterozygosity
<i>LysM<sup>cre</sup></i>	Lysozyme Cre
MCP-1	Monocyte Chemoattractant Protein-1
MMP	Matrix Metalloproteinase
MMP-2	Matrix Metalloproteinase-2
MMP-9	Matrix Metalloproteinase-9
NADPH	Nicotinamide adenine dinucleotide phosphate
NF1	Neurofibromatosis Type 1
<i>Nf1<sup>+/-</sup></i>	<i>Nf1</i> Heterozygosity
NIH	National Institutes of Health
OCT	Optimum Cutting Temperature
PBS	Phosphate Buffered Saline
Ras	p21 <sup>ras</sup>
ROS	Reactive Oxygen Species
SEM	Standard Error of the Mean
<i>Sm22<sup>cre</sup></i>	Smooth Muscle Protein 22 $\alpha$ Cre
VSMC	Vascular Smooth Muscle Cell
WT	Wild type

## **CHAPTER ONE**

DEVELOPMENT OF TWO NOVEL *NF1* HETEROZYGOUS ANEURYSM  
MODELS AND IDENTIFICATION OF MYELIOD CELLS AS THE PRIMARY  
EFFECTORS OF *NF1*<sup>+/-</sup> ANEURYSM FORMATION

## **INTRODUCTION**

### **Neurofibromatosis Type 1.**

Neurofibromatosis Type 1 (NF1) is a common autosomal dominant genetic disorder affecting 1 in 3,000 live births resulting from mutations in the *NF1* tumor suppressor gene (1, 2). The NF1 gene is located on chromosome 17 at position 17q11.2 (3) spanning over 350 kilobases accounting for 60 exons encoding the protein neurofibromin (4). Neurofibromin negatively regulates p21<sup>ras</sup> (Ras) activity via stimulation of its GTPase function (1, 5, 6). Mutations in *NF1* can be inherited; however, 30 to 50% of NF1 cases result from *de novo* mutations (7-9). Over 240 mutations have been described which cause NF1 (10) including deletions, duplications, frame shift mutations, insertions, nonsense mutations and substitutions (11). Mutations causing NF1 affect only one allele of the *NF1* gene although loss of heterozygosity (LOH) has been described in primary tumor samples from NF1 patients (12, 13). The clinical diagnosis of NF1 is made based on recommendations by the National Institutes of Health (NIH) where two of the seven following clinical findings are present: 1) six or more café-au-lait macules (5 mm or more pre-pubertal or 15 mm or more post-pubertal) 2) two or more neurofibromas or one plexiform neurofibroma 3) freckling in the axillary or inguinal regions 4) optic glioma 5) two or more Lisch nodules 6) bone lesions including sphenoid dysplasia or thinning of long bone cortex 7) a first degree relative with NF1 (14, 15). Therefore, haploinsufficiency of *NF1* causes

disease with complete penetrance (9) and a variety of clinical manifestations in several organ systems (7, 8).

Common non-neoplastic manifestations of NF1 can affect the integumentary, skeletal, nervous and cardiovascular systems characterized by café-au-lait spots, bone dysplasia, cutaneous neurofibromas and aneurysmal disease, respectively (16). Additionally, LOH can lead to neoplasms in the hematopoietic, gastrointestinal, and central nervous systems (16, 17). Previous studies have found decreased neurofibromin levels lead to phenotypic cellular changes such as increased proliferation and migration and decreased apoptosis in endothelial cells (18), fibroblasts (19), vascular smooth muscle cells (20), mast cells (21) and macrophages (22). Overall, NF1 is common genetic disease that affects many different cell types and tissues and results in a spectrum of clinical findings and severities.

### **Neurofibromatosis Type 1 and Cardiovascular Disease.**

Cardiovascular disease (CVD) is a serious but under-recognized complication of NF1 (23). NF1 patients with CVD display a wide range of lesions, affecting both arteries and veins, contributing to increased morbidity and mortality (24-26). Specifically, aneurysms or stenosis of the aortic, renal, and mesenteric arteries are the most common lesions (25). Most lesions occur by 50 years of age and are secondary to an underlying vasculopathy (23, 25). Importantly, these vascular lesions can progress over time or recur following treatment (27-29). Lesions affecting the renal arteries are the most common vascular abnormalities

identified in NF1 patients affecting up to 5% of patients (23). Patients may present with hypertension due to improper renovascular regulation of blood pressure secondary to intimal hyperplasia or renal vascular wall remodeling due to aneurysm formation (30). Renovascular hypertension usually presents by early adulthood and has been recognized during pregnancy as eclampsia or gestational hypertension (31, 32). Although renal lesions may present with hypertension, many vascular lesions located throughout the rest of the body may only be evident during unrelated imaging studies or at the time of a catastrophic vascular event. Though the frequency of NF1 vasculopathy is difficult to define due to a lack of routine screening and asymptomatic nature of many lesions (33), the prevalence of vascular lesions in large clinical series ranges between 2.0% to 6.4% (25, 26, 29).

Studies utilizing genetic mouse models which recapitulate NF1 vasocclusive disease reveal that heterozygous inactivation of *Nf1* (*Nf1*<sup>+/-</sup>) in bone marrow derived cells contributes to neointima hyperplasia and vessel lumen stenosis after arterial injury (22, 34, 35). Clinical studies demonstrate that NF1 patients have evidence of chronic inflammation and mobilization of a specific pro-inflammatory monocyte subset, characterized as CD14<sup>dim</sup>CD16<sup>hi</sup>, in their peripheral blood that has been linked to the development of vasocclusive disease and aneurysm formation in non-NF1 patients with CVD (22, 36, 37). Additionally, it was noted that in *Nf1*<sup>+/-</sup> mice the murine equivalent of CD14<sup>dim</sup>CD16<sup>hi</sup> monocytes characterized by the Ly6C<sup>hi</sup> membrane marker was increased in non-challenged 12-week old male mice (20). When both copies of *Nf1* were ablated in

myeloid cells alone the number of Ly6C<sup>hi</sup> monocytes increased further indicting a connection between neurofibromin insufficiency within myeloid cells and vascular inflammation (20). Despite these observations from clinical and murine studies, the pathogenesis of NF1 aneurysm disease is completely unknown partly due to a lack of animal models that mimic the human vascular disease. Given the mostly silent presentation of aneurysms in NF1 patients and the potential for catastrophic rupture of these lesions, understanding disease pathogenesis is critical for their prevention, early detection and treatment. Therefore, the specific aims addressed within this project include:

1. Development of a tractable murine model of *Nf1* heterozygous aneurysm formation.
2. Identification of the cellular mechanism leading to *Nf1* heterozygous aneurysm formation utilizing lineage-restricted transgenic mice.
3. Identification of biochemical processes leading to *Nf1* heterozygous aneurysm formation utilizing pharmacologic inhibition studies.

### **Neurofibromin.**

Neurofibromin, encoded by the NF1 tumor suppressor gene, is a GTPase activating protein (GAP) and functions as a negative regulator of Ras.

Neurofibromin accelerates intrinsic GTPase activity of Ras leading to the hydrolysis of active Ras-GTP to its inactive Ras-GDP form (5, 6, 38).

Neurofibromin has been shown to be expressed in many of the cells important for vessel homeostasis including vascular smooth muscle cells (VSMCs), endothelial



cells (39), myeloid cells (40) and fibroblasts (41) as well as cells associated with the central and peripheral nervous system including neurons, Schwann cells and oligodendrocytes (42). Additionally, studies have shown that at least one copy of functional *Nf1* is necessary for development. Developing embryos with homozygous deletion of *Nf1* die at embryonic day 13.5 and display cardiac malformations (43). Mice with heterozygous deletion of *Nf1* develop normally and do not display cardiac malformation or external phenotypic differences from their WT littermates although extended studies reveal that some *Nf1*<sup>+/-</sup> mice develop tumors and leukemia similar to those seen in NF1 patients (44).

### **Aneurysm Pathogenesis.**

Abdominal aortic aneurysms (AAA) affect up to 9% of adults 65 years and older (45, 46) with 15,000 patients dying each year in the United States from ruptured or dissected AAAs (47). Risk factors associated with AAA formation include smoking, male gender, advanced age, Caucasian race, atherosclerosis, hyperlipidemia, hypertension and family history of AAA (48). Additionally, several single gene disorders affecting the connective tissue of the vascular wall predispose younger patients to aneurysms of the aorta from the aortic root to the iliac bifurcation including Ehlers-Danlos syndrome, Loeys-Dietz syndrome, Marfan System, Turner syndrome and Familial thoracic aortic aneurysm and dissection (49). These genetic disorders indicate that connective tissue maintenance in the vascular wall is an important aspect of maintaining vascular homeostasis and withstanding the hemodynamic forces within the aorta. Matrix

metalloproteinases (MMPs), a family of proteases that possess the ability to degrade most extracellular matrix (ECM) components in the vascular wall, have been found to be more prevalent in AAA tissue than normal aortic tissue (50, 51). MMPs are secreted from many cell types within the vessel wall as inactive zymogen precursors and require extracellular activation to expose the protease active site (51). Specifically, pro-MMP-2 and pro-MMP-9, which degrade elastin, are secreted by VSMCs and macrophages, respectively (50, 52, 53). Activation of pro-MMPs can occur through many mechanisms including inflammation (54), oxidative stress (55), and other proteases such as plasmin (56). The active forms of both MMP-2 and MMP-9 have been found in higher concentrations within aneurysmal aortic tissue compared to normal aortic tissue (57). Importantly, Longo *et al.* (58) investigated the role of both MMP-2 and MMP-9 in aneurysm formation and found that complete genetic ablation of either protease inhibited aortic dilation. However, when WT macrophages were infused and challenged, only the MMP-9 knockout mice formed aneurysms, suggesting that MMP-2 from the vessel wall and MMP-9 from macrophages work in concert to induce aneurysms. Doxycyclin, a non-selective inhibitor of several MMPs has also been shown to efficiently inhibit aneurysm formation (59).

Besides matrix degradation, other hallmarks of aneurysm pathogenesis include oxidative stress and inflammation (60-62). Studies in animal models using angiotensin II (Ang II) have shown that chronic infusion of Ang II will induce AAA formation while showing an increase in oxidative stress, inflammation and matrix degradation within the aneurysmal tissue (63). Studies inducing AAAs with

Ang II have found that genetic or pharmacologic disruption of these biochemical processes can be protective. Specifically, Thomas *et al.* (64) showed that deletion of the p47<sup>phox</sup> subunit of the superoxide producing nicotinamide adenine dinucleotide phosphate (NADPH) oxidase complex (Nox) attenuated Ang II induced aneurysm formation in apolipoprotein E-deficient (*ApoE*<sup>-/-</sup>) mice. Several antioxidant agents have shown the ability to inhibit aneurysm formation in both murine (65) and rat (66) models of aneurysm formation although antioxidant treatments have not translated well to the human disease state. Finally, inflammatory cell recruitment and infiltration of the aortic media and adventitia has been observed in both human and murine diseased tissue. Specifically, monocytes are attracted to the cell wall by ECM degradation products (67), granulocyte macrophage colony-stimulating factor (68), monocyte chemoattractant protein-1 (MCP-1) (69), and RANTES (regulated on activation, normal T cell expressed and secreted) (70). VSMCs simulated with the inflammatory mediators Ang II or tumor necrosis factor-alpha secrete MCP-1 indicated a progression in which simulation of VSMCs causes release of MCP-1 and subsequent monocyte attraction (71, 72). Overall, examination of human aneurysmal tissue and murine genetic and pharmacologic studies indicate that the primary biologic processes driving aneurysm formation are the VMSC chemokine-driven recruitment of monocytes to areas of vascular inflammation, differentiation of those monocytes to macrophages, and subsequent damage to the wall by release and activation of MMPs.

## **Murine Models of Aneurysm Formation.**

Aneurysmal disease was initially studied by procurement of aneurysmal tissue from patients during aneurysm repair and performing IHC analysis to identify structural changes and cellular makeup of aneurysmal tissue compared to normal aortic tissue. These studies yielded a very limited view about how aneurysms developed and progressed. More recently aneurysm initiation and progression has been studied through the development of genetic and pharmacologically induced aneurysm models. Two genetic models of impaired ECM development and maintenance have been studied. First, the blotchy mouse contains a mutation of the *ATP7A* gene, which encodes a copper-transporting ATPase that leads to a copper deficiency (73). Lysyl oxidase is involved in the cross linking of collagen and elastin fibers for which copper is a co-factor (74), therefore defects in the ECM matrix predispose these mice as well as Menkes' disease patients with the equivalent mutations, to aneurysm formation. Alternatively, genetically engineered mice deficient in TIMP-1 (tissue inhibitor of metalloproteinases-1) show increased aneurysm formation due to increased activated MMPs breaking down the vascular wall ECM (75, 76). These models illustrate the importance of proper ECM formation and maintenance to aneurysm progression, but fail to address which factors translate from environmental risk to ECM breakdown and aneurysm formation.

Hyperlipidemic mice have been an important model for the induction and analysis of aneurysm formation by employing a well-established risk factor for aneurysm induction. Mice fed a high fat diet alone will develop atherosclerosis

and aneurysms over time. More recently, mice deficient in low-density lipoprotein receptor (LDLr) (77) or ApoE (78, 79) have been developed and allow for increased aneurysm formation when on a high fat diet for up to one year (80). *ApoE*<sup>-/-</sup> mice on a high fat diet formed aneurysms in the aorta near and under areas of atherosclerosis (80). The observation of aneurysm formation near atherosclerotic plaques containing foam cell macrophages indicates that inflammation and MMP release from macrophages may be the link between ECM degradation and the hyperlipidemic risk factor and ECM degradation (81). Additionally, this model indicates macrophage recruitment to the vascular wall may be an important early process in aneurysm formation.

Chemically-induced aneurysm formation represents the majority of current models being used for the investigation of aneurysm development and progression due to reduced amount of time required for induction. Elastase infusion into the infrarenal aorta has been used extensively and allows for aneurysm formation in 14 to 21 days (82). Elastase infusion leads to aneurysm formation by breaking down the elastin portion of the ECM in the infused segment. Due to the short time period of this model the progression of aneurysm formation can be reliably tracked. The limitation of this model is similar to the limitation of the genetic mouse models with ECM deficiency, the infusion itself breaks down the ECM rather than the vascular wall cells or recruited cells which likely do this during inflammation, repair and resolution.

Finally, Ang II infusion (500 to 1000 ng/kg/min) over 28 days via a subcutaneous osmotic mini-pump induces aneurysm formation in *LDLr*<sup>-/-</sup> and

*ApoE*<sup>-/-</sup> mice in the suprarenal aorta (63). Interestingly, Ang II at these doses only slightly increased blood pressure (83, 84). During subsequent studies, MMP inhibition prevented aneurysm formation (85) precluding blood pressure from being the sole mechanism of aneurysm formation in the Ang II infusion model. Ang II infusion has allowed for temporal characterization of the events leading to aneurysm formation (86). Macrophages accumulate within the first few days of infusion in the suprarenal aorta and are associated with elastin degradation. It is likely that Ang II stimulation of VSMCs results in the release of MCP-1 and MMP-2, which subsequently produces ECM degradation products. Both MCP-1 and the ECM degradation products attract monocytes to the stimulated site of the suprarenal aorta (87). Aneurysm formation has also been induced with Ang II infusion in WT C57B/6 mice allowing for a wild-type genetic background to be used. Aneurysms formed in WT mice were comparable in size to hyperlipidemic mice but occurred less frequently (88). Taken together, of the previous aneurysm studies utilizing various models of murine aneurysm induction, Ang II is very tractable model due to its limited time to induce aneurysms as well as its mechanism in which VSMCs are stimulated leading to inflammatory cell recruitment.

## **MATERIALS AND METHODS**

### **Animals.**

All protocols were approved by the Indiana University School of Medicine Institutional Animal Care and Use Committee. *Nf1*<sup>+/-</sup> mice were obtained from Tyler Jacks (Massachusetts Institute of Technology, Cambridge) and backcrossed 13 generations into the C57BL/6J strain. *Nf1*<sup>fl/fl</sup> mice were obtained from Luis Parada (University of Texas Southwestern Medical Center, Dallas) and backcrossed 13 generations into the 129SvJ strain. Lysozyme cre (*LysM*<sup>cre</sup>, stock 4781) and smooth muscle protein-22 $\alpha$  cre (*SM22*<sup>cre</sup>, stock 4746) mice were purchased from The Jackson Laboratory (Bar Harbor, ME) and maintained on C57BL/6 strain. *Nf1*<sup>fl/fl</sup> mice were inter-crossed with *LysMcre* or *SM22cre* mice to generate F1 C57BL/6  $\times$  129SvJ progeny. Specifically, *Nf1*<sup>fl/+</sup>;*LysMcre*, heterozygous loss of *Nf1* in myeloid cells only, and *Nf1*<sup>fl/+</sup>;*SM22cre*, heterozygous loss of *Nf1* in vascular smooth muscle cells (VSMCs) only, mice were used for experiments. Cre-mediated recombination was confirmed by PCR as previously described (89). LacZ lineage tracing of aortas from *Nf1*<sup>fl/+</sup>;*Rosa26*<sup>fl/+</sup>;*Sm22*<sup>cre</sup> mice revealed deep staining limited to the media of the vessel wall where VSMCs reside. LacZ lineage tracing of aortas from *Nf1*<sup>fl/+</sup>;*Rosa26*<sup>fl/+</sup>;*LysM*<sup>cre</sup> mice revealed very sparse staining limited to the vessel adventitia, a common area for limited numbers of macrophages under physiological conditions. *Nf1*<sup>+/-</sup> 129SvJ mice inter-crossed with *Nf1*<sup>+/-</sup> C57BL/6 mice generated F1 *Nf1*<sup>+/-</sup> and wild type

(WT) controls animals for experiments. All genotyping was performed according to Jackson Laboratory protocols or as previously described (89, 90).

### **Angiotensin II Infusion Abdominal Aortic Aneurysm Model.**

12 week-old WT and *Nf1*<sup>+/-</sup> male mice were infused with Angiotensin II (Ang II, 1500 ng/kg/min, Calbiochem, CA) or saline as previously described (91), with modification. In brief, animals were anesthetized by inhalation of an isoflurane (2%)/oxygen (98%) mixture, and an Alzet osmotic minipump (2006, Durect Corporation, CA) containing Ang II or saline was implanted into a subcutaneous pocket through an incision of the skin on the rear flank. The incision was closed using 5-0 prolene suture (Advanced Inventory Management). The incision site healed rapidly with no sign of infection. At indicated time points, the arterial tree was perfused at a constant physiologic pressure (100 mmHg) with 0.9% sodium chloride. Under a dissecting scope (Leica), a portion of the arterial tree was excised *en bloc* including carotid, aortic, iliac and femoral arteries after removal of adventitial fat. Some vessels were fixed with Zinc-formalin solution (1x, Anatech) before paraffin embedding.

### **Classification and Quantification of Abdominal Aortic Aneurysms.**

Digital images of harvested arteries were obtained with a Nikon camera on a Zeiss stereo-microscope (Carl Zeiss Inc) or a Nikon digital camera. The maximum external arterial diameters were measured using Metamorph 6.1 (Universal Imaging Systems Corp.) by a single observer blinded to the infusion



and/or treatment and genotype of the mice. Aneurysms were defined as an increase in the external aortic diameter of  $\geq 50\%$  as compared to control animals. Aortic aneurysm severity was rated from Type 0 to Type IV according to the method of Martin-McNulty et al. (92) with modification: Type 0, no aneurysm; Type I, discernable dilation 1.5 to 2 times the diameter of a normal corresponding artery; Type II, a single dilation that is more than 2 times the diameter of a normal corresponding artery; Type III, multiple dilations along the harvested vasculature with the largest dilation being 1.5 to 2 times the diameter of a normal corresponding artery; and Type IV, multiple dilations along the harvested vasculature with the largest dilation being more than 2 times the diameter of a normal corresponding artery.

### **Histopathology and Immunohistochemistry.**

Aortas were either paraffin or optimum cutting temperature (OCT) embedded and serial 5  $\mu\text{m}$  cross-sections were made through the length of the aorta at its largest diameter. Paraffin sections were stained with H&E (Anatech), Verhoeff's van Gieson (Sigma) for elastic lamina, Masson's trichrome (Sigma) for collagen, and Toluidine blue (Anatech) for mast cells. Elastic lamina preservation was graded as follows: grade 1, intact elastic lamina; grade 2, elastic lamina with some interruptions; and grade 3, severe elastin fragmentation. For immunohistochemistry, paraffin or OCT-embedded sections were de-waxed or acetone fixed, respectively, followed by low pH citrate antigen retrieval (DakoCytomation target retrieval solution citrate pH 6; Dako). Sections were

Protein Blocked (Dako) and incubated separately with anti-CD3 (1:100, BD Pharmingen), anti-B220 (1:100, BD Pharmingen), anti-alpha smooth muscle actin ( $\alpha$ -SMA, 1:200, Abcam), anti-Mac-3 (1:50, BD Pharmingen), anti-matrix metalloproteinase-2 (MMP2, 1:2000, Abcam) and anti-matrix metalloproteinase-9 (MMP9, 1:1000, Abcam) primary antibodies. Sections were incubated with the appropriate fluorescent secondary antibody (Alexa Flour 647 goat anti-rat IgG or Alexa Flour 488 goat anti-rat, life technologies) and visualized with fluorescent microscopy (Leica) or biotinylated secondary antibody (Vector Laboratories) followed by incubation with the ABC kit (Vector Lab), and visualized by 3,3'-diaminobenzidine (DAB; Vector Laboratories) and counterstained with hematoxylin. The average number of CD3<sup>+</sup>, B220<sup>+</sup>, F4/80<sup>+</sup>, Mac-3<sup>+</sup> and mast cells were calculated from five independent high power fields (HPF) from five sections at 50 $\mu$ m intervals. Some OCT embedded cross-sections were co-stained with fluorescent  $\alpha$ -SMA and anti-Mac-3 with Alexa Flour 488 goat anti-rat secondary.

### **Murine Blood Pressure Measurements.**

Blood pressure measurements were obtained as previously described (93), with modification. Mice were anesthetized with an isoflurane (2%)/oxygen (98%) mixture and placed on a heating block in a supine position. The femoral artery was exposed under a dissecting microscope (Leica). A heat-stretched polyethylene (PE)-50 tube (BD Biosciences) was inserted into the femoral artery. During the reading, the arterial line was connected to a pressure transducer (AD

Instruments, Colorado Springs, CO) and signal was acquired on a Blood Pressure Display Unit (StemTech, Milwaukee, WI), transmitting to a DI-205 signal interface (DATAQ Instruments, Akron, OH). Blood pressure readings were recorded with WinDAQ Version 2.15 software (DATAQ Instruments, Akron, OH). Blood pressure was recorded for three minutes with mean pressure reported.

### **Matrix Metalloproteinase Activity Analysis.**

To detect MMP activity in abdominal aortas, *in situ* zymography and gelatin zymography were performed as previously described (94). Briefly, for *in situ* zymography, fresh frozen, OCT-embedded aortic sections (10  $\mu$ m) from 18-day saline or Ang II infused WT and *Nf1*<sup>+/-</sup> mice were incubated with a dye-quenched gelatin substrate (DQ gelatin, Molecular Probes) according to the manufacturer's protocol. After cleavage of DQ-gelatin by gelatinolytic activity in the tissue, green fluorescence was photographed by fluorescence microscopy (Leica). Addition of EDTA (20 mM) in gelatin substrate before incubation was used to assess the specificity of MMP activity. For gelatin zymography, 10  $\mu$ g of homogenates lysed from fresh frozen segments of aorta from 18-day saline or Ang II infused WT and *Nf1*<sup>+/-</sup> mice in lysis buffer (50 mM Tris-HCl (pH 7.4), 0.2 M NaCl, and 10 mM CaCl<sub>2</sub>) were electrophoresed in a 10% SDS-polyacrylamide gel containing 1 mg/mL gelatin (Invitrogen). Gels were incubated for 36 hours (37°C) in zymography buffer (50 mmol Tris (pH 8.0), 10 mmol CaCl<sub>2</sub>, 0.05% Brij 35, 0.02% NaN<sub>3</sub>) and stained with Coomassie brilliant blue followed by destaining to visualize clear bands, indicating active proteinase.

### ***In situ* Superoxide Detection.**

To detect ROS generation in abdominal aortas, *in situ* dihydroethidium (DHE) staining was performed as previously described (95). OCT embedded cross-sections (10  $\mu\text{m}$ ) of abdominal aortas were incubated with DHE (5  $\mu\text{M}$ ) (Molecular Probes Inc.) for 30 minutes at 37°C, rinsed with phosphate buffered saline (PBS), and mounted with ProLong Gold Antifade Reagent (Invitrogen), and photographed using fluorescent microscopy.

### **Statistical Analysis.**

Quantitative results are shown as mean  $\pm$  standard error of the mean (SEM). All statistical analyses were performed using the Prism 5 (GraphPad Software). *P* values were obtained by the unpaired Student's *t*-test when comparison was between 2 groups, and by one-way analysis of variance (ANOVA) followed by a post hoc analysis using the Tukey's test when comparison was made among 3 or more groups. To determine significance of distribution data was subjected to Fisher's Exact test was used with Bonferroni correction. *P* values less than 0.05 were considered significant.

## **RESULTS**

### **Heterozygous inactivation of *Nf1* amplifies the incidence and severity of aneurysm formation within *ApoE*<sup>-/-</sup> mice.**

*ApoE*<sup>-/-</sup> mice are predisposed to aneurysm formation when fed an atherogenic diet. Intercrossing genetically engineered mice with *ApoE*<sup>-/-</sup> mice is a standard model to study genetic contributions to aneurysm formation in experimental progeny (96). To test the hypothesis that *Nf1* heterozygosity enhances aneurysm formation *in vivo*, *ApoE*<sup>-/-</sup> and *ApoE*<sup>-/-</sup>;*Nf1*<sup>+/-</sup> mice along with experimental controls (WT and *Nf1*<sup>+/-</sup> mice) were fed an atherogenic or normal chow diet for four months. Both *ApoE*<sup>-/-</sup> and *ApoE*<sup>-/-</sup>;*Nf1*<sup>+/-</sup> mice fed an atherogenic diet developed severe hypercholesterolemia and advanced atherosclerosis compared to mice fed normal chow (Table 1). WT and *Nf1*<sup>+/-</sup> mice fed a normal chow or atherogenic diet did not develop hypercholesterolemia or atherosclerosis. Heterozygosity of *Nf1* in *ApoE*<sup>-/-</sup> mice did not alter cholesterol, triglyceride or glucose levels compared to *ApoE*<sup>-/-</sup> mice, and no difference in body weight or atherosclerotic lesion size between the two experimental groups was noted (Table 1). However, gross inspection of the aorta and its branches from *ApoE*<sup>-/-</sup>;*Nf1*<sup>+/-</sup> and *ApoE*<sup>-/-</sup> mice fed an atherogenic diet revealed an increased incidence of aneurysm formation in *ApoE*<sup>-/-</sup>;*Nf1*<sup>+/-</sup> when compared to control mice (Figure 1A). Neither *ApoE*<sup>-/-</sup> nor *ApoE*<sup>-/-</sup>;*Nf1*<sup>+/-</sup> mice fed normal chow developed aneurysms (Figure 1A).

Quantification of the incidence and numbers of aneurysms in experimental mice fed an atherogenic diet revealed that 100 percent of *ApoE<sup>-/-</sup>;Nf1<sup>+/-</sup>* mice developed aneurysms compared to 40 percent of *ApoE<sup>-/-</sup>* mice, with a 16-fold increase in total number of aneurysms per animal (Figure 1B and 1C). The aneurysms were more severe in *ApoE<sup>-/-</sup>;Nf1<sup>+/-</sup>* mice as measured by a validated rating scale (Figure 1D) (92). These data indicate that heterozygous inactivation of *Nf1* augments aneurysm formation in *ApoE<sup>-/-</sup>* mice.

NF1 patients and *Nf1<sup>+/-</sup>* mice have evidence of vascular inflammation with mobilization of discrete populations of inflammatory monocytes linked to aneurysm formation (22, 34). Therefore, we characterized the cellular architecture and structural composition of aneurysms in atherogenic diet fed *ApoE<sup>-/-</sup>* and *ApoE<sup>-/-</sup>;Nf1<sup>+/-</sup>* mice. Consistent with larger aneurysms, histologic examination of aneurysmal tissue from *ApoE<sup>-/-</sup>;Nf1<sup>+/-</sup>* mice displayed enhanced disruption of medial architecture, arterial dilation, infiltration of inflammatory cells, and increased adventitial expansion compared to *ApoE<sup>-/-</sup>* mice fed an atherogenic diet (Figure 2A, 2B, and D). Trichrome staining identified enhanced collagen accumulation in the media and adventitia of *ApoE<sup>-/-</sup>;Nf1<sup>+/-</sup>* mice compared to *ApoE<sup>-/-</sup>* mice (Figure 2C), which is a hallmark of aneurysm formation (97).

Immunohistochemical (IHC) analysis of arterial cross-sections to identify the lineage of infiltrating immune cells populating the aneurysms revealed increased numbers of macrophages in both *ApoE<sup>-/-</sup>;Nf1<sup>+/-</sup>* and *ApoE<sup>-/-</sup>* mice fed an atherogenic diet (Figure 2D). Strikingly, the number of macrophages were

increased nearly 4-fold in *ApoE*<sup>-/-</sup>;*Nf1*<sup>+/-</sup> aortic cross-sections compared to *ApoE*<sup>-/-</sup> mice (*ApoE*<sup>-/-</sup>: 45.9 ± 3.3, n=7 versus *ApoE*<sup>-/-</sup>;*Nf1*<sup>+/-</sup>: 164.9 ± 16.8, n=7; *P*<.001), and these cells accounted for the majority of infiltrating cells in *ApoE*<sup>-/-</sup>;*Nf1*<sup>+/-</sup> aneurysms (Figure 2D). *ApoE*<sup>-/-</sup>;*Nf1*<sup>+/-</sup> mice also had a 2-fold increase in the accumulation of T cells and mast cells compared to *ApoE*<sup>-/-</sup> mice; however, these cells accounted for less than 5% of immune cells in aneurysms of *ApoE*<sup>-/-</sup>;*Nf1*<sup>+/-</sup> mice. Collectively, these data demonstrate that heterozygous inactivation of *Nf1* increases the frequency and severity of aneurysms with a corresponding increase in macrophage population.

**Table 1**

Blood serum chemistry and atherosclerotic lesion assessment

	Normal Chow Diet		Atherogenic Diet	
	<i>ApoE</i> <sup>-/-</sup>	<i>ApoE</i> <sup>-/-</sup> ; <i>Nf1</i> <sup>+/-</sup>	<i>ApoE</i> <sup>-/-</sup>	<i>ApoE</i> <sup>-/-</sup> ; <i>Nf1</i> <sup>+/-</sup>
<b>Body Mass (g)</b>	ND	ND	26.2 ± 1.3 (n=9)	25.54 ± 0.6 (n=10)
<b>Total Chol<sup>A</sup></b>	462.6 ± 11.2 (n=7)	438.8 ± 28.4 (n=8)	1576* ± 110.9 (n=9)	1458 <sup>†</sup> ± 81.2 (n=10)
<b>LDL Chol<sup>A</sup></b>	345.4 ± 24.8 (n=7)	356.6 ± 8.1 (n=8)	1351* ± 92.2 (n=9)	1279 <sup>†</sup> ± 63.9 (n=10)
<b>HDL Chol<sup>A</sup></b>	83.7 ± 4.2 (n=7)	75.8 ± 9.6 (n=8)	364.9* ± 174.4 (n=9)	167.8 <sup>†</sup> ± 34.6 (n=10)
<b>Triglyceride<sup>A</sup></b>	111.1 ± 6.1 (n=7)	88.0 ± 12.3 (n=8)	136.9 ± 12.3 (n=9)	150.7 <sup>†</sup> ± 10.4 (n=9)
<b>Fasting Glucose<sup>A</sup></b>	ND	ND	60.7 ± 4.2 (n=6)	51.8 ± 3.0 (n=6)
<b>Atherosclerotic Lesion Area (% of total aortic area)</b>	245.4 ± 15.1 (n=7)	223.8 ± 22.8 (n=8)	624.0* ± 118.6 (n=9)	523.8 <sup>†</sup> ± 33.3 (n=10)

\* = P < 0.05 *ApoE*<sup>-/-</sup> NCD versus *ApoE*<sup>-/-</sup> Atherogenic Diet<sup>†</sup> = P < 0.05 *ApoE*<sup>-/-</sup>;*Nf1*<sup>+/-</sup> NCD versus *ApoE*<sup>-/-</sup>;*Nf1*<sup>+/-</sup> Atherogenic Diet<sup>A</sup> = Measured in mg/dL

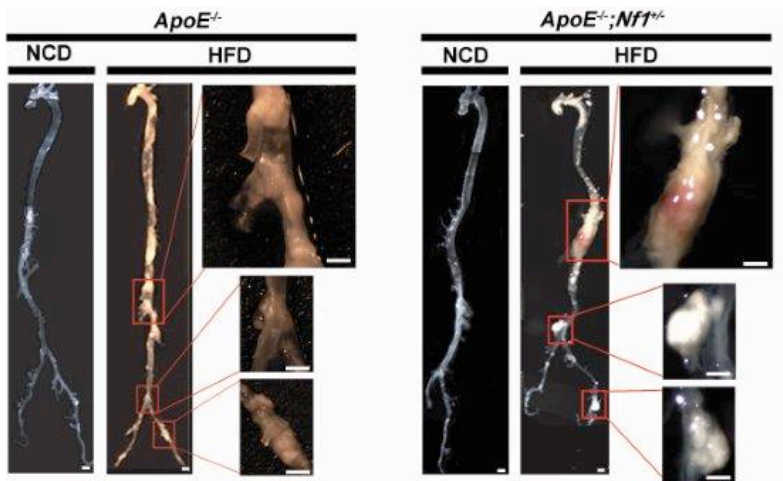
ND = Not Determined

Chol = Cholesterol

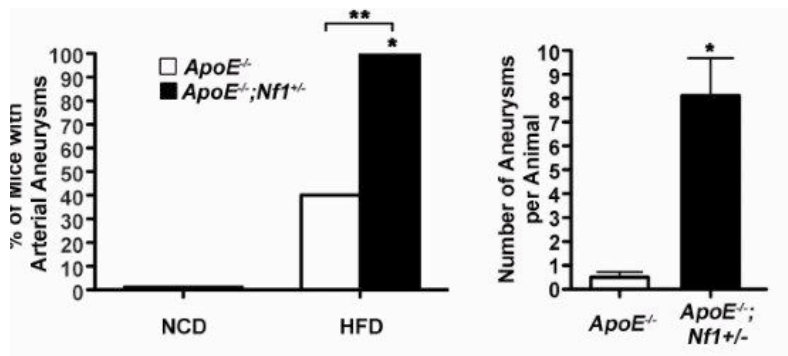


Figure 1

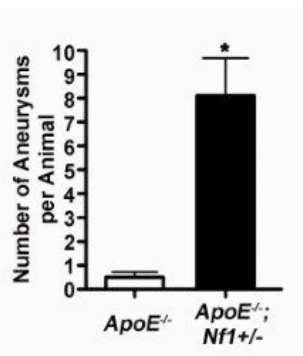
A



B



C



D

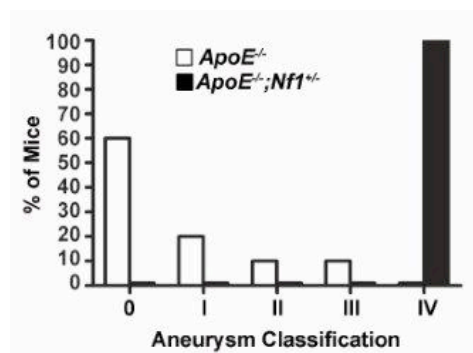


**Figure 1.** *ApoE*<sup>-/-</sup>;*Nf1*<sup>+/-</sup> mice fed a high fat diet have augmented aneurysm formation. **(A)** Representative photographs of the aorta and its branches from *ApoE*<sup>-/-</sup> and *ApoE*<sup>-/-</sup>;*Nf1*<sup>+/-</sup> mice fed a normal chow diet (NCD) or a high fat diet (HFD). Red boxes identify areas of aneurysm formation magnified in the panels on right. Scale bars: 1mm. **(B)** Quantification of aneurysm incidence, \**P*<0.0001 for NCD *ApoE*<sup>-/-</sup>;*Nf1*<sup>+/-</sup> (*n*= 10) versus HFD *ApoE*<sup>-/-</sup>;*Nf1*<sup>+/-</sup> (*n*=11). \*\**P*<0.01 for HFD *ApoE*<sup>-/-</sup> (*n*=10) versus HFD *ApoE*<sup>-/-</sup>;*Nf1*<sup>+/-</sup> (*n*=11). No statistical significance was observed (*P*=.08) for NCD *ApoE*<sup>-/-</sup> (*n*=10) versus HFD *ApoE*<sup>-/-</sup> (*n*=10). Analysis by Fisher's exact test with Bonferroni correction. **(C)** Average number of aneurysms per HFD mouse, \**P*<0.001 for *ApoE*<sup>-/-</sup> (*n*=10) versus *ApoE*<sup>-/-</sup>;*Nf1*<sup>+/-</sup> (*n*=11) by Student's t-test. **(D)** Severity index of aneurysms of HFD *ApoE*<sup>-/-</sup> (*n*=10) and HFD *ApoE*<sup>-/-</sup>;*Nf1*<sup>+/-</sup> (*n*=11). There was no aneurysm formation in NCD mice of either genotype.

**Figure 2**

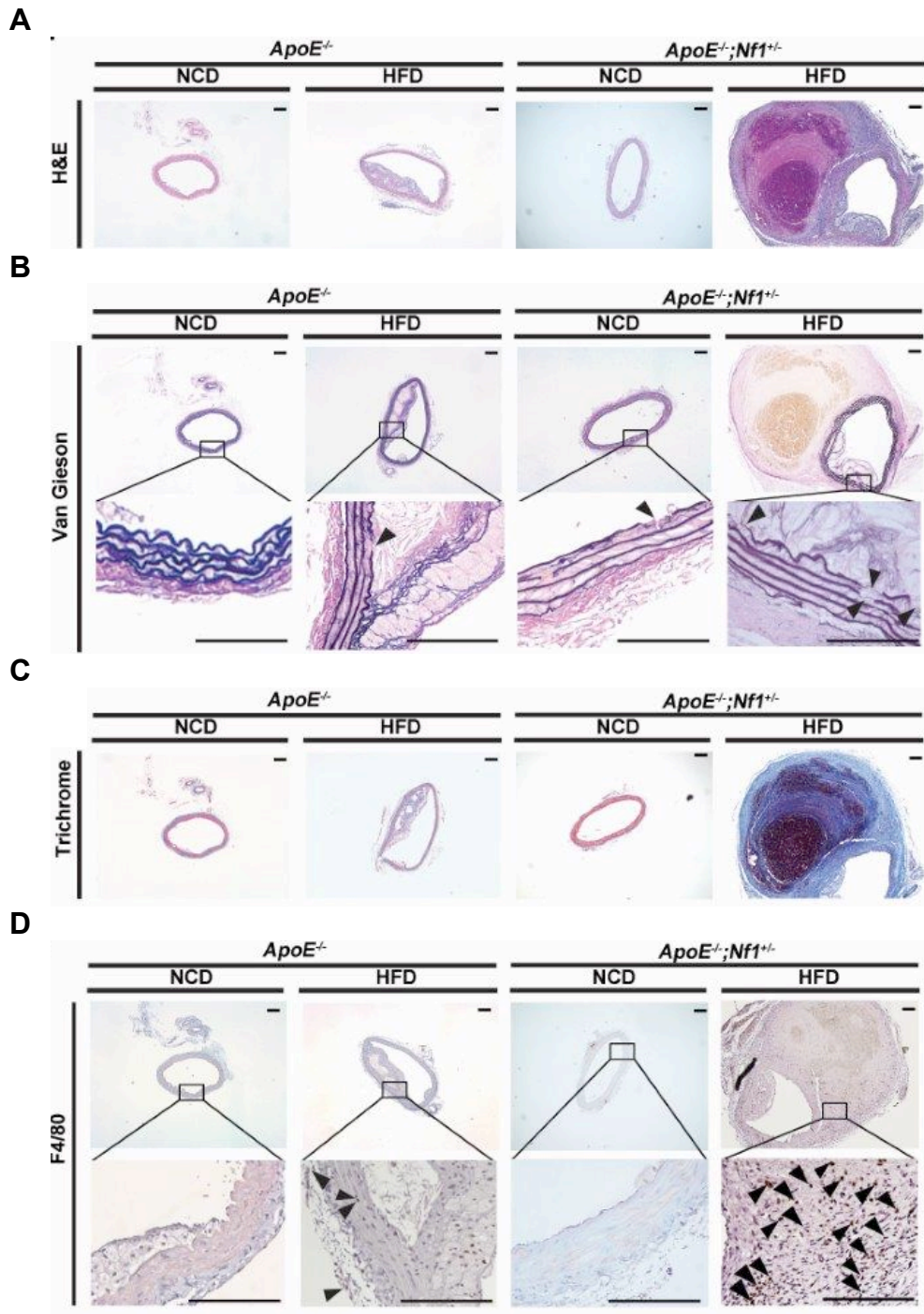


**Figure 2.** *ApoE*<sup>-/-</sup>;*Nf1*<sup>+/-</sup> mice fed a high fat diet have augmented histological aneurysm formation. Representative photomicrographs of abdominal aortic cross-sections from *ApoE*<sup>-/-</sup> and *ApoE*<sup>-/-</sup>;*Nf1*<sup>+/-</sup> mice on NCD or HFD stained with **(A)** H&E, **(B)** van Gieson for elastin, **(C)** Masson's trichrome for collagen or **(D)** anti-F4/80 for macrophages (brown cells, arrowheads). Arrowheads in **B** indicate degradation of the elastic lamina. Black boxes in **B** and **D** identify area that is magnified in lower panel. Scale bars: 50 μm.

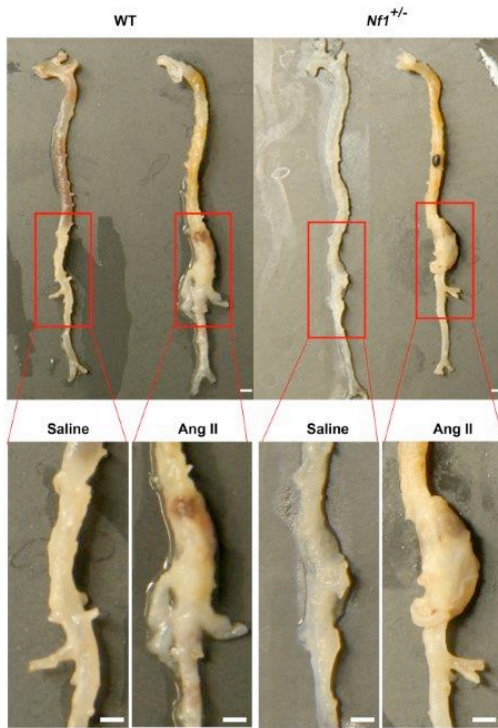
## **Heterozygous inactivation of *Nf1* amplifies the incidence and severity of aneurysm formation in angiotensin II-infused mice.**

To dissect the cellular mechanism of aneurysm formation and to confirm the effect of *Nf1* heterozygosity on aneurysm development in a more tractable system, we performed a second line of experiments in WT and *Nf1*<sup>+/-</sup> mice utilizing a different experimental model to interrogate disease pathogenesis. Angiotensin II (Ang II) infusion is another commonly used method of aneurysm induction and was adapted for use with modification (63, 98, 99). Infusion of Ang II induces inflammatory mediators and reactive oxygen species (ROS) within the arterial wall, producing abdominal aortic aneurysms that recapitulate human lesions (61, 95).

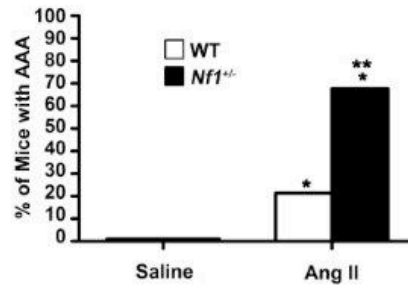
Infusion of Ang II increased aneurysm formation 3-fold in *Nf1*<sup>+/-</sup> mice compared to wild type mice (WT) (Figure 3A and 3B). Morphometric analysis of abdominal aortas from both genotypes revealed that Ang II-infused *Nf1*<sup>+/-</sup> mice had significantly larger aneurysms (Figure 4A and 4B). Further, *Nf1*<sup>+/-</sup> aneurysms display increased degradation of the elastic lamina and disorganized architecture which translated to a higher degree of aneurysm severity than WT aneurysms, which is reminiscent of lesions from NF1 patients (Figure 5A through 5C) (100). Importantly, Ang II infusion did not alter body weight or intra-arterial blood pressure in either genotype. Saline-infused *Nf1*<sup>+/-</sup> and WT mice did not form aneurysms (Figure 3A, 3B and 4A). These data indicate *Nf1* heterozygosity augments Ang II-induced aneurysm formation.

Figure 3

A



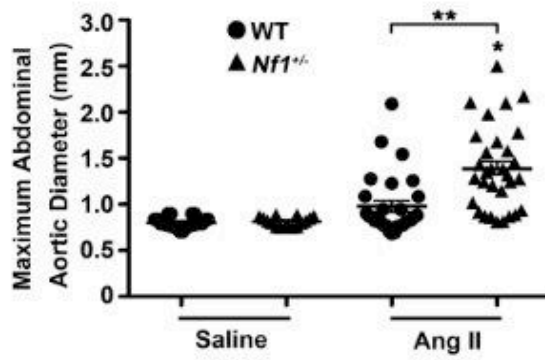
B



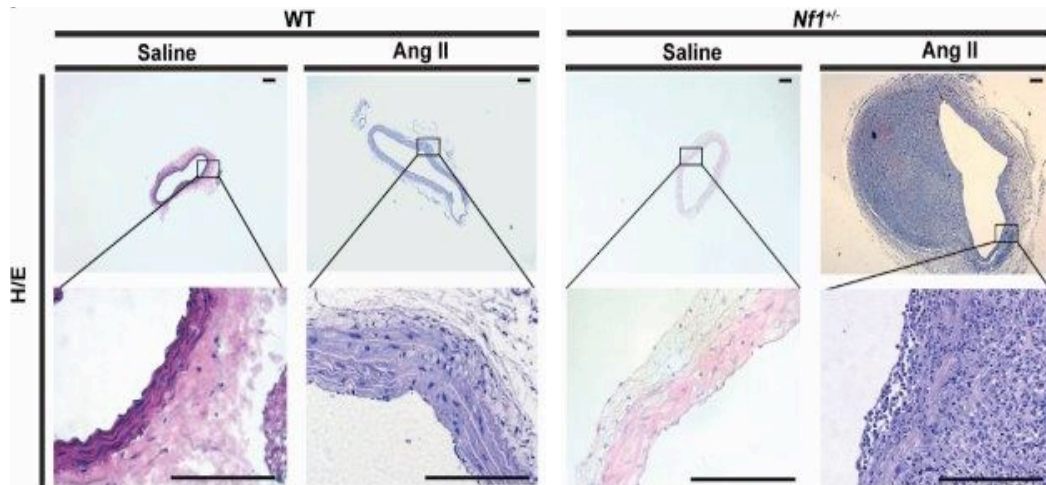
**Figure 3.** *Nf1*<sup>+/-</sup> mice have increased Ang II-induced abdominal aortic aneurysm formation. **(A)** Representative photographs of the aorta and branches from saline or Ang II-infused WT and *Nf1*<sup>+/-</sup> mice. Boxes identify area magnified in lower panel. Scale bars: 1mm. **(B)** Quantification of aneurysm incidence. \**P*<0.0083 for saline-infused WT (*n*=24) versus Ang II-infused WT (*n*=29) and Ang II-infused *Nf1*<sup>+/-</sup> (*n*=31). \*\**P*<0.0083 for saline-infused *Nf1*<sup>+/-</sup> (*n*=16) versus Ang II-infused *Nf1*<sup>+/-</sup>. Analysis by Fisher's exact test with Bonferonni correction.

Figure 4

A



B





**Figure 4.** *Nf1*<sup>+/-</sup> mice have larger Ang II-induced abdominal aortic aneurysms.

**(A)** Maximum abdominal aortic diameter of saline or Ang II-infused WT and *Nf1*<sup>+/-</sup> mice. Clustering around 1mm represents animals without aneurysm formation.

\**P*<0.05 for saline-infused *Nf1*<sup>+/-</sup> (*n*=16) versus Ang II-infused *Nf1*<sup>+/-</sup> (*n*=31).

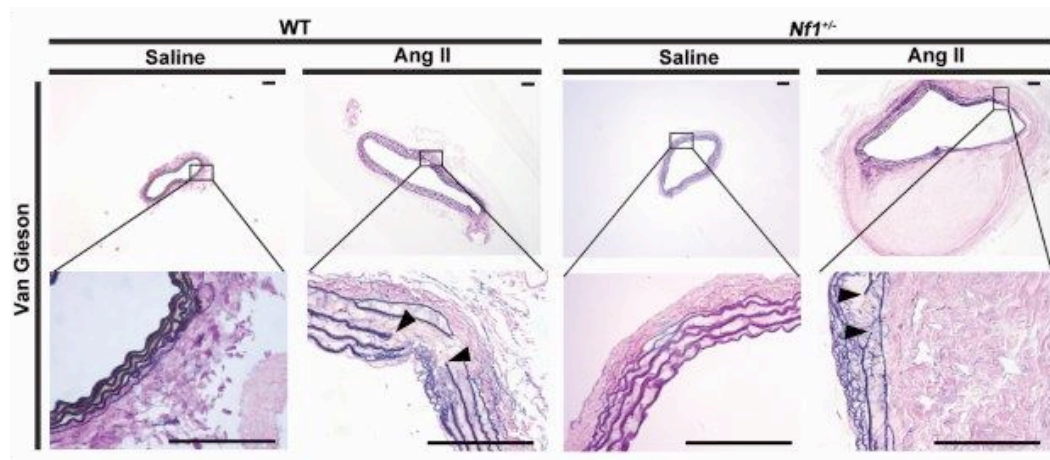
\*\**P*<0.05 for Ang II-infused WT (*n*=29) versus Ang II-infused *Nf1*<sup>+/-</sup> (*n*=31). No statistical significance was observed for saline-infused WT (*n*=24) versus Ang II-infused WT (*n*=29). Analysis by one-way analysis of variance (ANOVA) with

Tukey's test. Error bars denote the mean ± SEM. **(B)** Representative

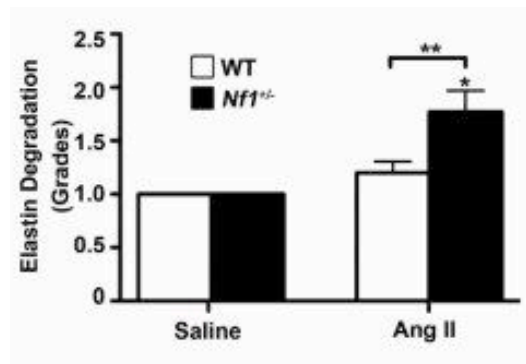
photomicrographs of abdominal aortic cross-sections from saline and Ang II-infused WT and *Nf1*<sup>+/-</sup> mice stained with H&E.

Figure 5

A



B



C

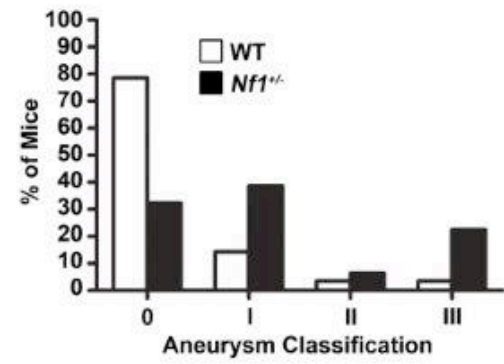


**Figure 5.** *Nf1*<sup>+/-</sup> mice display increased severity of Ang II-induced abdominal aortic aneurysms. **(A)** Representative photomicrographs of abdominal aortic cross-sections from saline and Ang II-infused WT and *Nf1*<sup>+/-</sup> mice stained with van Gieson. Boxed areas magnified in lower panel. Arrowheads indicate elastic lamina fragmentation. Scale bars: 50µm. **(B)** Grading of elastic lamina degradation in saline or Ang II-infused WT and *Nf1*<sup>+/-</sup> mice. \**P*<0.05 for saline-infused *Nf1*<sup>+/-</sup> (*n*=5) or WT (*n*=5) versus Ang II-infused *Nf1*<sup>+/-</sup> mice (*n*=13). \*\**P*<0.05 for Ang II-infused WT (*n*=15) versus Ang II-infused *Nf1*<sup>+/-</sup> mice. No statistical significance was observed for saline-infused WT or *Nf1*<sup>+/-</sup> versus Ang II-infused WT. **(C)** Aneurysm severity for Ang II-infused WT (*n*=29) or Ang II-infused *Nf1*<sup>+/-</sup> (*n*=31) mice. No aneurysms formed in saline-infused mice of either genotype.

***Nf1*<sup>+/-</sup> aneurysms are characterized by inflammatory cell infiltration, vascular smooth muscle cell expansion, and reactive oxygen species production.**

NF1 patients and *Nf1*<sup>+/-</sup> mice have increased populations of circulating inflammatory monocytes and pro-inflammatory cytokines linked to aneurysm formation (20, 22). Therefore, we sought to characterize the cellular and structural composition of WT and *Nf1*<sup>+/-</sup> aneurysms. Histologic examination of *Nf1*<sup>+/-</sup> aneurysms demonstrated significant dilation and degradation of the aortic wall, including increased disruption of the elastic lamina and adventitial expansion when compared to WT aneurysms (Figure 5A through 5C). Importantly, *Nf1*<sup>+/-</sup> aneurysms contained 4-times the number of macrophages compared to WT (Figure 6A and 6B). *Nf1*<sup>+/-</sup> macrophages co-localized to sites of elastic lamina degradation, medial rupture and adventitial expansion, indicating their potential role in aneurysm formation (Figure 5A and 6A). Ang II infusion also induced a significant expansion of vascular smooth muscle cells (VSMCs) in the media of *Nf1*<sup>+/-</sup> aortas compared to WT (Figure 7A and 7B). *Nf1*<sup>+/-</sup> VSMC expansion is consistent with previous findings that *Nf1*<sup>+/-</sup> VSMCs exhibit increased proliferation and migration in response to cytokines secreted by macrophages and vascular wall cells implicated in CVD (20, 101). Finally, co-staining with  $\alpha$ -smooth muscle actin ( $\alpha$ -SMA) and anti-Mac-3 illustrated VSMC expansion was within and near the vessel media while macrophage infiltration was primarily in the adventia as expected (Figure 8) (102, 103).

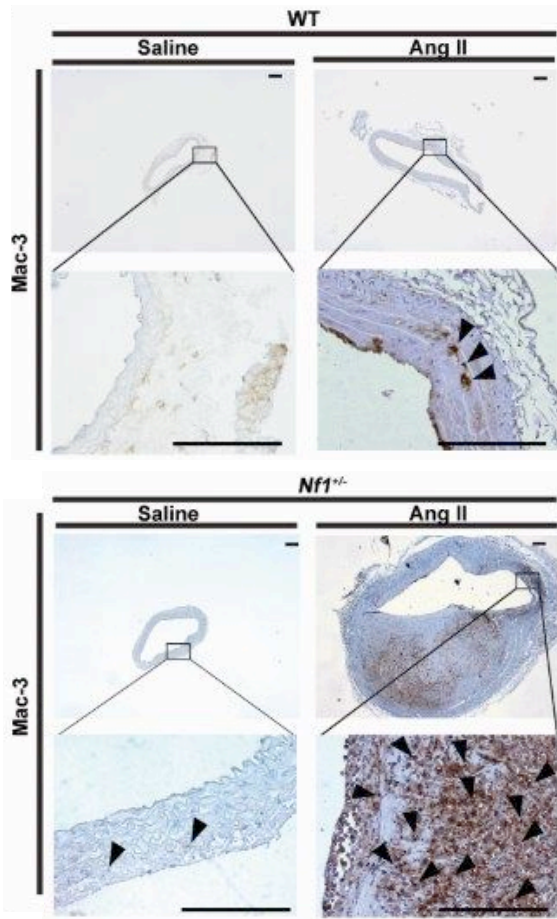
Genetic studies demonstrate that VSMC and macrophage secretion of MMPs (50, 52, 53) and ROS (61, 94, 104) are important molecular triggers for extracellular matrix (ECM) remodeling and aneurysm induction. Given the increased density of VSMCs and macrophages in *Nf1*<sup>+/-</sup> aneurysms, we measured expression and activation of matrix metalloproteinase-2 (MMP-2) and matrix metalloproteinase-9 (MMP-9) in aortas harvested from *Nf1*<sup>+/-</sup> and WT mice infused with Ang II or saline. Ang II infusion increased MMP activity and preferentially amplified MMP-9 expression in *Nf1*<sup>+/-</sup> aneurysms when compared with Ang II-infused WT aneurysms as determined by *in situ* zymography and immunohistochemistry (IHC) (Figure 9A and 9B). In addition, gelatin zymography of abdominal aortic explants from Ang II-infused WT and *Nf1*<sup>+/-</sup> mice corroborated increases of MMP activity in both genotypes with significantly enhanced activation of MMP-9 in *Nf1*<sup>+/-</sup> aortas alone (Figure 9C). Amplified MMP-9 expression in *Nf1*<sup>+/-</sup> aortas is an important observation since MMP-9 is largely derived from vessel wall macrophages (57, 105), which is consistent with the increased macrophage infiltration observed in *Nf1*<sup>+/-</sup> aneurysms.

We next assessed ROS production in abdominal aortic cross-sections from Ang II and saline-infused *Nf1*<sup>+/-</sup> and WT mice with dihydroethidium (DHE), a superoxide probe. Ang II infusion significantly increased superoxide production in *Nf1*<sup>+/-</sup> aortas when compared with WT aortas, while superoxide production was nearly undetectable in the aortas from saline-infused *Nf1*<sup>+/-</sup> and WT aortas (Figure 10A and 10B). Collectively, these data demonstrate that *Nf1* heterozygous aneurysms have evidence of increased inflammatory cell infiltration,

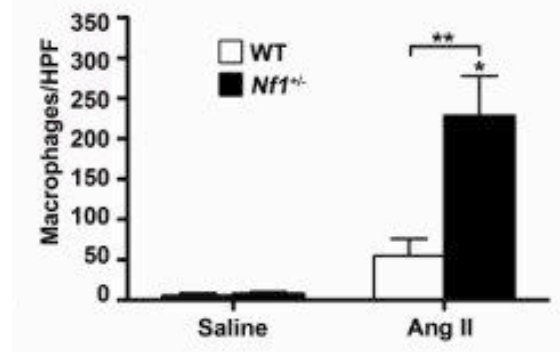
MMP activation, and ROS production, which are linked to abnormal arterial remodeling and disease progression.

Figure 6

A



B

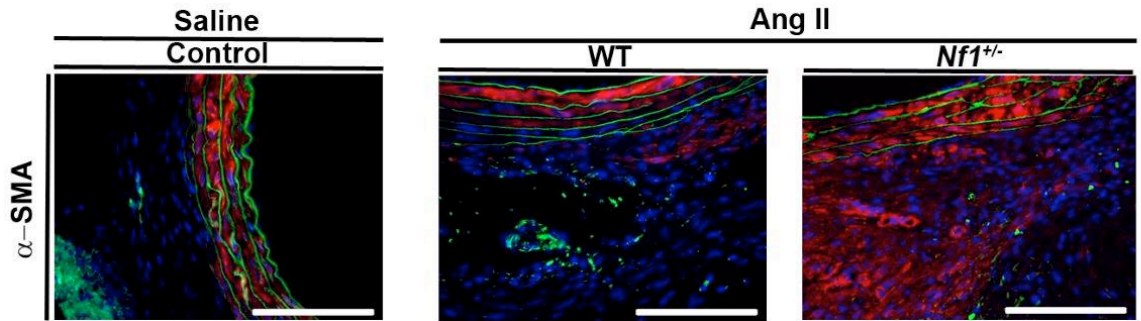


**Figure 6.** *Nf1<sup>+/-</sup>* mice have increased Mac3<sup>+</sup> macrophage infiltration in abdominal aortic aneurysms. **(A)** Representative photomicrographs of abdominal aortic cross-sections from saline and Ang II-infused WT and *Nf1<sup>+/-</sup>* mice stained anti-Mac-3 antibody (arrowheads). Boxed areas magnified in lower panel. Scale bars: 50 $\mu$ m. **(B)** Quantification of Mac3-positive macrophages per high-power field (HPF) in saline or Ang II-infused WT and *Nf1<sup>+/-</sup>* mice. \* $P$ <0.05 for saline-infused *Nf1<sup>+/-</sup>* ( $n$ =5) versus Ang II-infused *Nf1<sup>+/-</sup>* mice ( $n$ =5). \*\* $P$ <0.05 for Ang II-infused WT ( $n$ =5) versus Ang II-infused *Nf1<sup>+/-</sup>* mice. No statistical significance was observed for saline-infused WT ( $n$ =5) versus Ang II-infused WT. Analysis by one-way ANOVA with Tukey's test.

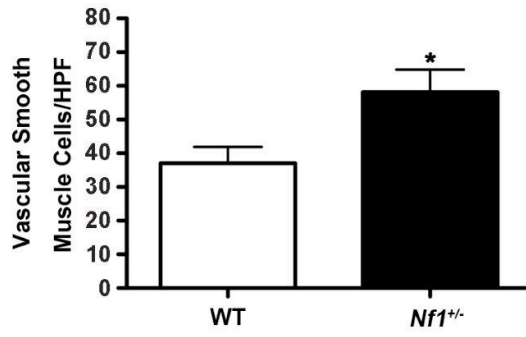


Figure 7

A



B



**Figure 7.** *Nf1*<sup>+/-</sup> mice have increased vascular smooth muscle cells in abdominal aortic aneurysms. **(A)** Representative photomicrographs of abdominal aortic cross-sections from Ang II-infused WT and *Nf1*<sup>+/-</sup> mice, stained with anti- $\alpha$  smooth muscle actin (red) to identify VSMCs. Cell nuclei are counterstained with DAPI (blue) and auto-fluorescence of murine tissue is visible (green). Saline-infused WT mice shown as control. Appearance of saline-infused *Nf1*<sup>+/-</sup> was similar to saline-infused WT staining. Scale bars: 50 $\mu$ m. **(B)** Quantification of VSMCs from Ang II-infused WT ( $n=5$ ) and *Nf1*<sup>+/-</sup> ( $n=5$ ) mice; \* $P<0.05$  for Ang II-infused WT versus Ang II-infused *Nf1*<sup>+/-</sup>, by Student's t-test.

Figure 8

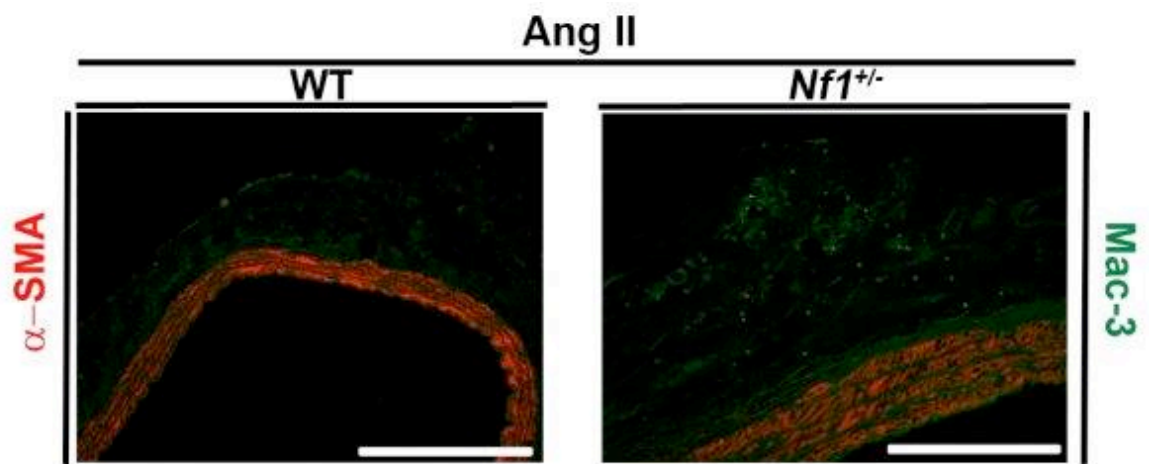
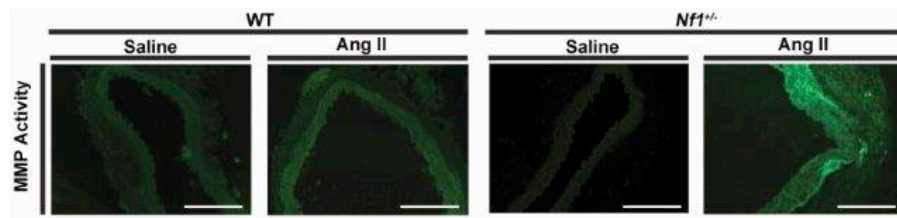


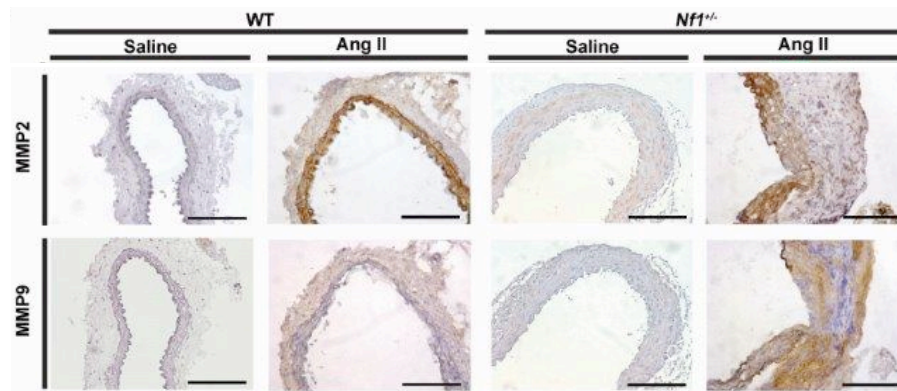
**Figure 8.** Relative location of macrophages and vascular smooth muscle cells in abdominal aortic aneurysms. Representative photomicrographs showing co-staining of Ang II-infused WT and *Nf1*<sup>+/-</sup> aortas with anti- $\alpha$ -SMA (red) and anti-Mac-3 (green). Scale bars: 50 $\mu$ m.

**Figure 9**

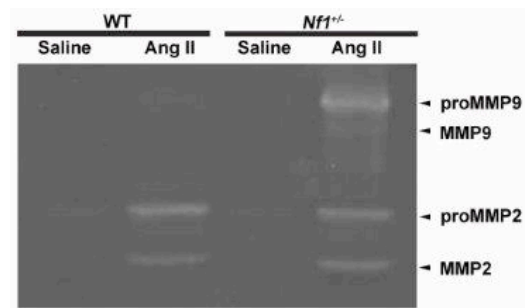
**A**



**B**



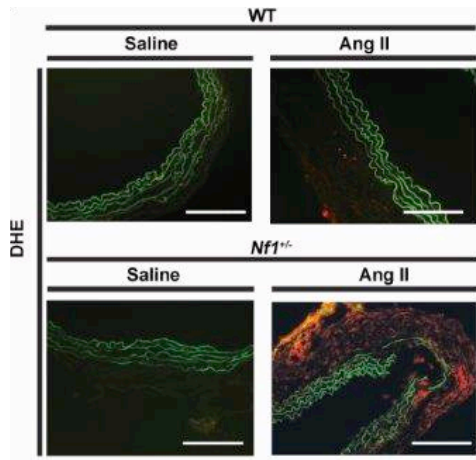
**C**



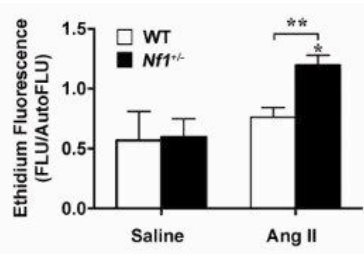
**Figure 9.** *Nf1*<sup>+/-</sup> mice have increased MMP activity and increased MMP-2 and MMP-9 expression in abdominal aortic aneurysms. **(A)** Representative photomicrographs of abdominal aortic cross-sections from saline and Ang II-infused WT and *Nf1*<sup>+/-</sup> mice. MMP activity (green) was visualized by *in situ* zymography **(B)** expression of MMP-2 and MMP-9 was detected by IHC staining with anti-MMP-2 (brown) and anti-MMP-9 (brown) antibodies. Scale bars: 50µm. **(C)** Representative zymogram showing abdominal aortic MMP-2 and MMP-9 levels for saline and Ang II-infused WT and *Nf1*<sup>+/-</sup> mice.

Figure 10

A



B



**Figure 10.** *Nf1*<sup>+/-</sup> mice have increased superoxide formation in abdominal aortic aneurysms. **(A)** Representative photomicrographs of abdominal aortic cross-sections from saline or Ang II-infused WT and *Nf1*<sup>+/-</sup> mice, showing superoxide production identified by *in situ* DHE staining (red). Auto-fluorescence of murine tissue is visible (green). **(B)** Quantification of ethidium fluorescence. \**P*<0.05 for Ang II-infused *Nf1*<sup>+/-</sup> (*n*=9) versus saline-infused WT (*n*=5) and *Nf1*<sup>+/-</sup> (*n*=3). \*\**P*<0.05 for Ang II-infused *Nf1*<sup>+/-</sup> versus Ang II-infused WT (*n*=8). Analysis by one-way ANOVA with Tukey's test.



**Heterozygous inactivation of *Nf1* in myeloid cells alone is sufficient to recapitulate *Nf1*<sup>+/-</sup> aneurysm formation.**

*Nf1*<sup>+/-</sup> mice have increased aneurysm formation characterized by increased macrophages and VSMCs and their secretory products, which are known to promote disease progression. Based on these observations, we generated transgenic mice with a single copy of the *Nf1* gene ablated in VSMCs or myeloid cells alone to determine the role of *Nf1* heterozygosity in VSMCs and myeloid cells on aneurysm formation. Briefly, *Nf1*<sup>fl/fl</sup> mice containing conditional *Nf1* alleles susceptible to *Cre*-mediated recombination (89) were inter-crossed with *SM22cre* or *LysMcre* transgenic mice, generating *Nf1*<sup>fl/+</sup>;*SM22cre* and *Nf1*<sup>fl/+</sup>;*LysMcre* progeny with *Nf1* heterozygous VSMCs (106) and myeloid cells (107), respectively. *Nf1*<sup>fl/fl</sup> mice underwent efficient *Cre*-mediated recombination when crossed with *LysMcre* (Figure 11) or *SM22cre* mice (35). Importantly, *LysMcre*-mediated recombination was seen in the aortic adventitia, a known location for macrophages, while the aortic media showed minimal *LysMcre*-mediated recombination.

*Nf1*<sup>fl/+</sup>;*SM22cre* and *Nf1*<sup>fl/+</sup>;*LysMcre* mice were infused with Ang II or saline and evaluated for aneurysm formation with controls (WT and *Nf1*<sup>+/-</sup> mice). *Nf1*<sup>fl/+</sup>;*LysMcre* mice infused with Ang II developed large aneurysms recapitulating the phenotype of *Nf1*<sup>+/-</sup> mice, while *Nf1*<sup>fl/+</sup>;*SM22cre* mice produced less severe aneurysms similar to WT mice (Figure 12A through 12D). Specifically, a 2.5-fold increase in AAA incidence was observed in *Nf1*<sup>fl/+</sup>;*LysMcre* mice compared with *Nf1*<sup>fl/+</sup>;*SM22cre* and WT mice (Figure 12B). Saline infusion failed to produce aortic

aneurysms in all genotypes. Additionally, Ang II-infused *Nf1<sup>fl/+</sup>;LysM<sup>cre</sup>* aneurysms displayed similar maximal dilation and aneurysm severity when compared to *Nf1<sup>+/-</sup>* mice (Figure 12C and 12D).

Histologic examination of H&E and van Gieson stained arterial cross-sections of *Nf1<sup>fl/+</sup>;LysM<sup>cre</sup>* aneurysms revealed increased elastic lamina degradation and adventitial expansion, similar to aneurysms harvested from Ang II-infused *Nf1<sup>+/-</sup>* mice (Figure 13A through 13C). Cross-sections from *Nf1<sup>fl/+</sup>;LysM<sup>cre</sup>* aortas demonstrated increased macrophage density similar to *Nf1<sup>+/-</sup>* aneurysms, while *Nf1<sup>fl/+</sup>;SM22<sup>cre</sup>* and WT mice contained significantly reduced macrophage numbers (Figure 14A). Similar to *Nf1<sup>+/-</sup>* mice, macrophages in *Nf1<sup>fl/+</sup>;LysM<sup>cre</sup>* mice were in close proximity to areas of adventitial expansion and elastic lamina degradation (Figure 13B and 14A). Additionally, *Nf1<sup>fl/+</sup>;LysM<sup>cre</sup>* and *Nf1<sup>fl/+</sup>;SM22<sup>cre</sup>* displayed similar MMP activity and DHE staining as *Nf1<sup>+/-</sup>* and WT mice, respectively (Figure 14B through 14D). Collectively, these data provide genetic evidence that heterozygous inactivation of *Nf1* in myeloid cells alone is sufficient to recapitulate *Nf1<sup>+/-</sup>* aneurysm formation *in vivo*, thereby implicating *Nf1<sup>+/-</sup>* monocytes and macrophages as the cellular trigger for aneurysm formation.

Figure 11

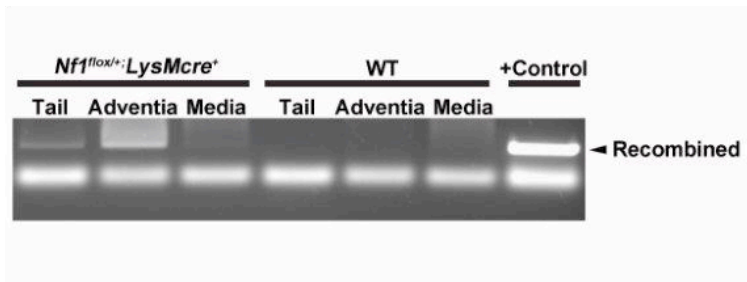
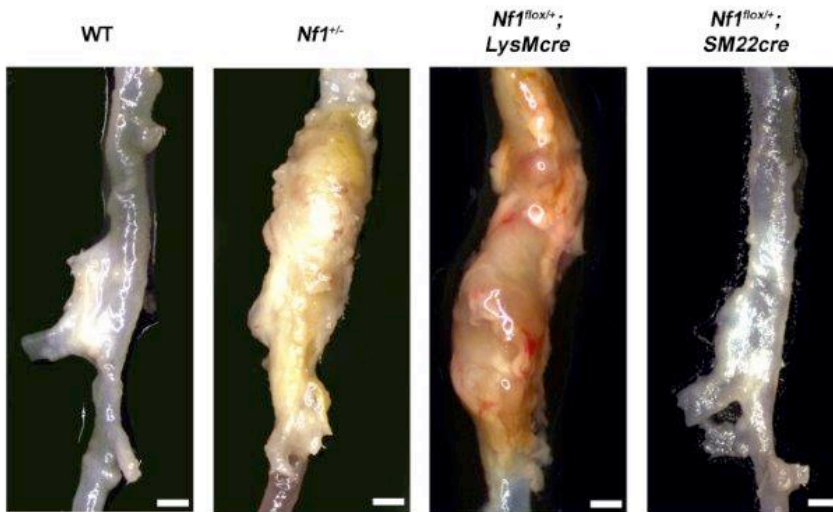


**Figure 11.** *Nf1<sup>fl/+</sup>;LysM<sup>cre</sup>* mice display efficient recombination.

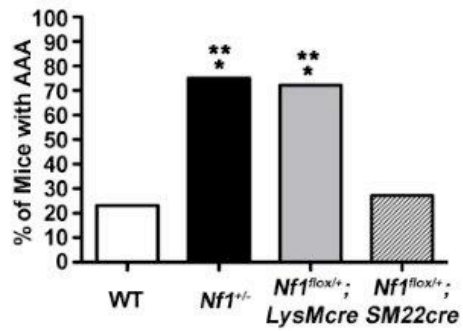
PCR analysis of abdominal aorta shows the specific location of the *cre*-mediated recombination of floxed *Nf1* gene in the vascular adventitia of 3 month old, non-infused *Nf1<sup>flox/+</sup>;LysM<sup>cre</sup>* mice. Arrowhead indicates *cre*-mediated recombination (280bp band). *Nf1<sup>flox/+</sup>;SM22<sup>cre</sup>* VSMCs were used as positive control.

Figure 12

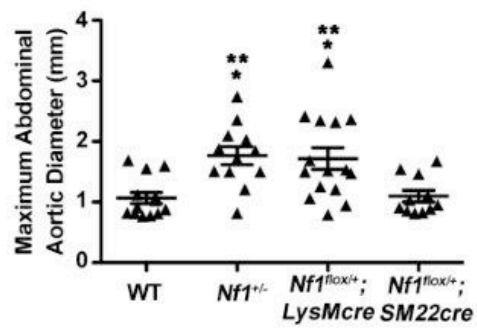
A



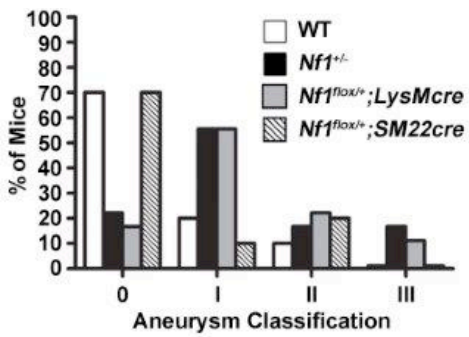
B



C



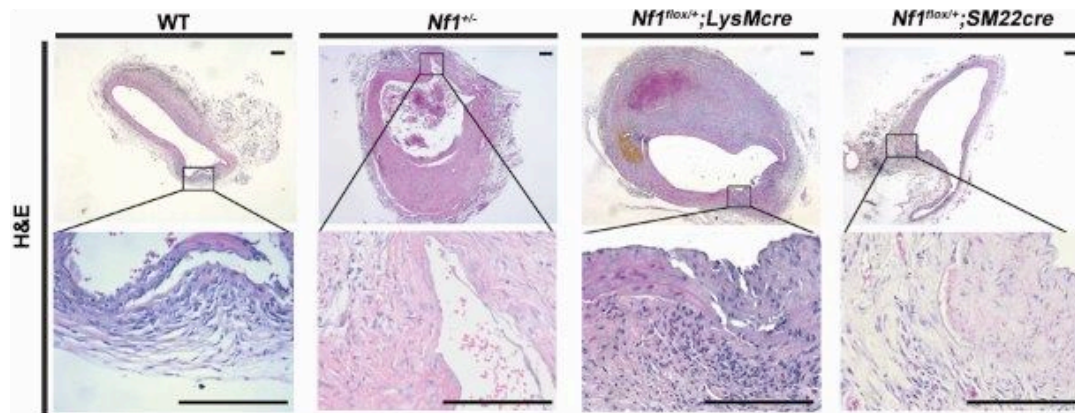
D



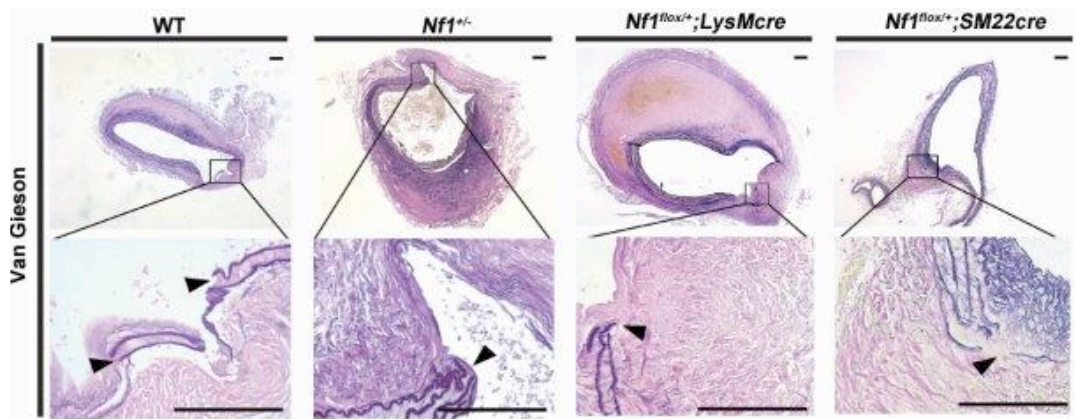
**Figure 12.** Heterozygous inactivation of *Nf1* in myeloid cells alone is sufficient to recapitulate *Nf1* abdominal aortic aneurysm formation. **(A)** Representative photographs of abdominal aortas from Ang II-infused WT, *Nf1*<sup>+/-</sup>, *Nf1*<sup>fl/+</sup>; *LysM*<sup>cre</sup> and *Nf1*<sup>fl/+</sup>; *SM22*<sup>cre</sup> mice. Scale bars: 1mm. Saline-infused WT, *Nf1*<sup>+/-</sup>, *Nf1*<sup>fl/+</sup>; *LysM*<sup>cre</sup> and *Nf1*<sup>fl/+</sup>; *SM22*<sup>cre</sup> mice did not form AAAs. **(B)** Quantification of AAA incidence. **(C)** Maximum abdominal aortic diameter of Ang II-infused WT, *Nf1*<sup>+/-</sup>, *Nf1*<sup>fl/+</sup>; *LysM*<sup>cre</sup> and *Nf1*<sup>fl/+</sup>; *SM22*<sup>cre</sup> mice. Clustering around 1mm represents animals without AAA formation. \**P*<0.05 for Ang II-infused WT (*n*=10) versus Ang II-infused *Nf1*<sup>+/-</sup> (*n*=9), and Ang II-infused WT versus *Nf1*<sup>fl/+</sup>; *LysM*<sup>cre</sup> (*n*=15). \*\**P*<0.05 for Ang II-infused *Nf1*<sup>fl/+</sup>; *SM22*<sup>cre</sup> (*n*=10) versus Ang II-infused *Nf1*<sup>+/-</sup>, and Ang II-infused *Nf1*<sup>fl/+</sup>; *SM22*<sup>cre</sup> versus Ang II-infused *Nf1*<sup>fl/+</sup>; *LysM*<sup>cre</sup>. Analysis by one-way ANOVA with Tukey's test. Error bars denote mean ± SEM. For **B** and **C**, no statistical significance was observed for Ang II-infused WT versus Ang II-infused *Nf1*<sup>fl/+</sup>; *SM22*<sup>cre</sup>, or Ang II-infused *Nf1*<sup>+/-</sup> versus Ang II-infused *Nf1*<sup>fl/+</sup>; *LysM*<sup>cre</sup>. **(D)** Severity index of AAAs for Ang II-infused WT (*n*=10), *Nf1*<sup>+/-</sup> (*n*=9), *Nf1*<sup>fl/+</sup>; *LysM*<sup>cre</sup> (*n*=15) and *Nf1*<sup>fl/+</sup>; *SM22*<sup>cre</sup> mice (*n*=10).

Figure 13

A



B



C

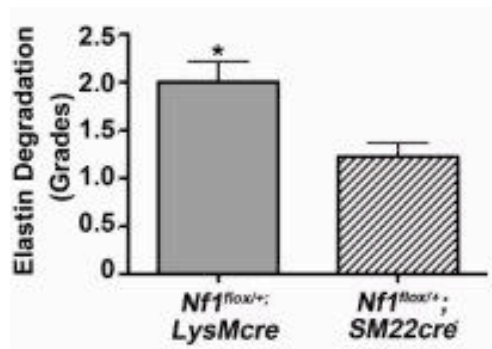
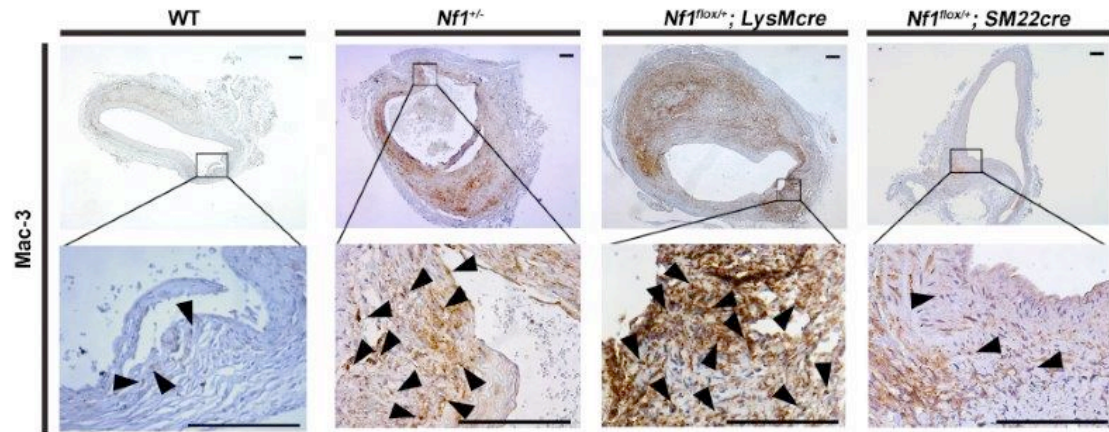


**Figure 13.** *Nf1<sup>fl/+</sup>;LysM<sup>cre</sup>* mice have enlarged and more severe abdominal aortic aneurysms similar to *Nf1<sup>+/-</sup>* mice. **(A)** Representative photomicrographs of abdominal aortic cross-sections from Ang II-infused WT, *Nf1<sup>+/-</sup>*, *Nf1<sup>fl/+</sup>;LysM<sup>cre</sup>* and *Nf1<sup>fl/+</sup>;SM22<sup>cre</sup>*, stained with H&E or **(B)** van Gieson for elastin. Boxes identify area that is magnified in lower panel. Arrowheads identify fragmentation of elastic lamina in van Gieson photomicrographs and yellow staining identifies ECM. Saline infusion did not produce AAAs in any genotype. Scale bars: 50µm. **(C)** Grading of elastic lamina degradation in Ang II-infused *Nf1<sup>fl/+</sup>;LysM<sup>cre</sup>* and *Nf1<sup>fllox/+</sup>;SM22<sup>cre</sup>* mice. \**P*<0.05 for *Nf1<sup>fl/+</sup>;LysM<sup>cre</sup>* (*n*=12) versus *Nf1<sup>fl/+</sup>;SM22<sup>cre</sup>* (*n*=9). No statistical significance in elastic lamina degradation grade was observed between *Nf1<sup>fl/+</sup>;LysM<sup>cre</sup>* and *Nf1<sup>+/-</sup>* mice or *Nf1<sup>fl/+</sup>;SM22<sup>cre</sup>* and WT mice.

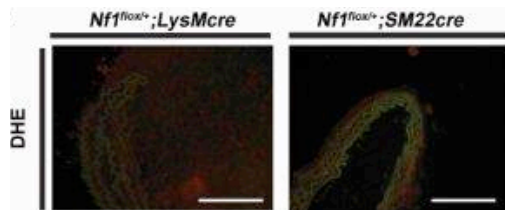


Figure 14

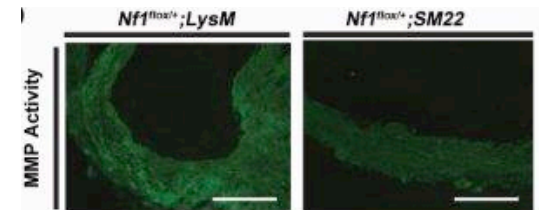
A



B



C



D

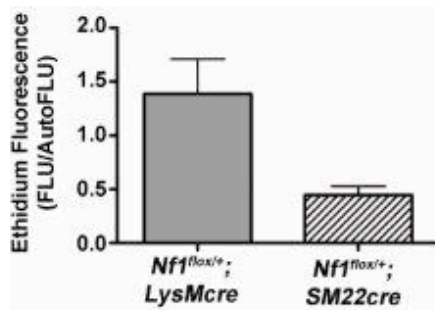


**Figure 14.** *Nf1<sup>fl/+</sup>;LysM<sup>cre</sup>* aneurysms contain increased macrophage infiltration, MMP activity and superoxide levels similar to *Nf1<sup>+/-</sup>* mice. **(A)** Representative photomicrographs of abdominal aortic cross-sections from Ang II infused WT, *Nf1<sup>+/-</sup>*, *Nf1<sup>fl/+</sup>;LysM<sup>cre</sup>*, and *Nf1<sup>fl/+</sup>;SM22<sup>cre</sup>* mice stained with anti-Mac-3 antibody for macrophages (brown cells, arrowheads). Black boxes specify area that is magnified in lower panel. Scale bars: 50  $\mu$ m. **(B)** Representative photomicrographs showing MMP activity in *Nf1<sup>fl/+</sup>;LysM<sup>cre</sup>* and *Nf1<sup>fl/+</sup>;SM22<sup>cre</sup>* mice. Scale bars: 50 $\mu$ m. **(C)** Representative photomicrographs of abdominal aortic cross-sections from Ang II-infused *Nf1<sup>fl/+</sup>;LysM<sup>cre</sup>* and *Nf1<sup>fl/+</sup>;SM22<sup>cre</sup>* mice, showing superoxide production identified by *in situ* DHE staining (red). Auto-fluorescence of murine tissue is visible (green). Scale bars: 50 $\mu$ m. **(D)** Bar graph depicts quantification of ethidium fluorescence.

## **DISCUSSION**

Cardiovascular disease is an important under recognized non-neoplastic manifestation in NF1 patients, which contributes significantly to debilitating morbidities and early mortality and encompasses a variety of pathologies (23). Many of these vascular pathologies, including aneurysm formation and arterial stenosis, are often clinically silent, making an accurate measure of both disease frequency and burden difficult to determine (33). Thus, an understanding of the initiation and progression of these vascular pathologies is critical to facilitate cardiovascular disease risk screening, early recognition, and intervention in NF1 patients.

A major limitation in understanding NF1 aneurysm disease has been the lack of an animal model that closely recapitulates the human disease. In the current study, two common murine models of aneurysmal disease were adapted to *Nf1* heterozygous mice, which provide novel approaches to examine the cellular and molecular mechanisms that regulate NF1 aneurysm formation. In both experimental models, histologic analysis of *Nf1*<sup>+/-</sup> aneurysms revealed increased macrophage infiltration, MMP-9 expression and activation, and ROS production, which are molecular and cellular signatures of aneurysm formation observed in other experimental animals independent of neurofibromin deficiency (56, 57, 108, 109). These observations suggest that vascular inflammation and macrophage secretory products are critical factors in NF1 aneurysmal disease consistent with aneurysm formation in other diseases with chronic inflammation

(56, 64, 109). This is an important observation since it has been previously demonstrated that NF1 patients without known cardiovascular disease have increased numbers of CD14<sup>dim</sup>CD16<sup>hi</sup> circulating pro-inflammatory monocytes and elevated levels of inflammatory cytokines including IL1 $\beta$  and IL-6 (22), which have been previously linked to vascular disease in non-NF1 subjects in large population studies (37).

To directly determine the contribution of neurofibromin-deficient myeloid cells to *Nf1*<sup>+/-</sup> aneurysm formation, lineage-restricted transgenic mice were utilized to specifically ablate a single *Nf1* allele in myeloid cells alone. Heterozygous inactivation of the *Nf1* gene in myeloid cells alone was sufficient to reproduce the aneurysm phenotype observed in *Nf1*<sup>+/-</sup> mice. Importantly, despite significant expansion of *Nf1*<sup>+/-</sup> VSMCs in arterial walls, aneurysm frequency and severity in transgenic mice harboring a single *Nf1* allele in VSMCs were similar to WT controls. Collectively, this genetic study directly implicates neurofibromin-deficient myeloid cells as the critical cellular effectors of aneurysm formation in *Nf1*<sup>+/-</sup> mice.

Neurofibromin negatively regulates the Ras signaling cascade in multiple mammalian cell types by accelerating the conversion of active Ras-GTP to its inactive GDP confirmation (5). Loss of this function in *Nf1* heterozygous cells and subsequent augmentation of Ras signaling and activation of its downstream effectors including the Ras-Mek-Erk and Ras-PI-3K pathways, render cells hypersensitive to a number of growth factors contributing to the variety and the complexity of disease manifestations observed in NF1 patients (12, 22, 34, 101,

110-112). Interestingly, myeloid cells and their progenitor cells are particularly sensitive to Ras activation and demonstrate multiple gain-of-function phenotypes contributing to myelo-proliferative disease, plexiform neurofibroma formation, bone disease, and vasocclusive disease in various animal models of NF1 disease (22, 34, 111-114). Relevant to the current study, myeloid cells secrete growth factors and cytokines that are well established mediators of cardiovascular disease including atherosclerosis (115), vessel occlusion (34), and aneurysm formation (116). In view of our recent report that neurofibromin-deficient myeloid cells are the primary mediators of *Nf1*<sup>+/-</sup> arterial stenosis (34), the observation that *Nf1*<sup>+/-</sup> mice develop more frequent and severe aneurysms mediated via heterozygous inactivation of *Nf1* in myeloid cells alone highlights the global pathogenic consequences of neurofibromin-deficient myeloid cells to diverse NF1 clinical manifestations, including cardiovascular disease.

Myeloid cell recruitment and infiltration of the vessel wall to initiate elastic lamina degradation are essential steps in the pathogenesis of aneurysm formation (56). Ang II facilitates aneurysm formation via activation of VSCMs and monocytes, which secrete cytokines and chemotactic factors leading to enhanced production of MMPs, resulting in vascular inflammation and vessel wall remodeling (63, 117). Though several molecular ligand-receptor signaling cascades contribute to the progression of aneurysmal disease, pharmacologic inhibition or genetic disruption of monocyte chemotactic protein-1 (MCP-1) binding to its primary receptor, CCR2, significantly reduces aneurysm formation (117-119). This signaling axis is particularly interesting since pro-inflammatory

monocytes co-express high cell surface levels of the CCR2 receptor (120, 121). Therefore, increased CD14<sup>dim</sup>CD16<sup>hi</sup> pro-inflammatory monocytes found within NF1 patients may be an important factor leading to the increased incidence of CVD and aneurysm formation. Whether *Nf1*<sup>+/-</sup> macrophages are mobilized from the bone marrow, to the blood and into the vascular wall or proliferate locally within the wall of the aorta from the recently described common myeloid progenitor remains to be elucidated (117, 122).

Another striking observation in this study is the increased production of ROS and MMPs in *Nf1*<sup>+/-</sup> vessel walls and developing aneurysms. Production of ROS and MMPs by various cell types is known to be critical for aneurysm formation in several model systems. Genetic or pharmacologic disruption of MMP-2 and MMP-9 in mice decreases aneurysm formation (58, 123). These findings suggest that MMPs, released by resident and infiltrating vascular wall cells, are key molecular events in aneurysm formation. Given these observations, our current study suggests that increased levels of MMP-9 observed in *Nf1* heterozygous aneurysms may play a significant role in NF1 aneurysm progression, warranting further investigation to examine whether genetic modification and pharmacologic inhibition of MMP-9 activity alone can inhibit aneurysm initiation and progression in our *Nf1* experimental system.

Increased ROS levels are also detected in various human and murine cardiovascular lesions including aneurysms (61, 94). Moreover, evidence suggests that ROS overproduction facilitates MMP activation and contributes to vascular inflammation and vessel wall remodeling (124). Loss of neurofibromin

has been shown to directly stimulate the adenylyl cyclase/cyclic AMP pathway amplifying mitochondrial ROS production in *Drosophila melanogaster*, independent of the Ras/Raf pathway (125). Conversely, constitutively active Ras mutations dramatically increase ROS production in mammalian hematopoietic progenitor cells via NADPH oxidase (NOX2) activation without increasing mitochondrial ROS (126). Although these studies differ in regards to the source of ROS production due to neurofibromin deficiency, increased ROS from either source has the ability to activate MMPs in the vascular wall potentially leading to aneurysm formation. These prior experimental observations highlight the need to unravel the potentially complicated redox state within neurofibromin-deficient cells, which could trigger oxidant stress in various tissues including the vessel wall.

Previous studies have also identified increased expression of ROS producing-NOX subunits p22<sup>phox</sup> and p47<sup>phox</sup> within aortic aneurysms of non-NF1 patients and mice (61, 127). Genetic disruption of p47<sup>phox</sup> significantly diminishes oxidative stress and subsequent aneurysm formation in mice infused with Ang II (64). These data suggest a role of NOX proteins as producers of ROS in aneurysm pathogenesis, indicating potential sources for the observed *Nf1*<sup>+/-</sup> production of ROS. Further, these studies also provide rationale for transgenic murine studies using cell specific deletion of p47<sup>phox</sup> and gp91<sup>phox</sup> within endothelial cells, VSMCs and/or monocytes/macrophages in *Nf1*<sup>+/-</sup> mice to test whether specific NOX isoform(s) contribute to ROS overproduction and subsequent aneurysm development.

Together, the current study establishes the first animal models of NF1 aneurysm disease and identifies myeloid cells as the critical cellular effectors. Given the utility of these *Nf1* aneurysm models, additional studies will refine the biochemical triggers for NF1 vascular disease using genetic and pharmacologic approaches. These insights could provide the pre-clinical data for future human studies in NF1 patients to identify early cardiovascular disease and potential therapeutic strategies for prevention and treatment of vascular disease.



## **CHAPTER TWO**

IDENTIFICATION OF EXCESSIVE INFLAMMATION AND OXIDATIVE STRESS  
AS CRITICAL BIOCHEMICAL PROCESSES LEADING TO *NF1*<sup>+/-</sup> ANEURYSM  
FORMATION

## **INTRODUCTION**

### **Cardiovascular Disease and Oxidative Stress.**

Reactive oxygen species (ROS), including superoxide, hydrogen peroxide, peroxide, hydroxyl radical and hydroxyl ion, play an important role as signaling molecules intracellularly and intercellularly in response to growth factors and chemical stimulation (128-130). ROS can rapidly react and oxidize lipids and proteins resulting in chemical and structural modification which under appropriate redox regulation can lead to proper signal transduction (131). However, when the redox state is not properly regulated oxidation of lipids, proteins and DNA can occur in a detrimental manner and has been implicated in many diseases processes including cardiovascular disease (132), neurodegeneration (133), diabetes (134) and aging (135). The production of ROS results primarily from professional oxidases, such as those in the NADPH oxidase (NOX) family, and as a byproduct of inefficient aerobic metabolism by mitochondria (136).

The NOX family of professional oxidases includes NOX1, NOX2, NOX3, NOX4, NOX5, dual oxidase-1 (DUOX1) and DUOX2. While the NOX proteins produce superoxide, the DUOX proteins may use superoxide generated by NOX proteins to produce hydrogen peroxide (137, 138). NOX2 is the most thoroughly studied enzyme of the NOX family and is found in phagocytic cells producing superoxide, which is expelled during the oxidative burst as part of innate immunity (139). The superoxide-producing active complex of NOX2 is made up of 6 subunits including gp91phox and p22phox (flavocytochrome b<sub>558</sub>) which are

located in the plasma membrane, as well as 4 regulatory subunits that reside in the cytoplasm while inactive including p40phox, p47phox, p67phox, and Rac (140). Of note, chronic granulomatous disease (CGD) patients are characterized by the absence of the p91phox component of NOX2, resulting in the inability to clear bacteria and debris. Additionally, CGD patients develop granulomas due to a defect in the potent oxidative burst resulting in granuloma formation, indicating the physiological importance of this complex (141).

Regulation of NOX2 is multidimensional in both cellular location and signal transduction. Inactive flavocytochrome  $b_{558}$  is stored within intracellular granules while p40phox, p47phox and p67phox make up an inactive dephosphorylated complex within the cytoplasm (142, 143). Inactive Rac is GDP-bound and complexed with Rho-GDI (144). Upon stimulation, granules containing flavocytochrome  $b_{558}$  fuse to phagosomes and interact with the phosphorylated p47phox, p40phox, p67phox complex and active GTP-bound Rac forming the active oxidase (145). Phosphorylation has been shown to be dependent on Ras-Mek-Erk signaling pathway indicating a potential role in NF1 for inappropriate activation of NOX2 (146). Phosphatidylinositol-3,4,5-triphosphate which is generated by PI-3K, also under control of neurofibromin, is required to bind with p40phox to allow for association of the phosphorylated p40phox, p47phox and p67phox complex with the plasma membrane and flavocytochrome  $b_{558}$  (147). Finally, Rac activation has also been shown to be important in cross-talk between the Ras-Mek-ERK pathway and the PI-3K pathway further linking neurofibromin regulated pathways and NOX2 activation (148).

Although many members of the NOX family are currently being investigated for their role in CVD, the main focus has been on the role of NOX2 due to its ability to produce the largest amount of superoxide in a short time, as well as its expression in phagocytes, which are commonly found associated with and implicated in cardiovascular lesion formation. Immunohistochemical studies have identified increased expression of p22phox and p47phox within aortic aneurysms of non-NF1 patients and mice (61, 127). Additionally, *in vivo* studies of p47phox-deficient mice implicate p47phox as a critical mediator of aneurysm formation (64). These findings underscore the importance of the NOX2 subunits, in the development of aneurysmal tissue and also show that inhibition may be a viable therapeutic target.

Mitochondrial superoxide formation via aerobic respiration may also be an important contributor to CVD (149). Mitochondria produce ATP via a proton gradient established through oxidative phosphorylation by transferring electrons from NADH or FADH<sub>2</sub> to oxygen, producing water (150). In normal conditions 1 to 2% of electrons form superoxide rather than water and are quickly dismutated to hydrogen peroxide by superoxide dismutase. If the electron transport chain becomes uncoupled, a large amount of superoxide can be released into the cytoplasm, leading to intracellular, intercellular and extracellular damage of lipids, protein, and DNA. Regulation of mitochondrial respiration, and therefore ROS release, has been shown to be mediated via the adenylyl cyclase/cyclic AMP/protein kinase A pathway. Decreases in neurofibromin lead to a reduction in protein kinase A and decreased mitochondrial respiration and greater ROS

production. The converse was also true when Nf1 was overexpressed in *Drosophila* or cyclic AMP was supplemented; efficient mitochondrial respiration was increased and ROS was decreased leading to a protective oxidative state and increased lifespan (125).

Overall, oxidative stress displays a causal relationship in cardiovascular disease and in affected individuals in the general population. Studies presented above indicate that NF1 patients may have increased oxidative burden compared to the general population, resulting in the earlier onset and increased severity of CVD. Mechanisms leading to the oxidative burden may be complexed and from multiple cellular sources warranting further investigation to identify therapeutic targets.

### **HMG-CoA Reductase inhibitors and Cardiovascular Disease.**

HMG-CoA Reductase inhibitors, or statins, were originally developed as a potential cancer treatment to attenuate oncogenic Ras activity by reducing isoprenoid synthesis, an intermediate in cholesterol synthesis, that is necessary for proteins to interact with the plasma membrane (151). Statins have a long history of being used to reduce cholesterol levels and therefore reduce the risk of coronary artery disease (CAD) in patients (152). It was believed that the cholesterol lowering affect of statins was the mechanism of reduced CAD in patients on statins. More recently, large clinical studies have noted that subjects receiving statins have a greater protection from CAD than placebo subjects with

similar cholesterol levels, indicating a mechanism independent of cholesterol reduction (153).

Several hypotheses exist explaining the mechanisms of the observed pleiotropic effects of statins, which seem to work in concert to provide cardiovascular protection. It is hypothesized that of HMG-CoA reductase inhibition reduces the amount of lipid intermediates in the cholesterol synthesis pathway, including geranyl pyrophosphate, farnesyl pyrophosphate and isopentenyl pyrophosphate(151). Many proteins rely on post-translational modification and attachment of these lipids to enable trafficking and membrane binding within the cell. Importantly, Ras and Ras-like proteins, including Rho and Rac, are heavily dependent on post-translational prenylation for proper functioning (151, 154). Reduction in Ras and Rac activity could lead to reduced NOX2 activation and explain the antioxidant affects of statins (155). In addition to cholesterol and possible ROS reductions, statins have multiple potential effects on vascular endothelium. Hypercholesterolemia impairs nitric oxide synthesis and release, both critical functions to multiple components of atherosclerosis (156-158). Importantly, decreased nitric oxide synthesis allows for vasoconstriction, clot formation, VSMC proliferation and leukocyte recruitment, all hallmarks of both atherosclerosis and aneurysm formation (159). Statins have been shown to directly upregulate endothelial nitric oxide synthase leading to proper functioning of the endothelium, even before cholesterol levels have been reduced (160, 161). Overall, HMG-CoA reductase inhibition has beneficial effects in maintaining vessel wall homeostasis and reducing CVD.

## **Apocynin and Cardiovascular Disease.**

Oxidative stress is a known component of many forms of cardiovascular disease. Antioxidant therapy has shown encouraging potential in various murine models of cardiovascular disease but has translated poorly to the clinic (155). Apocynin (4-hydroxy-3-methoxy-acetophenone), a plant extract, has been shown to function as a potent antioxidant (162). Apocynin is a monomer that is thought to be a general antioxidant in this natural form; however, in cells which express myeloperoxidase apocynin can be dimerized or trimerized, both of which display the specific ability to block the association of p47phox with gp91phox thereby inhibiting superoxide formation by NOX2 (163). Myeloperoxidase is expressed in many hematopoietic cell types including macrophages, monocytes and neutrophils (164, 165). Importantly, myeloperoxidase is not expressed in VSMCs or endothelial cells indicating the majority of benefit seen in studies utilizing apocynin were largely from NOX2 inhibition in myeloid cells (166).

Apocynin has shown efficacy in the treatment of CVD in multiple animal models. In a rat model of hypertension, apocynin attenuated vascular wall superoxide formation, eliminating hypertension by allowing nitric oxide to diffuse freely, restoring normal VSMC relaxation (167, 168). Apocynin has also been found to reduce atherosclerotic progression in hypercholesterolemic mice, indicating the importance of ROS in those disease processes while highlighting the ability of apocynin to inhibit multiple types of CVD. Although apocynin has shown impressive efficacy in mouse models of CVD, no clinical trials have evaluated its use in human CVD. Currently, only one human clinical trial has

been completed, which investigated inhaled apocynin in mild asthmatics. The study observed no adverse effects of apocynin administration, as well as a reduction of hydrogen peroxide, nitrate and nitrite in exhaled breath condensate up to 2 hours after nebulization (169). By suggesting that apocynin is well tolerated in humans and can lead to a reduction in ROS, this trial provides a strong case for further investigation into potential uses for apocynin and future clinical trials.



## **MATERIALS AND METHODS**

### **Patient Recruitment.**

NF1 patients were recruited by the Indiana University NF1 Clinic at Riley Hospital for Children. All patients received a physical examination and a medical history was taken to confirm the diagnosis of NF1 according to the NIH clinical criteria (14, 15). Patients with a history of cancer, on anti-cancer drugs or pregnant were excluded from the study. All patients gave informed consent prior to participation in the study.

### **Comet assay.**

Blood samples were collected from NF1 patients ( $37.6 \pm 9.7$  years) and sex and age-matched controls ( $40.2 \pm 8.1$  years) into EDTA vacutainer tubes (BD Biosciences). Mononuclear cells from approximately 16mLs of blood were isolated by centrifugation using Ficoll-Paque Plus (GE Healthcare) (170). Mononuclear cells were assayed for oxidative DNA damage as previously described, with modification (171). Following cellular lysis, slides were treated Formamidopyrimidine DNA glycosylase (FPG) which recognized and removed oxidized purines, causing a DNA break (172).

### **Simvastatin administration.**

When indicated, simvastatin (Besse, OH) was administered as a suspension in water at 1 mg/kg/day via oral gavage beginning 7 days prior to

Ang II or saline infusion and continued throughout the course of experimentation. Water was administered via oral gavage to control mice in an equivalent volume as simvastatin.

**Apocynin administration.**

When indicated, Apocynin (also known as acetovanillone, 100mg/kg/day, Arcos Organics) was administered in drinking water beginning 7 days prior to Ang II or saline infusion and continued throughout the course of experimentation. Control mice received water at a similar volume.

## **RESULTS**

### **NF1 patients have evidence of oxidative stress in white blood cells.**

NF1 patients without known cardiovascular disease have evidence of chronic vascular inflammation as evidenced by increased circulating pro-inflammatory monocytes (22). Other disease processes characterized as having chronic vascular inflammation, such as diabetes, have been linked to increase oxidative stress (173). Therefore, we sought to investigate markers of oxidative stress in white blood cell samples from NF1 patients using the comet assay to analyze DNA damage. Briefly, cells are dispersed into individual cells and embedded in agarose on a microscope slide and lysed. Formamidopyrimidine DNA glycosylase (FPG) was added to cleave any oxidized DNA bases. Upon electrophoresis large DNA strands will not be able to move through the agar while smaller DNA pieces, caused by FPG cleavage, will migrate forming a comet tail-like appearance which can be quantified to assess oxidative DNA damage (172). NF1 patients displayed nearly a 2-fold increase in the amount of oxidative DNA damage as compared to control patients (Figure 15). This data indicates that circulating white blood cells are overproducing ROS even before differentiating to macrophages during extravasation into the vessel wall. Additionally, this data supports our previous hypothesis that myeloid cells are predominant producer of ROS in the vessel wall.

**Figure 15**

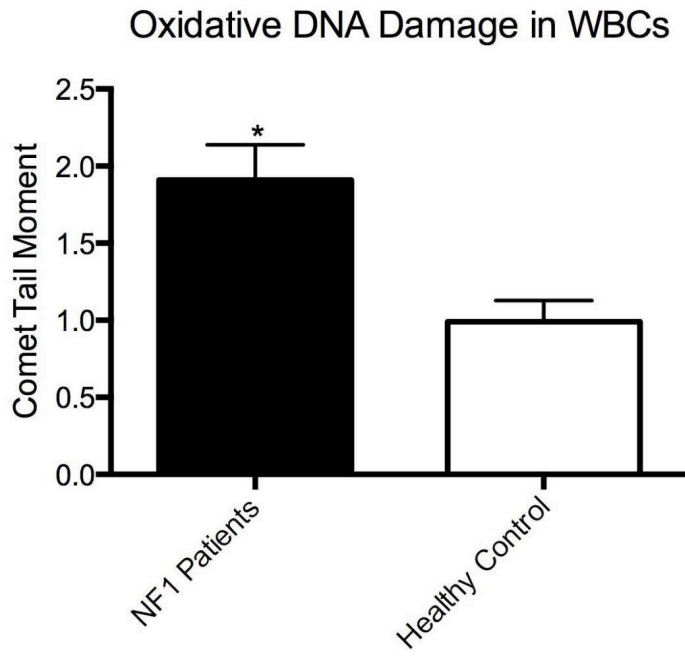


**Figure 15.** NF1 patients have increased DNA damage.

Quantification of mean comet tail moment in white blood cells from NF1 and control patients. \* $P < 0.05$  for NF1 ( $n=10$ ) versus control ( $n=28$ ).

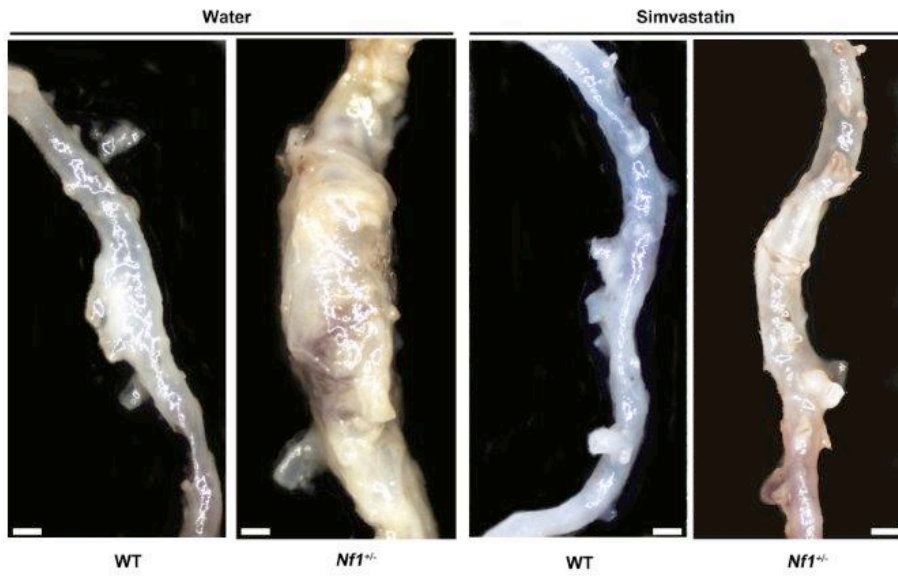
### **Simvastatin attenuates Ang II-induced AAA formation in *Nf1*<sup>+/-</sup> mice.**

HMG-CoA reductase inhibitors are clinically efficacious in the prevention of several manifestations of CVD, including aneurysm formation (174), which is in part attributable to their anti-inflammatory and antioxidant properties (175). Recent studies revealed that daily statin therapy significantly reduces arterial stenosis in *Nf1*<sup>+/-</sup> mice in part by inhibiting macrophage functions central to disease progression (34). Therefore, we tested whether simvastatin would reduce *Nf1*<sup>+/-</sup> aneurysm formation given our genetic data implicating the essential function of macrophages in both the initiation and progression of aneurysmal disease as well as previous findings of chronic inflammation and oxidative stress. WT and *Nf1*<sup>+/-</sup> mice were treated with daily low-dose simvastatin (1 mg/kg/day) or water for 7 days prior to initiation of Ang II infusion and continued for 35 days. Low-dose simvastatin reduced AAAs in Ang II-infused *Nf1*<sup>+/-</sup> mice by greater than 2-fold compared to water-treated controls (Figure 16A, 16B and 17A) without affecting blood pressure or serum cholesterol levels. Corresponding decreases in aortic diameter and severity in Ang II-infused *Nf1*<sup>+/-</sup> mice were also observed (Figure 16C and 16D). There was no significant difference in AAA incidence, maximum aortic diameter, or severity in Ang II-infused WT mice in either treatment group (Figure 16A through 16D). However, simvastatin treatment reduced arterial remodeling, macrophage infiltration (Figure 17A through 17C) MMP-9 expression and activation, and ROS production (Figure 18A through 18D) in arterial cross-sections from *Nf1*<sup>+/-</sup> mice when compared to water treatment. These results demonstrate that simvastatin prevents Ang II-induced

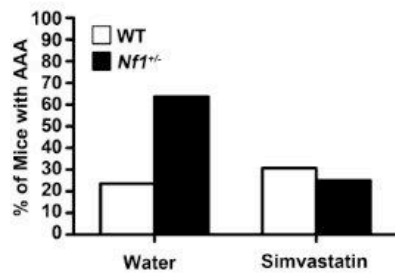
AAA formation in *Nf1*<sup>+/-</sup> mice, providing a potential therapeutic for NF1 aneurysmal disease.

Figure 16

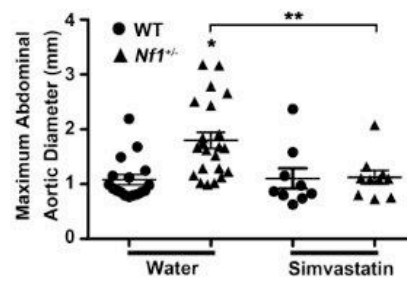
A



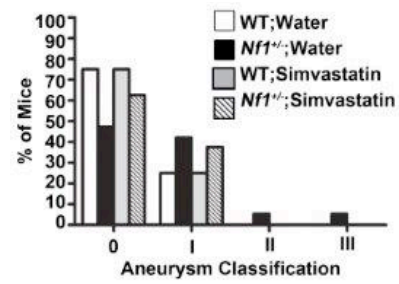
B



C



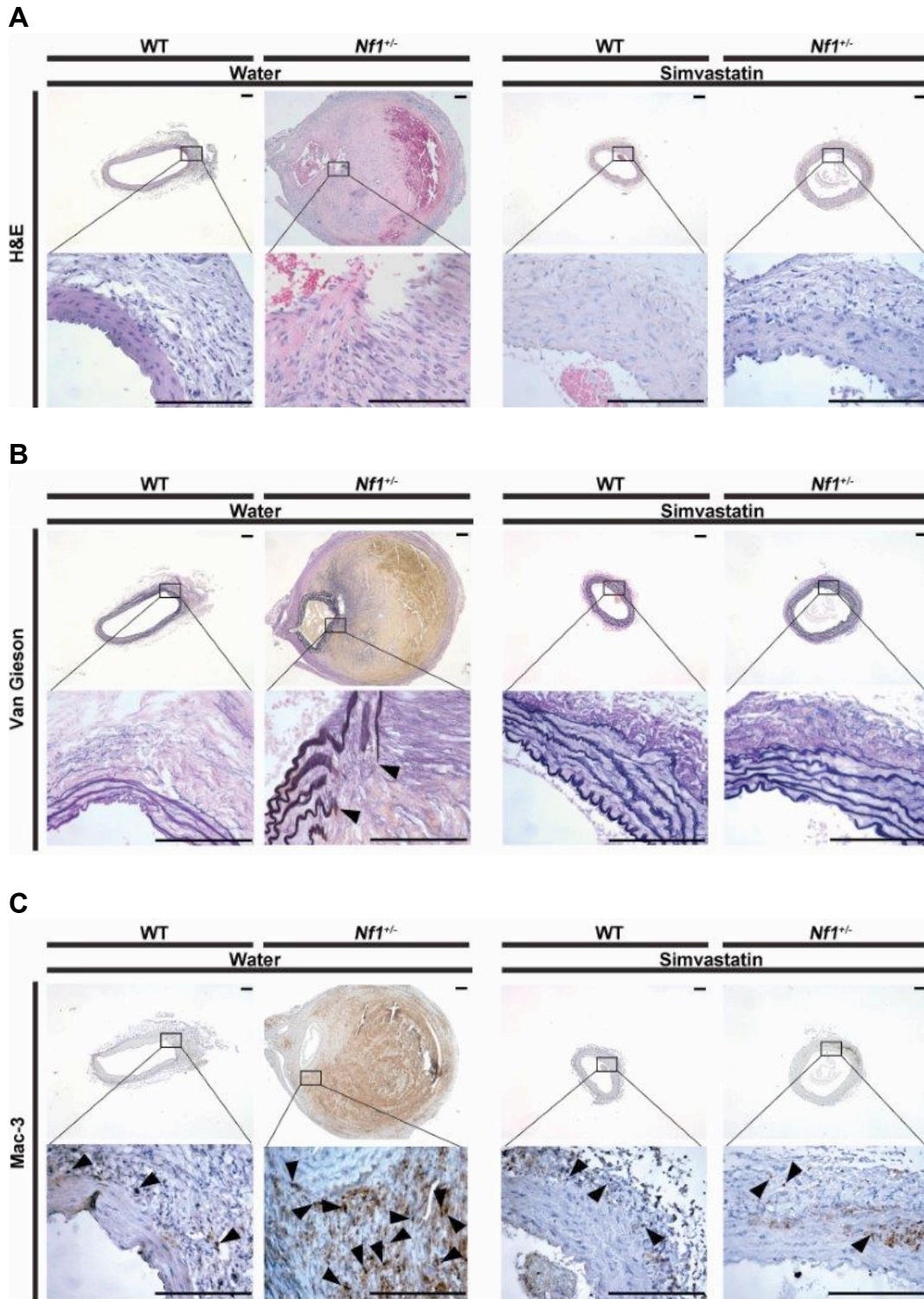
D





**Figure 16.** Simvastatin reduces Ang II-induced *Nf1*<sup>+/-</sup> abdominal aortic aneurysms. **(A)** Representative photographs of abdominal aortas from water or simvastatin-treated, Ang II-infused WT and *Nf1*<sup>+/-</sup> mice. Scale bars: 1mm. **(B)** Quantification of aneurysm incidence in water or simvastatin-treated, Ang II-infused mice. **(C)** Maximum abdominal aortic diameter of water or simvastatin-treated, Ang II-infused WT and *Nf1*<sup>+/-</sup> mice. Clustering around 1mm represents animals without aneurysm formation. \**P*<0.05 for water-treated WT (*n*=17) versus water-treated *Nf1*<sup>+/-</sup> (*n*=22). \*\**P*<0.05 for water-treated *Nf1*<sup>+/-</sup> versus simvastatin-treated *Nf1*<sup>+/-</sup> (*n*=10). Analysis by one-way ANOVA with Tukey's test. Error bars denote the mean ± S.E.M. For **C**, no statistical significance was observed for water-treated WT versus simvastatin-treated WT (*n*=13). **(D)** Severity index of AAAs of Ang II-infused WT and *Nf1*<sup>+/-</sup> mice treated with water (WT, *n*=17; *Nf1*<sup>+/-</sup>, *n*=22) or simvastatin (WT, *n*=9; *Nf1*<sup>+/-</sup>, *n*=10). For **B-D**, saline-infused WT or *Nf1*<sup>+/-</sup> mice in either treatment group did not form aneurysms.

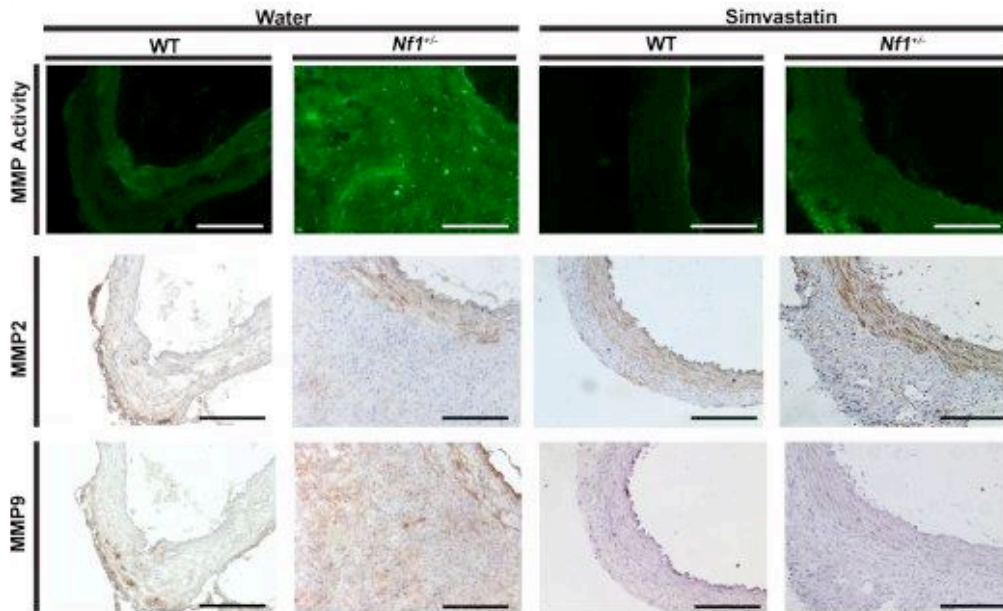
Figure 17



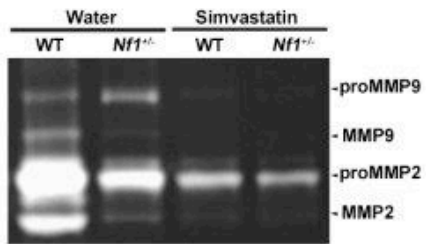
**Figure 17.** Simvastatin reduces Ang II-induced *Nf1*<sup>+/-</sup> abdominal aortic aneurysms and macrophage infiltration. Representative photomicrographs of abdominal aortic cross-sections from water or simvastatin-treated, Ang II-infused WT and *Nf1*<sup>+/-</sup> mice stained with (A) H&E, (B) van Gieson for elastin or (C) anti-Mac-3 (arrowheads). Boxes specify area magnified in lower panel. Saline-infused WT and *Nf1*<sup>+/-</sup> mice treated with water or simvastatin did not produce aneurysms. In A, arrowheads identify fragmentation of elastic lamina and yellow staining identifies ECM. Scale bars: 50µm.

Figure 18

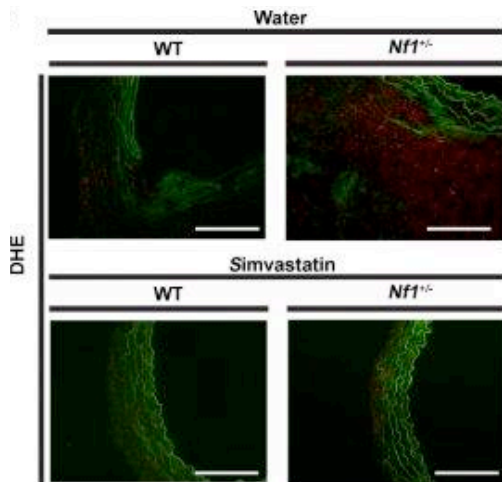
A



B



C



D

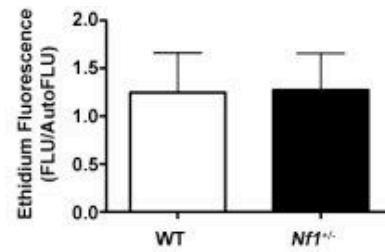


**Figure 18.** Simvastatin attenuates Ang II-induced *Nf1*<sup>+/-</sup> MMP expression and activation and superoxide production. **(A)** Representative photomicrographs of abdominal aortic cross-sections from water or simvastatin treated, Ang II-infused WT and *Nf1*<sup>+/-</sup> mice. MMP activity (green) was visualized by *in situ* zymography and expression of MMP-2 and MMP-9 was detected by IHC staining with anti-MMP-2 (brown) and anti-MMP-9 antibodies (brown). Scale bars, 50µm. **(B)** Representative zymogram showing abdominal aortic MMP-2 and MMP-9 levels from water or simvastatin treated, Ang II-infused WT and *Nf1*<sup>+/-</sup> mice. **(C)** Representative photomicrographs of abdominal aortic cross-sections from water or simvastatin treated, Ang II-infused WT and *Nf1*<sup>+/-</sup> mice showing ROS identified by *in situ* DHE staining (red). Auto fluorescence of murine tissue is visible (green). **(D)** Quantification of ethidium fluorescence for simvastatin-treated, Ang II-infused WT and *Nf1*<sup>+/-</sup>.

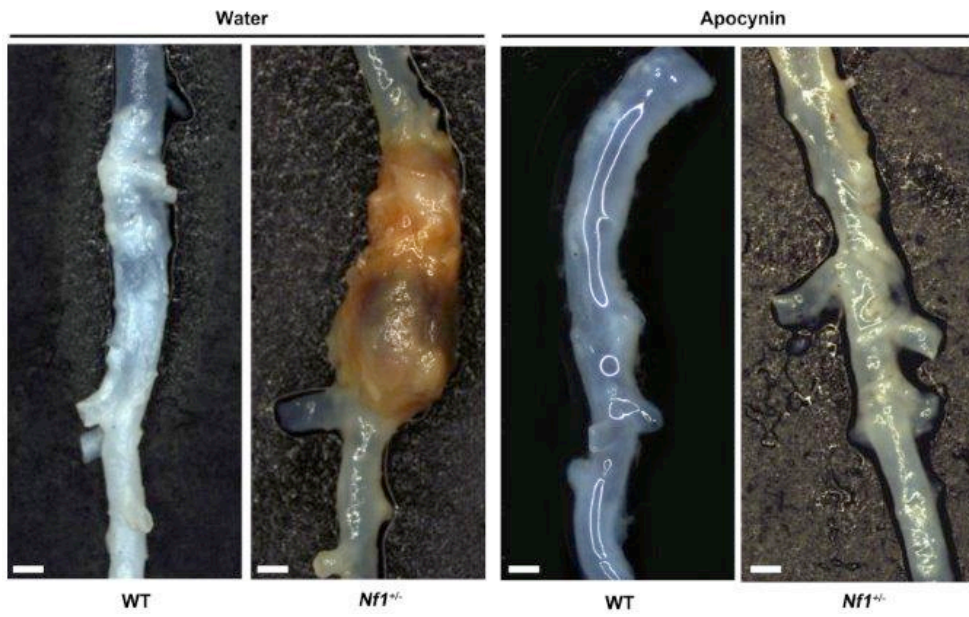
### **Apocynin attenuates Ang II-induced AAA formation in *Nf1*<sup>+/-</sup> mice.**

Increased production of ROS has been demonstrated in several animal models of CVD and antioxidant therapy has shown some utility in reversing many of these processes (65). Based on our observation that NF1 patients have increased oxidative DNA damage and that *Nf1*<sup>+/-</sup> aortas have evidence of increased ROS in response to Ang II infusion, we sought to explore the ability of antioxidant therapy, using apocynin, in attenuating *Nf1*<sup>+/-</sup> aneurysm formation. Though generally recognized as a non-specific antioxidant, recent evidence suggests that apocynin may inhibit superoxide production in cells containing myeloperoxidase, including macrophages and monocytes (166, 176).

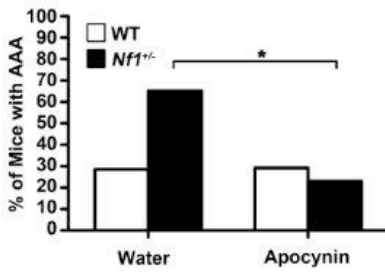
WT and *Nf1*<sup>+/-</sup> mice were treated with apocynin for 7 days prior to initiation of Ang II infusion and continued for 35 days thereafter. Apocynin reduced AAAs in Ang II-infused *Nf1*<sup>+/-</sup> mice by greater than 2-fold compared to water-treated controls, while apocynin did not have a significant effect on WT mice (Figure 19A and 19B). Additionally, decreases in both maximum abdominal aortic diameter and aneurysm severity were also noted in apocynin-treated *Nf1*<sup>+/-</sup> mice while apocynin-treated WT mice did not display a difference in either parameter (Figure 19C and 19D). Remodeling of the arterial wall, macrophage infiltration and ROS production was significantly reduced in apocynin-treated *Nf1*<sup>+/-</sup> mice when compared to water-treated controls (Figure 20 and 21). These results identify overproduction of ROS as a significant contributor to *Nf1*<sup>+/-</sup> aneurysm formation and provide evidence that antioxidants may be a viable therapeutic option.

Figure 19

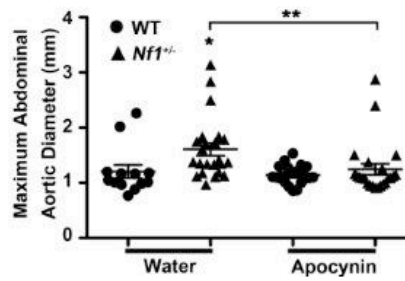
A



B



C



D

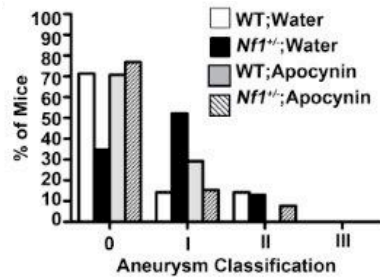
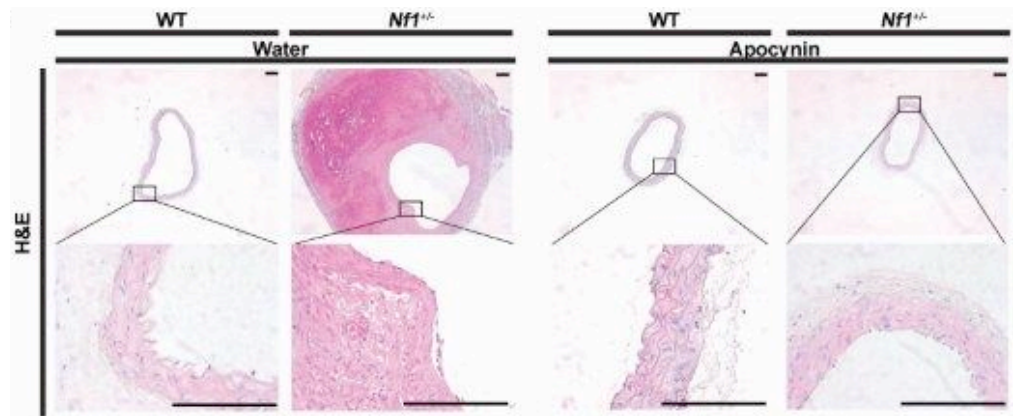


**Figure 19.** Apocynin reduces Ang II-induced *Nf1*<sup>+/-</sup> abdominal aortic aneurysms. **(A)** Representative photographs of abdominal aortas from water or apocynin-treated, Ang II-infused WT and *Nf1*<sup>+/-</sup> mice. Scale bars: 1mm. **(B)** Quantification of aneurysm incidence in water or apocynin-treated, Ang II-infused mice. \**P*<0.0083 for water-treated *Nf1*<sup>+/-</sup> (*n*=23) versus apocynin-treated *Nf1*<sup>+/-</sup> (*n*=26). Analysis by Fisher's exact test with Bonferroni Correction. **(C)** Maximum abdominal aortic diameter of water or apocynin-treated, Ang II-infused WT and *Nf1*<sup>+/-</sup> mice. Clustering around 1mm represents animals without aneurysm formation. \**P*<0.05 for water-treated WT (*n*=14) versus water-treated *Nf1*<sup>+/-</sup> (*n*=23). \*\**P*<0.05 for water-treated *Nf1*<sup>+/-</sup> versus apocynin-treated *Nf1*<sup>+/-</sup> (*n*=26). Analysis by one-way ANOVA with Tukey's post hoc test. Error bars denote the mean ± S.E.M. For **B** and **C**, no statistical significance was observed for water-treated WT versus apocynin-treated WT (*n*=24). **(D)** Severity index of AAAs of Ang II-infused WT and *Nf1*<sup>+/-</sup> mice treated with water (WT, *n*=14; *Nf1*<sup>+/-</sup>, *n*=23) or apocynin (WT, *n*=24; *Nf1*<sup>+/-</sup>, *n*=26). For **B-D**, saline-infused WT or *Nf1*<sup>+/-</sup> mice in either treatment group did not form aneurysms.

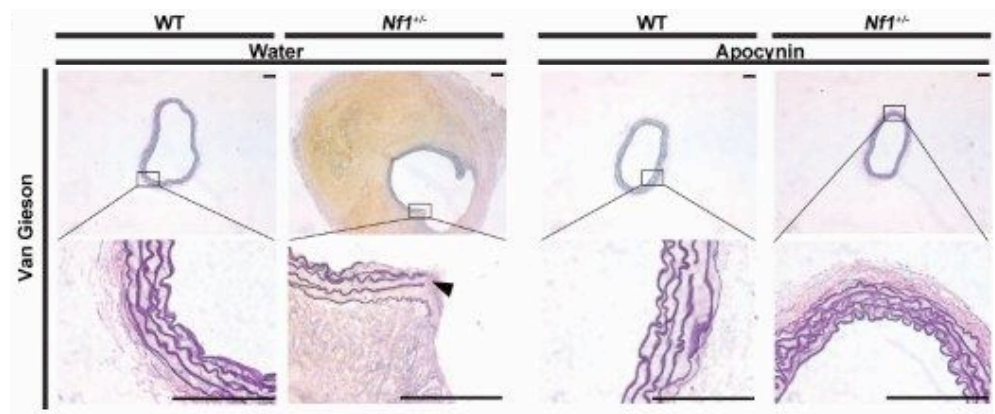


Figure 20

A



B



C

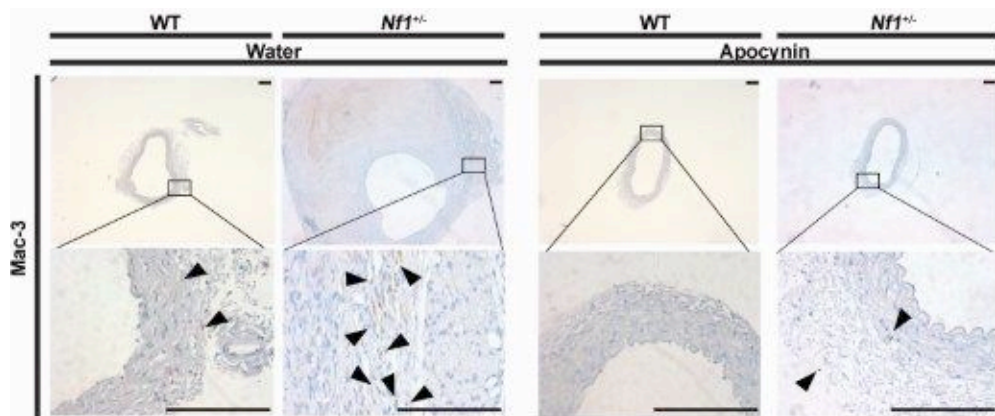
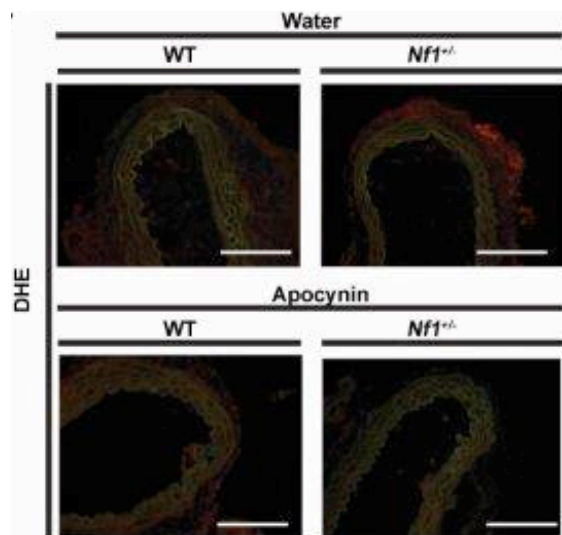


**Figure 20.** Apocynin prevents Ang II-induced AAA formation in *Nf1*<sup>+/-</sup> mice.

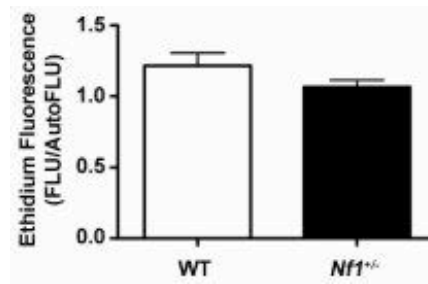
(A) Representative photomicrographs of abdominal aortic cross-sections from water or apocynin-treated, Ang II-infused WT and *Nf1*<sup>+/-</sup> mice stained with H&E, (B) van Gieson for elastin or (C) anti-Mac-3 (arrowheads). Boxes specify area magnified in lower panel. Saline-infused WT and *Nf1*<sup>+/-</sup> mice treated with water or apocynin did not produce aneurysms. In B, arrowhead identifies fragmentation of elastic lamina and yellow staining identifies ECM. Scale bars: 50µm.

Figure 21

A



B



**Figure 21.** Apocynin reduces Ang II-induced superoxide formation in *Nf1*<sup>+/-</sup> mice.

**(A)** Representative photomicrographs of abdominal aortic cross-sections from water or apocynin treated, Ang II-infused WT and *Nf1*<sup>+/-</sup> mice showing ROS identified by *in situ* DHE staining (red). Auto-fluorescence of murine tissue is visible (green). **(B)** Quantification of ethidium fluorescence for apocynin-treated, Ang II-infused WT and *Nf1*<sup>+/-</sup>.

## DISCUSSION

Cardiovascular disease, and specifically aneurysm formation, has hallmark pathologic features including macrophage infiltration and oxidative stress. NF1 patients and *Nf1* heterozygous mice display evidence of chronic vascular inflammation characterized by an increase in circulating pro-inflammatory monocytes (20, 22). *Nf1* heterozygous mice displayed larger and more severe aneurysms compared to WT; however, overall comparisons between the aneurysms showed similar features of macrophage infiltration, elastic lamina degradation, MMP activity and superoxide formation. It is therefore likely that *Nf1*<sup>+/-</sup> aneurysm formation progresses via a similar pathogenesis to WT, and the increased incidence and severity is the result of increased circulating pro-inflammatory monocytes and increased oxidative stress produced from these monocytes and differentiated macrophages.

Therefore, excessive vascular inflammation and oxidative stress within NF1 patients and mice provide a rational target for therapeutic intervention. Statins are efficacious in reducing inflammation and oxidative stress independent of their lipid lowering capacity in both human trials and animal models (175, 177, 178). Specifically, statins reduce post-translational modification of proteins such as Ras and Rac, potentially resulting in reduced Ras activation and NADPH activation, respectively, in aneurysm-inducing neurofibromin-deficient myeloid cells (151, 154). Additionally, statins have positive effects on the vascular endothelium within the first month of treatment, demonstrated by increased nitric

oxide synthesis and improved vascular homeostasis (160, 161). The safety profile is additionally important which makes them advantageous for use in pediatric patients, as evidenced by recent trials in NF1 children (179), which may be important since evidence of vascular inflammation was identified in adolescent NF1 patients (22).

In the current study, simvastatin dramatically reduced *Nf1*<sup>+/-</sup> aneurysm formation with corresponding attenuation of MMP-9 activation and ROS production, lending strong evidence to the role of inflammation and oxidative stress in NF1 aneurysm development, as well as a potential therapeutic option for patients. Importantly, simvastatin was administered at a relatively low dose compared to other studies, which likely explains the absence of aneurysm attenuation in WT mice. These findings indicate NF1 patients and mice may be more susceptible to the positive effects of simvastatin at a lower dose than non-NF1 patients, due to increases in both Ras activation and Rac activation of NOX2 in untreated patients. Based on our pre-clinical findings that low-dose statin treatment attenuates aneurysm formation and vasocclusive disease (20), it is possible that statins could be a viable therapeutic intervention in NF1 patients for the prevention and treatment of CVD.

To further evaluate the biochemical mechanisms of NF1 aneurysm formation and identify another possible therapeutic for the treatment of NF1 CVD, *Nf1* heterozygous mice were treated with the antioxidant and NOX2 inhibitor, apocynin. Treatment reduced aneurysm incidence to near WT levels while significantly attenuating MMP activity and superoxide formation. These results,

as well as increased oxidative damage in white blood cells of NF1 patients, strongly suggest ROS derived from monocytes and/or macrophages as the biochemical mechanism leading to NF1 aneurysm formation. Apocynin inhibition of NOX2 may also reduce the homing or inflammatory activity of neurofibromin-deficient myeloid cells, similar to findings in a WT pain model (180).

Together, these results indicate *Nf1*<sup>+/-</sup> aneurysmal disease progresses via a similar pathogenic mechanism to normal aneurysm development; however, due to the increases in inflammation and ROS, larger and more severe aneurysms are produced. Additionally, we provide pharmacologic evidence that aneurysm formation in *Nf1*<sup>+/-</sup> mice is significantly attenuated by daily low-dose administration of the HMG-CoA reductase inhibitor simvastatin, as well as the NOX2 inhibitor apocynin. Finally, these studies provide compelling pre-clinical evidence implicating simvastatin and apocynin as possible therapeutic interventions for both the prevention and treatment of NF1 cardiovascular disease.

## REFERENCES

1. Riccardi, V.M. 1991. Neurofibromatosis: past, present, and future. *N Engl J Med* 324:1283-1285.
2. Lammert, M., Friedman, J.M., Kluwe, L., and Mautner, V.F. 2005. Prevalence of neurofibromatosis 1 in German children at elementary school enrollment. *Arch Dermatol* 141:71-74.
3. Wallace, M.R., Marchuk, D.A., Andersen, L.B., Letcher, R., Odeh, H.M., Saulino, A.M., Fountain, J.W., Brereton, A., Nicholson, J., Mitchell, A.L., et al. 1990. Type 1 neurofibromatosis gene: identification of a large transcript disrupted in three NF1 patients. *Science* 249:181-186.
4. Li, Y., O'Connell, P., Breidenbach, H.H., Cawthon, R., Stevens, J., Xu, G., Neil, S., Robertson, M., White, R., and Viskochil, D. 1995. Genomic organization of the neurofibromatosis 1 gene (NF1). *Genomics* 25:9-18.
5. Viskochil, D., Buchberg, A.M., Xu, G., Cawthon, R.M., Stevens, J., Wolff, R.K., Culver, M., Carey, J.C., Copeland, N.G., Jenkins, N.A., et al. 1990. Deletions and a translocation interrupt a cloned gene at the neurofibromatosis type 1 locus. *Cell* 62:187-192.
6. Xu, G.F., O'Connell, P., Viskochil, D., Cawthon, R., Robertson, M., Culver, M., Dunn, D., Stevens, J., Gesteland, R., White, R., et al. 1990. The neurofibromatosis type 1 gene encodes a protein related to GAP. *Cell* 62:599-608.



7. Huson, S.M., and Hughes, R.A.C. 1994. *The Neurofibromatoses : a pathogenetic and clinical overview*. London ; New York: Chapman & Hall Medical. xiii, 487 p., 484 p. of plates pp.
8. Riccardi, V.M. 1986. *Neurofibromatosis: phenotype, natural history and pathogenesis*. Baltimore: Johns Hopkins University Press.
9. Huson, S.M., Compston, D.A., Clark, P., and Harper, P.S. 1989. A genetic study of von Recklinghausen neurofibromatosis in south east Wales. I. Prevalence, fitness, mutation rate, and effect of parental transmission on severity. *J Med Genet* 26:704-711.
10. Rasmussen, S.A., and Friedman, J.M. 2000. NF1 gene and neurofibromatosis 1. *Am J Epidemiol* 151:33-40.
11. Upadhyaya, M., Shaw, D.J., and Harper, P.S. 1994. Molecular basis of neurofibromatosis type 1 (NF1): mutation analysis and polymorphisms in the NF1 gene. *Hum Mutat* 4:83-101.
12. Ward, B.A., and Gutmann, D.H. 2005. Neurofibromatosis 1: From lab bench to clinic. *Pediatric Neurology* 32:221-228.
13. Thomas, L., Mautner, V.F., Cooper, D.N., and Upadhyaya, M. 2012. Molecular heterogeneity in malignant peripheral nerve sheath tumors associated with neurofibromatosis type 1. *Hum Genomics* 6:18.
14. DeBella, K., Szudek, J., and Friedman, J.M. 2000. Use of the national institutes of health criteria for diagnosis of neurofibromatosis 1 in children. *Pediatrics* 105:608-614.

15. Gutmann, D.H., Aylsworth, A., Carey, J.C., Korf, B., Marks, J., Pyeritz, R.E., Rubenstein, A., and Viskochil, D. 1997. The diagnostic evaluation and multidisciplinary management of neurofibromatosis 1 and neurofibromatosis 2. *JAMA* 278:51-57.
16. Riccardi, V.M. 2010. Neurofibromatosis type 1 is a disorder of dysplasia: the importance of distinguishing features, consequences, and complications. *Birth Defects Res A Clin Mol Teratol* 88:9-14.
17. Side, L., Taylor, B., Cayouette, M., Conner, E., Thompson, P., Luce, M., and Shannon, K. 1997. Homozygous inactivation of the NF1 gene in bone marrow cells from children with neurofibromatosis type 1 and malignant myeloid disorders. *N Engl J Med* 336:1713-1720.
18. Bajaj, A., Li, Q.F., Zheng, Q., and Pumiglia, K. 2012. Loss of NF1 expression in human endothelial cells promotes autonomous proliferation and altered vascular morphogenesis. *PLoS ONE* 7:e49222.
19. Atit, R.P., Crowe, M.J., Greenhalgh, D.G., Wenstrup, R.J., and Ratner, N. 1999. The Nf1 tumor suppressor regulates mouse skin wound healing, fibroblast proliferation, and collagen deposited by fibroblasts. *J Invest Dermatol* 112:835-842.
20. Stansfield, B.K., Bessler, W.K., Mali, R., Mund, J.A., Downing, B., Li, F., Sarchet, K.N., Distasi, M.R., Conway, S.J., Kapur, R., et al. 2013. Heterozygous inactivation of the Nf1 gene in myeloid cells enhances neointima formation via a rosuvastatin-sensitive cellular pathway. *Hum Mol Genet* 22:977-988.

21. Chen, S., Burgin, S., McDaniel, A., Li, X., Yuan, J., Chen, M., Khalaf, W., Clapp, D.W., and Yang, F.C. 2010. Nf1-/- Schwann cell-conditioned medium modulates mast cell degranulation by c-Kit-mediated hyperactivation of phosphatidylinositol 3-kinase. *Am J Pathol* 177:3125-3132.
22. Lasater, E.A., Li, F., Bessler, W.K., Estes, M.L., Vemula, S., Hingtgen, C.M., Dinauer, M.C., Kapur, R., Conway, S.J., and Ingram, D.A., Jr. 2010. Genetic and cellular evidence of vascular inflammation in neurofibromin-deficient mice and humans. *J Clin Invest* 120:859-870.
23. Friedman, J.M., Arbiser, J., Epstein, J.A., Gutmann, D.H., Huot, S.J., Lin, A.E., McManus, B., and Korf, B.R. 2002. Cardiovascular disease in neurofibromatosis 1: report of the NF1 Cardiovascular Task Force. *Genet Med* 4:105-111.
24. Rasmussen, S.A., Yang, Q., and Friedman, J.M. 2001. Mortality in neurofibromatosis 1: an analysis using U.S. death certificates. *Am J Hum Genet* 68:1110-1118.
25. Oderich, G.S., Sullivan, T.M., Bower, T.C., Gloviczki, P., Miller, D.V., Babovic-Vuksanovic, D., Macedo, T.A., and Stanson, A. 2007. Vascular abnormalities in patients with neurofibromatosis syndrome type I: clinical spectrum, management, and results. *J Vasc Surg* 46:475-484.
26. Rosser, T.L., Vezina, G., and Packer, R.J. 2005. Cerebrovascular abnormalities in a population of children with neurofibromatosis type 1. *Neurology* 64:553-555.

27. Criado, E., Izquierdo, L., Lujan, S., Puras, E., and del Mar Espino, M. 2002. Abdominal aortic coarctation, renovascular, hypertension, and neurofibromatosis. *Ann Vasc Surg* 16:363-367.
28. Ghosh, P.S., Rothner, A.D., Emch, T.M., Friedman, N.R., and Moodley, M. 2013. Cerebral vasculopathy in children with neurofibromatosis type 1. *J Child Neurol* 28:95-101.
29. Rea, D., Brandsema, J.F., Armstrong, D., Parkin, P.C., deVeber, G., MacGregor, D., Logan, W.J., and Askalan, R. 2009. Cerebral arteriopathy in children with neurofibromatosis type 1. *Pediatrics* 124:e476-483.
30. Fossali, E., Signorini, E., Intermite, R.C., Casalini, E., Lovaria, A., Maninetti, M.M., and Rossi, L.N. 2000. Renovascular disease and hypertension in children with neurofibromatosis. *Pediatr Nephrol* 14:806-810.
31. Sharma, J.B., Gulati, N., and Malik, S. 1991. Maternal and perinatal complications in neurofibromatosis during pregnancy. *Int J Gynaecol Obstet* 34:221-227.
32. Edwards, J.N., Fooks, M., and Davey, D.A. 1983. Neurofibromatosis and severe hypertension in pregnancy. *Br J Obstet Gynaecol* 90:528-531.
33. Lehrnbecher, T., Gassel, A.M., Rauh, V., Kirchner, T., and Huppertz, H.I. 1994. Neurofibromatosis presenting as a severe systemic vasculopathy. *Eur J Pediatr* 153:107-109.

34. Stansfield, B.K., Bessler, W.K., Mali, R., Mund, J.A., Downing, B., Li, F., Sarchet, K.N., Distasi, M.R., Conway, S.J., Kapur, R., et al. 2012. Heterozygous Inactivation of the Nf1 Gene in Myeloid Cells Enhances Neointima Formation via a Rosuvastatin-Sensitive Cellular Pathway. *Hum Mol Genet*.
35. Xu, J., Ismat, F.A., Wang, T., Yang, J., and Epstein, J.A. 2007. NF1 regulates a Ras-dependent vascular smooth muscle proliferative injury response. *Circulation* 116:2148-2156.
36. Grage-Griebenow, E., Flad, H.D., and Ernst, M. 2001. Heterogeneity of human peripheral blood monocyte subsets. *J Leukoc Biol* 69:11-20.
37. Schlitt, A., Heine, G.H., Blankenberg, S., Espinola-Klein, C., Dopheide, J.F., Bickel, C., Lackner, K.J., Iz, M., Meyer, J., Darius, H., et al. 2004. CD14+CD16+ monocytes in coronary artery disease and their relationship to serum TNF-alpha levels. *Thromb Haemost* 92:419-424.
38. Martin, G.A., Viskochil, D., Bollag, G., McCabe, P.C., Crosier, W.J., Haubruck, H., Conroy, L., Clark, R., O'Connell, P., Cawthon, R.M., et al. 1990. The GAP-related domain of the neurofibromatosis type 1 gene product interacts with ras p21. *Cell* 63:843-849.
39. Norton, K.K., Xu, J., and Gutmann, D.H. 1995. Expression of the neurofibromatosis I gene product, neurofibromin, in blood vessel endothelial cells and smooth muscle. *Neurobiol Dis* 2:13-21.

40. Hiatt, K.K., Ingram, D.A., Zhang, Y., Bollag, G., and Clapp, D.W. 2001. Neurofibromin GTPase-activating protein-related domains restore normal growth in *Nf1*<sup>-/-</sup> cells. *J Biol Chem* 276:7240-7245.
41. DeClue, J.E., Cohen, B.D., and Lowy, D.R. 1991. Identification and characterization of the neurofibromatosis type 1 protein product. *Proc Natl Acad Sci U S A* 88:9914-9918.
42. Daston, M.M., Scrable, H., Nordlund, M., Sturbaum, A.K., Nissen, L.M., and Ratner, N. 1992. The protein product of the neurofibromatosis type 1 gene is expressed at highest abundance in neurons, Schwann cells, and oligodendrocytes. *Neuron* 8:415-428.
43. Brannan, C.I., Perkins, A.S., Vogel, K.S., Ratner, N., Nordlund, M.L., Reid, S.W., Buchberg, A.M., Jenkins, N.A., Parada, L.F., and Copeland, N.G. 1994. Targeted disruption of the neurofibromatosis type-1 gene leads to developmental abnormalities in heart and various neural crest-derived tissues. *Genes Dev* 8:1019-1029.
44. Jacks, T., Shih, T.S., Schmitt, E.M., Bronson, R.T., Bernards, A., and Weinberg, R.A. 1994. Tumour predisposition in mice heterozygous for a targeted mutation in *Nf1*. *Nat Genet* 7:353-361.
45. Scott, R.A., Ashton, H.A., and Kay, D.N. 1991. Abdominal aortic aneurysm in 4237 screened patients: prevalence, development and management over 6 years. *Br J Surg* 78:1122-1125.

46. Newman, A.B., Arnold, A.M., Burke, G.L., O'Leary, D.H., and Manolio, T.A. 2001. Cardiovascular disease and mortality in older adults with small abdominal aortic aneurysms detected by ultrasonography: the cardiovascular health study. *Ann Intern Med* 134:182-190.
47. Kent, K.C., Zwolak, R.M., Jaff, M.R., Hollenbeck, S.T., Thompson, R.W., Schermerhorn, M.L., Sicard, G.A., Riles, T.S., and Cronenwett, J.L. 2004. Screening for abdominal aortic aneurysm: a consensus statement. *J Vasc Surg* 39:267-269.
48. Kent, K.C., Zwolak, R.M., Egorova, N.N., Riles, T.S., Manganaro, A., Moskowitz, A.J., Gelijns, A.C., and Greco, G. 2010. Analysis of risk factors for abdominal aortic aneurysm in a cohort of more than 3 million individuals. *J Vasc Surg* 52:539-548.
49. Halushka, M.K. 2012. Single gene disorders of the aortic wall. *Cardiovasc Pathol* 21:240-244.
50. Freestone, T., Turner, R.J., Coady, A., Higman, D.J., Greenhalgh, R.M., and Powell, J.T. 1995. Inflammation and matrix metalloproteinases in the enlarging abdominal aortic aneurysm. *Arterioscler Thromb Vasc Biol* 15:1145-1151.
51. Thompson, R.W., and Parks, W.C. 1996. Role of matrix metalloproteinases in abdominal aortic aneurysms. *Ann N Y Acad Sci* 800:157-174.

52. Thompson, R.W., Holmes, D.R., Mertens, R.A., Liao, S., Botney, M.D., Mecham, R.P., Welgus, H.G., and Parks, W.C. 1995. Production and localization of 92-kilodalton gelatinase in abdominal aortic aneurysms. An elastolytic metalloproteinase expressed by aneurysm-infiltrating macrophages. *J Clin Invest* 96:318-326.
53. Siefert, S.A., and Sarkar, R. 2012. Matrix metalloproteinases in vascular physiology and disease. *Vascular* 20:210-216.
54. Huang, Q., Lan, F., Wang, X., Yu, Y., Ouyang, X., Zheng, F., Han, J., Lin, Y., Xie, Y., Xie, F., et al. 2014. IL-1beta-induced activation of p38 promotes metastasis in gastric adenocarcinoma via upregulation of AP-1/c-fos, MMP2 and MMP9. *Mol Cancer* 13:18.
55. Gasche, Y., Copin, J.C., Sugawara, T., Fujimura, M., and Chan, P.H. 2001. Matrix metalloproteinase inhibition prevents oxidative stress-associated blood-brain barrier disruption after transient focal cerebral ischemia. *J Cereb Blood Flow Metab* 21:1393-1400.
56. Gong, Y., Hart, E., Shchurin, A., and Hoover-Plow, J. 2008. Inflammatory macrophage migration requires MMP-9 activation by plasminogen in mice. *J Clin Invest* 118:3012-3024.
57. Rizas, K.D., Ippagunta, N., and Tilson, M.D., 3rd. 2009. Immune cells and molecular mediators in the pathogenesis of the abdominal aortic aneurysm. *Cardiol Rev* 17:201-210.



58. Longo, G.M., Xiong, W., Greiner, T.C., Zhao, Y., Fiotti, N., and Baxter, B.T. 2002. Matrix metalloproteinases 2 and 9 work in concert to produce aortic aneurysms. *J Clin Invest* 110:625-632.
59. Pyo, R., Lee, J.K., Shipley, J.M., Curci, J.A., Mao, D., Ziporin, S.J., Ennis, T.L., Shapiro, S.D., Senior, R.M., and Thompson, R.W. 2000. Targeted gene disruption of matrix metalloproteinase-9 (gelatinase B) suppresses development of experimental abdominal aortic aneurysms. *J Clin Invest* 105:1641-1649.
60. Weintraub, N.L. 2009. Understanding abdominal aortic aneurysm. *N Engl J Med* 361:1114-1116.
61. Miller, F.J., Jr., Sharp, W.J., Fang, X., Oberley, L.W., Oberley, T.D., and Weintraub, N.L. 2002. Oxidative stress in human abdominal aortic aneurysms: a potential mediator of aneurysmal remodeling. *Arterioscler Thromb Vasc Biol* 22:560-565.
62. Guzik, B., Sagan, A., Ludew, D., Mrowiecki, W., Chwala, M., Bujak-Gizycka, B., Filip, G., Grudzien, G., Kapelak, B., Zmudka, K., et al. 2013. Mechanisms of oxidative stress in human aortic aneurysms - Association with clinical risk factors for atherosclerosis and disease severity. *Int J Cardiol*.
63. Daugherty, A., Manning, M.W., and Cassis, L.A. 2000. Angiotensin II promotes atherosclerotic lesions and aneurysms in apolipoprotein E-deficient mice. *J Clin Invest* 105:1605-1612.

64. Thomas, M., Gavrilu, D., McCormick, M.L., Miller, F.J., Jr., Daugherty, A., Cassis, L.A., Dellsperger, K.C., and Weintraub, N.L. 2006. Deletion of p47phox attenuates angiotensin II-induced abdominal aortic aneurysm formation in apolipoprotein E-deficient mice. *Circulation* 114:404-413.
65. Kaneko, H., Anzai, T., Morisawa, M., Kohno, T., Nagai, T., Anzai, A., Takahashi, T., Shimoda, M., Sasaki, A., Maekawa, Y., et al. 2011. Resveratrol prevents the development of abdominal aortic aneurysm through attenuation of inflammation, oxidative stress, and neovascularization. *Atherosclerosis* 217:350-357.
66. Bao, W., Morimoto, K., Hasegawa, T., Sasaki, N., Yamashita, T., Hirata, K., Okita, Y., and Okada, K. 2014. Orally administered dipeptidyl peptidase-4 inhibitor (alogliptin) prevents abdominal aortic aneurysm formation through an antioxidant effect in rats. *J Vasc Surg* 59:1098-1108.
67. Maeda, I., Mizoiri, N., Briones, M.P., and Okamoto, K. 2007. Induction of macrophage migration through lactose-insensitive receptor by elastin-derived nonapeptides and their analog. *J Pept Sci* 13:263-268.
68. Sho, E., Sho, M., Hoshina, K., Kimura, H., Nakahashi, T.K., and Dalman, R.L. 2004. Hemodynamic forces regulate mural macrophage infiltration in experimental aortic aneurysms. *Exp Mol Pathol* 76:108-116.

69. Middleton, R.K., Bown, M.J., Lloyd, G.M., Jones, J.L., London, N.J., and Sayers, R.D. 2009. Characterisation of Interleukin-8 and monocyte chemoattractant protein-1 expression within the abdominal aortic aneurysm and their association with mural inflammation. *Eur J Vasc Endovasc Surg* 37:46-55.
70. Colonnello, J.S., Hance, K.A., Shames, M.L., Wyble, C.W., Ziporin, S.J., Leidenfrost, J.E., Ennis, T.L., Upchurch, G.R., Jr., and Thompson, R.W. 2003. Transient exposure to elastase induces mouse aortic wall smooth muscle cell production of MCP-1 and RANTES during development of experimental aortic aneurysm. *J Vasc Surg* 38:138-146.
71. Schubl, S., Tsai, S., Ryer, E.J., Wang, C., Hu, J., Kent, K.C., and Liu, B. 2009. Upregulation of protein kinase cdelta in vascular smooth muscle cells promotes inflammation in abdominal aortic aneurysm. *J Surg Res* 153:181-187.
72. Marchesi, C., Rehman, A., Rautureau, Y., Kasal, D.A., Briet, M., Leibowitz, A., Simeone, S.M., Ebrahimian, T., Neves, M.F., Offermanns, S., et al. 2013. Protective role of vascular smooth muscle cell PPARgamma in angiotensin II-induced vascular disease. *Cardiovasc Res* 97:562-570.
73. Majamaa, K., and Myllyla, V.V. 1993. A disorder of collagen biosynthesis in patients with cerebral artery aneurysm. *Biochim Biophys Acta* 1225:48-52.

74. Siegel, R.C., Pinnell, S.R., and Martin, G.R. 1970. Cross-linking of collagen and elastin. Properties of lysyl oxidase. *Biochemistry* 9:4486-4492.
75. Silence, J., Collen, D., and Lijnen, H.R. 2002. Reduced atherosclerotic plaque but enhanced aneurysm formation in mice with inactivation of the tissue inhibitor of metalloproteinase-1 (TIMP-1) gene. *Circ Res* 90:897-903.
76. Lemaitre, V., Soloway, P.D., and D'Armiento, J. 2003. Increased medial degradation with pseudo-aneurysm formation in apolipoprotein E-knockout mice deficient in tissue inhibitor of metalloproteinases-1. *Circulation* 107:333-338.
77. Ishibashi, S., Goldstein, J.L., Brown, M.S., Herz, J., and Burns, D.K. 1994. Massive xanthomatosis and atherosclerosis in cholesterol-fed low density lipoprotein receptor-negative mice. *J Clin Invest* 93:1885-1893.
78. Zhang, S.H., Reddick, R.L., Piedrahita, J.A., and Maeda, N. 1992. Spontaneous hypercholesterolemia and arterial lesions in mice lacking apolipoprotein E. *Science* 258:468-471.
79. Plump, A.S., Smith, J.D., Hayek, T., Aalto-Setälä, K., Walsh, A., Verstuyft, J.G., Rubin, E.M., and Breslow, J.L. 1992. Severe hypercholesterolemia and atherosclerosis in apolipoprotein E-deficient mice created by homologous recombination in ES cells. *Cell* 71:343-353.

80. Tangirala, R.K., Rubin, E.M., and Palinski, W. 1995. Quantitation of atherosclerosis in murine models: correlation between lesions in the aortic origin and in the entire aorta, and differences in the extent of lesions between sexes in LDL receptor-deficient and apolipoprotein E-deficient mice. *J Lipid Res* 36:2320-2328.
81. Newby, A.C., George, S.J., Ismail, Y., Johnson, J.L., Sala-Newby, G.B., and Thomas, A.C. 2009. Vulnerable atherosclerotic plaque metalloproteinases and foam cell phenotypes. *Thromb Haemost* 101:1006-1011.
82. Anidjar, S., Salzman, J.L., Gentric, D., Lagneau, P., Camilleri, J.P., and Michel, J.B. 1990. Elastase-induced experimental aneurysms in rats. *Circulation* 82:973-981.
83. Daugherty, A., Manning, M.W., and Cassis, L.A. 2001. Antagonism of AT2 receptors augments angiotensin II-induced abdominal aortic aneurysms and atherosclerosis. *Br J Pharmacol* 134:865-870.
84. Manning, M.W., Cassi, L.A., Huang, J., Szilvassy, S.J., and Daugherty, A. 2002. Abdominal aortic aneurysms: fresh insights from a novel animal model of the disease. *Vasc Med* 7:45-54.
85. Manning, M.W., Cassis, L.A., and Daugherty, A. 2003. Differential effects of doxycycline, a broad-spectrum matrix metalloproteinase inhibitor, on angiotensin II-induced atherosclerosis and abdominal aortic aneurysms. *Arterioscler Thromb Vasc Biol* 23:483-488.

86. Saraff, K., Babamusta, F., Cassis, L.A., and Daugherty, A. 2003. Aortic dissection precedes formation of aneurysms and atherosclerosis in angiotensin II-infused, apolipoprotein E-deficient mice. *Arterioscler Thromb Vasc Biol* 23:1621-1626.
87. Yao, H.L., Gao, F.H., Li, Z.Z., Wu, H.X., Xu, M.D., Zhang, Z., and Dai, Q.Y. 2012. Monocyte chemoattractant protein-1 mediates angiotensin II-induced vascular smooth muscle cell proliferation via SAPK/JNK and ERK1/2. *Mol Cell Biochem* 366:355-362.
88. Deng, G.G., Martin-McNulty, B., Sukovich, D.A., Freay, A., Halks-Miller, M., Thinnes, T., Loskutoff, D.J., Carmeliet, P., Dole, W.P., and Wang, Y.X. 2003. Urokinase-type plasminogen activator plays a critical role in angiotensin II-induced abdominal aortic aneurysm. *Circ Res* 92:510-517.
89. Zhu, Y., Romero, M.I., Ghosh, P., Ye, Z., Charnay, P., Rushing, E.J., Marth, J.D., and Parada, L.F. 2001. Ablation of NF1 function in neurons induces abnormal development of cerebral cortex and reactive gliosis in the brain. *Genes Dev* 15:859-876.
90. Zhang, Y.Y., Vik, T.A., Ryder, J.W., Srour, E.F., Jacks, T., Shannon, K., and Clapp, D.W. 1998. Nf1 regulates hematopoietic progenitor cell growth and ras signaling in response to multiple cytokines. *J Exp Med* 187:1893-1902.

91. Police, S.B., Putnam, K., Thatcher, S., Batifoulier-Yiannikouris, F., Daugherty, A., and Cassis, L.A. 2010. Weight loss in obese C57BL/6 mice limits adventitial expansion of established angiotensin II-induced abdominal aortic aneurysms. *Am J Physiol Heart Circ Physiol* 298:H1932-1938.
92. Martin-McNulty, B., Tham, D.M., da Cunha, V., Ho, J.J., Wilson, D.W., Rutledge, J.C., Deng, G.G., Vergona, R., Sullivan, M.E., and Wang, Y.X. 2003. 17 Beta-estradiol attenuates development of angiotensin II-induced aortic abdominal aneurysm in apolipoprotein E-deficient mice. *Arterioscler Thromb Vasc Biol* 23:1627-1632.
93. Janssen, B.J., De Celle, T., Debets, J.J., Brouns, A.E., Callahan, M.F., and Smith, T.L. 2004. Effects of anesthetics on systemic hemodynamics in mice. *Am J Physiol Heart Circ Physiol* 287:H1618-1624.
94. Satoh, K., Nigro, P., Matoba, T., O'Dell, M.R., Cui, Z., Shi, X., Mohan, A., Yan, C., Abe, J., Illig, K.A., et al. 2009. Cyclophilin A enhances vascular oxidative stress and the development of angiotensin II-induced aortic aneurysms. *Nat Med* 15:649-656.
95. Tieu, B.C., Lee, C., Sun, H., Lejeune, W., Recinos, A., 3rd, Ju, X., Spratt, H., Guo, D.C., Milewicz, D., Tilton, R.G., et al. 2009. An adventitial IL-6/MCP1 amplification loop accelerates macrophage-mediated vascular inflammation leading to aortic dissection in mice. *J Clin Invest* 119:3637-3651.

96. Meir, K.S., and Leitersdorf, E. 2004. Atherosclerosis in the apolipoprotein-E-deficient mouse: a decade of progress. *Arterioscler Thromb Vasc Biol* 24:1006-1014.
97. Rizzo, R.J., McCarthy, W.J., Dixit, S.N., Lilly, M.P., Shively, V.P., Flinn, W.R., and Yao, J.S. 1989. Collagen types and matrix protein content in human abdominal aortic aneurysms. *J Vasc Surg* 10:365-373.
98. Kanematsu, Y., Kanematsu, M., Kurihara, C., Tsou, T.L., Nuki, Y., Liang, E.I., Makino, H., and Hashimoto, T. 2010. Pharmacologically induced thoracic and abdominal aortic aneurysms in mice. *Hypertension* 55:1267-1274.
99. Daugherty, A., and Cassis, L.A. 2004. Mouse models of abdominal aortic aneurysms. *Arterioscler Thromb Vasc Biol* 24:429-434.
100. Miyazaki, T., Ohta, F., Daisu, M., and Hoshii, Y. 2004. Extracranial vertebral artery aneurysm ruptured into the thoracic cavity with neurofibromatosis type 1: case report. *Neurosurgery* 54:1517-1520; discussion 1520-1511.
101. Li, F., Munchhof, A.M., White, H.A., Mead, L.E., Krier, T.R., Fenoglio, A., Chen, S., Wu, X., Cai, S., Yang, F.C., et al. 2006. Neurofibromin is a novel regulator of RAS-induced signals in primary vascular smooth muscle cells. *Hum Mol Genet* 15:1921-1930.



102. Lopez-Candales, A., Holmes, D.R., Liao, S., Scott, M.J., Wickline, S.A., and Thompson, R.W. 1997. Decreased vascular smooth muscle cell density in medial degeneration of human abdominal aortic aneurysms. *Am J Pathol* 150:993-1007.
103. Bobryshev, Y.V., and Lord, R.S. 2001. Vascular-associated lymphoid tissue (VALT) involvement in aortic aneurysm. *Atherosclerosis* 154:15-21.
104. Yajima, N., Masuda, M., Miyazaki, M., Nakajima, N., Chien, S., and Shyy, J.Y. 2002. Oxidative stress is involved in the development of experimental abdominal aortic aneurysm: a study of the transcription profile with complementary DNA microarray. *J Vasc Surg* 36:379-385.
105. Galis, Z.S., Sukhova, G.K., Kranzhofer, R., Clark, S., and Libby, P. 1995. Macrophage foam cells from experimental atheroma constitutively produce matrix-degrading proteinases. *Proc Natl Acad Sci U S A* 92:402-406.
106. Holtwick, R., Gotthardt, M., Skryabin, B., Steinmetz, M., Potthast, R., Zetsche, B., Hammer, R.E., Herz, J., and Kuhn, M. 2002. Smooth muscle-selective deletion of guanylyl cyclase-A prevents the acute but not chronic effects of ANP on blood pressure. *Proc Natl Acad Sci U S A* 99:7142-7147.
107. Clausen, B.E., Burkhardt, C., Reith, W., Renkawitz, R., and Forster, I. 1999. Conditional gene targeting in macrophages and granulocytes using LysMcre mice. *Transgenic Res* 8:265-277.

108. Nagasawa, A., Yoshimura, K., Suzuki, R., Mikamo, A., Yamashita, O., Ikeda, Y., Tsuchida, M., and Hamano, K. 2013. Important role of the angiotensin II pathway in producing matrix metalloproteinase-9 in human thoracic aortic aneurysms. *J Surg Res*.
109. Gallo, A., Saad, A., Ali, R., Dardik, A., Tellides, G., and Geirsson, A. 2012. Circulating interferon-gamma-inducible Cys-X-Cys chemokine receptor 3 ligands are elevated in humans with aortic aneurysms and Cys-X-Cys chemokine receptor 3 is necessary for aneurysm formation in mice. *J Thorac Cardiovasc Surg* 143:704-710.
110. Munchhof, A.M., Li, F., White, H.A., Mead, L.E., Krier, T.R., Fenoglio, A., Li, X., Yuan, J., Yang, F.C., and Ingram, D.A. 2006. Neurofibroma-associated growth factors activate a distinct signaling network to alter the function of neurofibromin-deficient endothelial cells. *Hum Mol Genet* 15:1858-1869.
111. Chang, T., Krisman, K., Theobald, E.H., Xu, J., Akutagawa, J., Lauchle, J.O., Kogan, S., Braun, B.S., and Shannon, K. 2013. Sustained MEK inhibition abrogates myeloproliferative disease in Nf1 mutant mice. *J Clin Invest* 123:335-339.
112. Staser, K., Park, S.J., Rhodes, S.D., Zeng, Y., He, Y.Z., Shew, M.A., Gehlhausen, J.R., Cerabona, D., Menon, K., Chen, S., et al. 2013. Normal hematopoiesis and neurofibromin-deficient myeloproliferative disease require Erk. *J Clin Invest* 123:329-334.

113. Yang, F.C., Ingram, D.A., Chen, S., Zhu, Y., Yuan, J., Li, X., Yang, X., Knowles, S., Horn, W., Li, Y., et al. 2008. Nf1-dependent tumors require a microenvironment containing Nf1+/- and c-kit-dependent bone marrow. *Cell* 135:437-448.
114. Yang, F.C., Chen, S., Robling, A.G., Yu, X., Nebesio, T.D., Yan, J., Morgan, T., Li, X., Yuan, J., Hock, J., et al. 2006. Hyperactivation of p21ras and PI3K cooperate to alter murine and human neurofibromatosis type 1-haploinsufficient osteoclast functions. *J Clin Invest* 116:2880-2891.
115. Businaro, R., Tagliani, A., Buttari, B., Profumo, E., Ippoliti, F., Di Cristofano, C., Capoano, R., Salvati, B., and Rigano, R. 2012. Cellular and molecular players in the atherosclerotic plaque progression. *Ann N Y Acad Sci* 1262:134-141.
116. Nordon, I.M., Hinchliffe, R.J., Holt, P.J., Loftus, I.M., and Thompson, M.M. 2009. Review of current theories for abdominal aortic aneurysm pathogenesis. *Vascular* 17:253-263.
117. Ishibashi, M., Egashira, K., Zhao, Q., Hiasa, K., Ohtani, K., Ihara, Y., Charo, I.F., Kura, S., Tsuzuki, T., Takeshita, A., et al. 2004. Bone marrow-derived monocyte chemoattractant protein-1 receptor CCR2 is critical in angiotensin II-induced acceleration of atherosclerosis and aneurysm formation in hypercholesterolemic mice. *Arterioscler Thromb Vasc Biol* 24:e174-178.

118. MacTaggart, J.N., Xiong, W., Knispel, R., and Baxter, B.T. 2007. Deletion of CCR2 but not CCR5 or CXCR3 inhibits aortic aneurysm formation. *Surgery* 142:284-288.
119. de Waard, V., Bot, I., de Jager, S.C., Talib, S., Egashira, K., de Vries, M.R., Quax, P.H., Biessen, E.A., and van Berkel, T.J. 2010. Systemic MCP1/CCR2 blockade and leukocyte specific MCP1/CCR2 inhibition affect aortic aneurysm formation differently. *Atherosclerosis* 211:84-89.
120. Swirski, F.K., Libby, P., Aikawa, E., Alcaide, P., Luscinskas, F.W., Weissleder, R., and Pittet, M.J. 2007. Ly-6Chi monocytes dominate hypercholesterolemia-associated monocytosis and give rise to macrophages in atheromata. *J Clin Invest* 117:195-205.
121. Getts, D.R., Terry, R.L., Getts, M.T., Muller, M., Rana, S., Shrestha, B., Radford, J., Van Rooijen, N., Campbell, I.L., and King, N.J. 2008. Ly6c+ "inflammatory monocytes" are microglial precursors recruited in a pathogenic manner in West Nile virus encephalitis. *J Exp Med* 205:2319-2337.
122. Psaltis, P.J., Harbuzariu, A., Delacroix, S., Witt, T.A., Holroyd, E.W., Spoon, D.B., Hoffman, S.J., Pan, S., Kleppe, L.S., Mueske, C.S., et al. 2012. Identification of a monocyte-predisposed hierarchy of hematopoietic progenitor cells in the adventitia of postnatal murine aorta. *Circulation* 125:592-603.

123. Bigatel, D.A., Elmore, J.R., Carey, D.J., Cizmeci-Smith, G., Franklin, D.P., and Youkey, J.R. 1999. The matrix metalloproteinase inhibitor BB-94 limits expansion of experimental abdominal aortic aneurysms. *J Vasc Surg* 29:130-138; discussion 138-139.
124. Rajagopalan, S., Meng, X.P., Ramasamy, S., Harrison, D.G., and Galis, Z.S. 1996. Reactive oxygen species produced by macrophage-derived foam cells regulate the activity of vascular matrix metalloproteinases in vitro. Implications for atherosclerotic plaque stability. *J Clin Invest* 98:2572-2579.
125. Tong, J.J., Schriener, S.E., McCleary, D., Day, B.J., and Wallace, D.C. 2007. Life extension through neurofibromin mitochondrial regulation and antioxidant therapy for neurofibromatosis-1 in *Drosophila melanogaster*. *Nat Genet* 39:476-485.
126. Hole, P.S., Pearn, L., Tonks, A.J., James, P.E., Burnett, A.K., Darley, R.L., and Tonks, A. 2010. Ras-induced reactive oxygen species promote growth factor-independent proliferation in human CD34+ hematopoietic progenitor cells. *Blood* 115:1238-1246.
127. Lassegue, B., San Martin, A., and Griendling, K.K. 2012. Biochemistry, physiology, and pathophysiology of NADPH oxidases in the cardiovascular system. *Circ Res* 110:1364-1390.

128. DeYulia, G.J., Jr., Carcamo, J.M., Borquez-Ojeda, O., Shelton, C.C., and Golde, D.W. 2005. Hydrogen peroxide generated extracellularly by receptor-ligand interaction facilitates cell signaling. *Proc Natl Acad Sci U S A* 102:5044-5049.
129. Rhee, S.G. 1999. Redox signaling: hydrogen peroxide as intracellular messenger. *Exp Mol Med* 31:53-59.
130. Lander, H.M. 1997. An essential role for free radicals and derived species in signal transduction. *FASEB J* 11:118-124.
131. Ray, P.D., Huang, B.W., and Tsuji, Y. 2012. Reactive oxygen species (ROS) homeostasis and redox regulation in cellular signaling. *Cell Signal* 24:981-990.
132. Harrison, D., Griending, K.K., Landmesser, U., Hornig, B., and Drexler, H. 2003. Role of oxidative stress in atherosclerosis. *Am J Cardiol* 91:7A-11A.
133. Andersen, J.K. 2004. Oxidative stress in neurodegeneration: cause or consequence? *Nat Med* 10 Suppl:S18-25.
134. Paravicini, T.M., and Touyz, R.M. 2006. Redox signaling in hypertension. *Cardiovasc Res* 71:247-258.
135. Haigis, M.C., and Yankner, B.A. 2010. The aging stress response. *Mol Cell* 40:333-344.
136. Cadenas, E., and Davies, K.J. 2000. Mitochondrial free radical generation, oxidative stress, and aging. *Free Radic Biol Med* 29:222-230.

137. Geiszt, M., Witta, J., Baffi, J., Lekstrom, K., and Leto, T.L. 2003. Dual oxidases represent novel hydrogen peroxide sources supporting mucosal surface host defense. *FASEB J* 17:1502-1504.
138. Lassegue, B., and Griendling, K.K. 2010. NADPH oxidases: functions and pathologies in the vasculature. *Arterioscler Thromb Vasc Biol* 30:653-661.
139. Babior, B.M., Lambeth, J.D., and Nauseef, W. 2002. The neutrophil NADPH oxidase. *Arch Biochem Biophys* 397:342-344.
140. Chanock, S.J., el Benna, J., Smith, R.M., and Babior, B.M. 1994. The respiratory burst oxidase. *J Biol Chem* 269:24519-24522.
141. Pollock, J.D., Williams, D.A., Gifford, M.A., Li, L.L., Du, X., Fisherman, J., Orkin, S.H., Doerschuk, C.M., and Dinauer, M.C. 1995. Mouse model of X-linked chronic granulomatous disease, an inherited defect in phagocyte superoxide production. *Nat Genet* 9:202-209.
142. Borregaard, N., Heiple, J.M., Simons, E.R., and Clark, R.A. 1983. Subcellular localization of the b-cytochrome component of the human neutrophil microbicidal oxidase: translocation during activation. *J Cell Biol* 97:52-61.
143. Lapouge, K., Smith, S.J., Groemping, Y., and Rittinger, K. 2002. Architecture of the p40-p47-p67phox complex in the resting state of the NADPH oxidase. A central role for p67phox. *J Biol Chem* 277:10121-10128.

144. Abo, A., Pick, E., Hall, A., Totty, N., Teahan, C.G., and Segal, A.W. 1991. Activation of the NADPH oxidase involves the small GTP-binding protein p21rac1. *Nature* 353:668-670.
145. Heyworth, P.G., Bohl, B.P., Bokoch, G.M., and Curnutte, J.T. 1994. Rac translocates independently of the neutrophil NADPH oxidase components p47phox and p67phox. Evidence for its interaction with flavocytochrome b558. *J Biol Chem* 269:30749-30752.
146. Hazan-Halevy, I., Levy, T., Wolak, T., Lubarsky, I., Levy, R., and Paran, E. 2005. Stimulation of NADPH oxidase by angiotensin II in human neutrophils is mediated by ERK, p38 MAP-kinase and cytosolic phospholipase A2. *J Hypertens* 23:1183-1190.
147. Hannigan, M.O., Huang, C.K., and Wu, D.Q. 2004. Roles of PI3K in neutrophil function. *Curr Top Microbiol Immunol* 282:165-175.
148. Ingram, D.A., Hiatt, K., King, A.J., Fisher, L., Shivakumar, R., Derstine, C., Wenning, M.J., Diaz, B., Travers, J.B., Hood, A., et al. 2001. Hyperactivation of p21(ras) and the hematopoietic-specific Rho GTPase, Rac2, cooperate to alter the proliferation of neurofibromin-deficient mast cells in vivo and in vitro. *J Exp Med* 194:57-69.
149. Victor, V.M., Apostolova, N., Herance, R., Hernandez-Mijares, A., and Rocha, M. 2009. Oxidative stress and mitochondrial dysfunction in atherosclerosis: mitochondria-targeted antioxidants as potential therapy. *Curr Med Chem* 16:4654-4667.



150. Boveris, A., Cadenas, E., and Stoppani, A.O. 1976. Role of ubiquinone in the mitochondrial generation of hydrogen peroxide. *Biochem J* 156:435-444.
151. Van Aelst, L., and D'Souza-Schorey, C. 1997. Rho GTPases and signaling networks. *Genes Dev* 11:2295-2322.
152. 1998. Prevention of cardiovascular events and death with pravastatin in patients with coronary heart disease and a broad range of initial cholesterol levels. The Long-Term Intervention with Pravastatin in Ischaemic Disease (LIPID) Study Group. *N Engl J Med* 339:1349-1357.
153. 1998. Influence of pravastatin and plasma lipids on clinical events in the West of Scotland Coronary Prevention Study (WOSCOPS). *Circulation* 97:1440-1445.
154. Hall, A. 1998. Rho GTPases and the actin cytoskeleton. *Science* 279:509-514.
155. Tinkel, J., Hassanain, H., and Khouri, S.J. 2012. Cardiovascular antioxidant therapy: a review of supplements, pharmacotherapies, and mechanisms. *Cardiol Rev* 20:77-83.
156. Ignarro, L.J., Buga, G.M., Wood, K.S., Byrns, R.E., and Chaudhuri, G. 1987. Endothelium-derived relaxing factor produced and released from artery and vein is nitric oxide. *Proc Natl Acad Sci U S A* 84:9265-9269.
157. Radomski, M.W., Rees, D.D., Dutra, A., and Moncada, S. 1992. S-nitroso-glutathione inhibits platelet activation in vitro and in vivo. *Br J Pharmacol* 107:745-749.

158. Garg, U.C., and Hassid, A. 1989. Nitric oxide-generating vasodilators and 8-bromo-cyclic guanosine monophosphate inhibit mitogenesis and proliferation of cultured rat vascular smooth muscle cells. *J Clin Invest* 83:1774-1777.
159. Harrison, D.G. 1997. Cellular and molecular mechanisms of endothelial cell dysfunction. *J Clin Invest* 100:2153-2157.
160. Anderson, T.J., Meredith, I.T., Yeung, A.C., Frei, B., Selwyn, A.P., and Ganz, P. 1995. The effect of cholesterol-lowering and antioxidant therapy on endothelium-dependent coronary vasomotion. *N Engl J Med* 332:488-493.
161. O'Driscoll, G., Green, D., and Taylor, R.R. 1997. Simvastatin, an HMG-coenzyme A reductase inhibitor, improves endothelial function within 1 month. *Circulation* 95:1126-1131.
162. Van den Worm, E., Beukelman, C.J., Van den Berg, A.J., Kroes, B.H., Labadie, R.P., and Van Dijk, H. 2001. Effects of methoxylation of apocynin and analogs on the inhibition of reactive oxygen species production by stimulated human neutrophils. *Eur J Pharmacol* 433:225-230.
163. Ximenes, V.F., Kanegae, M.P., Rissato, S.R., and Galhiane, M.S. 2007. The oxidation of apocynin catalyzed by myeloperoxidase: proposal for NADPH oxidase inhibition. *Arch Biochem Biophys* 457:134-141.
164. Schultz, J., and Kaminker, K. 1962. Myeloperoxidase of the leucocyte of normal human blood. I. Content and localization. *Arch Biochem Biophys* 96:465-467.

165. Bos, A., Wever, R., and Roos, D. 1978. Characterization and quantification of the peroxidase in human monocytes. *Biochim Biophys Acta* 525:37-44.
166. Heumuller, S., Wind, S., Barbosa-Sicard, E., Schmidt, H.H., Busse, R., Schroder, K., and Brandes, R.P. 2008. Apocynin is not an inhibitor of vascular NADPH oxidases but an antioxidant. *Hypertension* 51:211-217.
167. Taylor, N.E., Glocka, P., Liang, M., and Cowley, A.W., Jr. 2006. NADPH oxidase in the renal medulla causes oxidative stress and contributes to salt-sensitive hypertension in Dahl S rats. *Hypertension* 47:692-698.
168. Jin, L., Beswick, R.A., Yamamoto, T., Palmer, T., Taylor, T.A., Pollock, J.S., Pollock, D.M., Brands, M.W., and Webb, R.C. 2006. Increased reactive oxygen species contributes to kidney injury in mineralocorticoid hypertensive rats. *J Physiol Pharmacol* 57:343-357.
169. Ghosh, M., Wang, H.D., and McNeill, J.R. 2004. Role of oxidative stress and nitric oxide in regulation of spontaneous tone in aorta of DOCA-salt hypertensive rats. *Br J Pharmacol* 141:562-573.
170. Yoder, M.C., Mead, L.E., Prater, D., Krier, T.R., Mroueh, K.N., Li, F., Krasich, R., Temm, C.J., Prchal, J.T., and Ingram, D.A. 2007. Redefining endothelial progenitor cells via clonal analysis and hematopoietic stem/progenitor cell principals. *Blood* 109:1801-1809.
171. Azqueta, A., Gutzkow, K.B., Brunborg, G., and Collins, A.R. 2011. Towards a more reliable comet assay: optimising agarose concentration, unwinding time and electrophoresis conditions. *Mutat Res* 724:41-45.

172. Collins, A.R. 2014. Measuring oxidative damage to DNA and its repair with the comet assay. *Biochim Biophys Acta* 1840:794-800.
173. Devaraj, S., Glaser, N., Griffen, S., Wang-Polagruto, J., Miguelino, E., and Jialal, I. 2006. Increased monocytic activity and biomarkers of inflammation in patients with type 1 diabetes. *Diabetes* 55:774-779.
174. Takagi, H., Matsui, M., and Umemoto, T. 2010. A meta-analysis of clinical studies of statins for prevention of abdominal aortic aneurysm expansion. *J Vasc Surg* 52:1675-1681.
175. Athyros, V.G., Kakafika, A.I., Tziomalos, K., Karagiannis, A., and Mikhailidis, D.P. 2009. Pleiotropic effects of statins--clinical evidence. *Curr Pharm Des* 15:479-489.
176. Simons, J.M., Hart, B.A., Ip Vai Ching, T.R., Van Dijk, H., and Labadie, R.P. 1990. Metabolic activation of natural phenols into selective oxidative burst agonists by activated human neutrophils. *Free Radic Biol Med* 8:251-258.
177. Scalia, R., Gooszen, M.E., Jones, S.P., Hoffmeyer, M., Rimmer, D.M., 3rd, Trocha, S.D., Huang, P.L., Smith, M.B., Lefer, A.M., and Lefer, D.J. 2001. Simvastatin exerts both anti-inflammatory and cardioprotective effects in apolipoprotein E-deficient mice. *Circulation* 103:2598-2603.
178. Zhang, Y., Naggar, J.C., Welzig, C.M., Beasley, D., Moulton, K.S., Park, H.J., and Galper, J.B. 2009. Simvastatin inhibits angiotensin II-induced abdominal aortic aneurysm formation in apolipoprotein E-knockout mice: possible role of ERK. *Arterioscler Thromb Vasc Biol* 29:1764-1771.

179. Krab, L.C., de Goede-Bolder, A., Aarsen, F.K., Pluijm, S.M., Bouman, M.J., van der Geest, J.N., Lequin, M., Catsman, C.E., Arts, W.F., Kushner, S.A., et al. 2008. Effect of simvastatin on cognitive functioning in children with neurofibromatosis type 1: a randomized controlled trial. *JAMA* 300:287-294.
180. Hackel, D., Pflucke, D., Neumann, A., Viebahn, J., Mousa, S., Wischmeyer, E., Roewer, N., Brack, A., and Rittner, H.L. 2013. The connection of monocytes and reactive oxygen species in pain. *PLoS ONE* 8:e63564.

## CURRICULUM VITAE

Brandon David Downing

### EDUCATION

#### *Undergraduate*

2004-2008 Indianapolis, IN	Purdue University	B.S.: Biology
-------------------------------	-------------------	---------------

#### *Graduate*

2008-2014	Indiana University Indianapolis, IN	Ph.D.: Biochemistry Minor: Life Sciences
-----------	--	---

### RESEARCH EXPERIENCE

#### **Indiana University School of Medicine**

Graduate Student, Department of Biochemistry & Molecular Biology, 2008-2014.  
Dr. David Ingram Jr., M.D.  
Dissertation Title: Myeloid Cells Induce Neurofibromatosis Type 1 Aneurysm  
Formation Through Inflammation and Oxidative Stress

#### **Indiana University School of Medicine**

Laboratory Assistant, Department of Biochemistry & Molecular Biology, 2007-  
2008.  
Dr. Ronald Wek, Ph.D.

#### **Purdue University, Indianapolis**

Undergraduate Research, Department of Biology, 2005-2008.  
Dr. Anna Malkova, Ph.D.

### AWARDS and HONORS

2012	Cleveland Clinic Student Award, Midwest Society of Pediatric Research. Nationwide Children's Hospital, Columbus, OH, October 4-5, 2012.
------	---

2012	Outstanding Poster Presentation Award, Indiana Clinical and Translational Sciences Institute 4 <sup>th</sup> Annual Meeting. Indianapolis, IN, August 31, 2012.
------	---

2008	Chancellor's Award for Outstanding Undergraduate Research. IUPUI, Indianapolis, IN
2008	Top 10 Male Students. IUPUI, Indianapolis, IN
2007	Bowling-Jones-Russo Undergraduate Research Award. IUPUI, Indianapolis, IN

#### GRANTS and FELLOWSHIPS

2011-2013	Indiana Clinical and Translational Sciences Institute (CTSI) Predoctoral training grant
2007	Undergraduate Research Opportunities Program Science Fellowship, Indiana University-Purdue University, Indianapolis, Indiana
2006	Undergraduate Research Opportunities Program Travel Funding, Indiana University-Purdue University, Indianapolis, Indiana

#### PEER REVIEWED PUBLICATIONS

- Li F\*, **Downing BD\***, Smiley LC, Mund JA, DiStasi MR, Bessler WK, Sarchet KN, Hinds DM, Kamendulis LM, Hingtgen CM, Case J, Clapp DW, Conway SJ, Stansfield BK, Ingram DA. "Neurofibromin Deficient Myeloid Cells are Critical Mediators of Aneurysm Formation *In Vivo*." *Circulation*. 2014;129(11):1213-1224. \*Authors contributed equally.
- Stansfield BK, Bessler WK, Mail R, Mund JA, **Downing BD**, Kapur R, Ingram DA. "Ras-Mek-Erk Signaling Directly Regulates *Nf1* heterozygous Neointima Formation." *American Journal of Pathology*. 2013;184(1):79-85.
- Stansfield BK, Bessler WK, Mali R, Mund JA, **Downing B**, Li F, Sarchet KN, DiStasi MR, Conway SJ, Kapur R, Ingram DA. "Heterozygous inactivation of the *Nf1* gene in Myeloid Cells Enhances Neointima Formation via a Rosuvastation-Sensitive Cellular Pathway." *Human Molecular Genetics*. 2013;22(5):977-88.
- **Downing B**, Morgan R, Vanhulle K, Deem A, Malkova A. "Large inverted repeats in the vicinity of a single double-strand break strongly affect repair in yeast diploids lacking Rad51." *Mutation Research*. 2008;645(1-2):9-18.

- Deem A., Barker K., Vanhulle K., **Downing B.**, Vayl A., Malkova A. “Defective break-induced replication leads to half-crossovers in *Saccharomyces cerevisiae*.” *Genetics*. 2008;179(4):1845-1860.
- Vanhulle K., Lemoine F. J., Narayanan V., **Downing B.**, Hull K., McCullough C., Bellinger M., Lobachev K., Petes T.D., Malkova A. “Inverted DNA repeats channel repair of distant double-strand breaks into chromatid fusions and chromosomal rearrangements”, *Mol. and Cell. Biol.* 2007;27(7):2601-2614.

## ABSTRACTS

- **Downing B.**, Li F, Bessler WK, Stansfield BK, Mund JA, Sarchet K, Distasi MR, Ingram DA. “Myeloid Cells Induce *Nf1*<sup>+/-</sup> Aneurysm Formation via Activation of NADPH Oxidase.” National Clinical and Translational Sciences Predoctoral Programs Meeting, Mayo Clinic, Rochester, MN, May 5-7, 2013. (oral presentation)
- Stansfield B, Bessler W, Mund J, **Downing B.**, Mali R, Kapur R, Ingram D. Heterozygous inactivation of the *Nf1* gene in Myeloid Cells Enhances Neointima Formation via a Rosuvastatin-Sensitive Cellular Pathway. Midwest Society for Pediatric Research, Nationwide Children’s Hospital, Columbus, OH, October 4-5, 2012. (oral presentation)
- **Downing B.**, Li F., Ingram D.A. Monocyte/macrophages are the primary effectors of *Nf1*<sup>+/-</sup> aneurysm formation via increased activation of the NADPH oxidase system. 1<sup>st</sup> annual South-Central Regional M.D./Ph.D. Conference. Louisville, KY, September 8, 2012.
- **Downing B.**, Li F., Distasi M.C., Smiley L.C., Stansfield B.K., Sarchet K., Mund J.A., Bessler W.K., Ingram D.A. Myeloid cells are the primary effectors of Neurofibromatosis Type 1 aneurysms via the NADPH oxidase system. Indiana Clinical and Translational Sciences Institute 4<sup>th</sup> Annual Meeting. Indianapolis, IN, Aug 31, 2012.
- **Downing B.**, Li F., Bessler W.K., Stansfield B.K., Mund J.A., Sarchet K., Distasi M.C., Smiley L.C., Ingram D.A. Monocyte/macrophages are the primary effectors of *Nf1*<sup>+/-</sup> aneurysm formation via increased activation of the NADPH oxidase system. Gordon Research Conference: NOX Family NADPH Oxidases. Waterville Valley, NH, June 3-8, 2012.
- Distasi MR, Ortiz MA, Campana GL, **Downing B.**, Mund JA, Miller SJ, Labarrere CA, Ingram DA, Unthank JL. Role of NAD(P)H Oxidase in Obesity-Induced Impaired Compensation to Subcritical Limb Ischemia. Gordon Research Conference: NOX Family NADPH Oxidases. Waterville Valley, NH, June 3-8, 2012.



- **Downing B.**, Li F., Bessler W.K., Stansfield B.K., Mund J.A., Sarchet K., Distasi M.C., Smiley L.C., Ingram D.A. Monocyte/macrophages are the primary effectors of *Nf1*<sup>+/-</sup> aneurysm formation via increased activation of the NADPH oxidase system. Gordon Research Seminar: NOX Family NADPH Oxidases. Waterville Valley, NH, June 2-3, 2012. (oral presentation)
- **Downing B.**, Li F., Bessler W.K., Stansfield B.K., Mund J.A., Sarchet K., Distasi M.C., Ingram D.A. Myeloid cells induce *Nf1*<sup>+/-</sup> aneurysms via activation of NADPH oxidase. National Clinical and Translational Sciences Predoctoral Programs Meeting. Rochester, MN, May 6-8 2012.
- Stansfield B., Bessler W., Mund J., Sarchet K., **Downing B.**, Distasi M., Smiley L., Li F., Ingram D. Monocyte/macrophages are the primary effectors of *Nf1*<sup>+/-</sup> vaso-occlusive disease. Children's Tumor Foundation: NF Conference. Jackson Hole, WY, June 11-14, 2011.
- Malkova A., **Downing B.**, VanHulle K., and Deem A. Single-strand annealing between inverted repeats initiated by double-strand breaks. FASEB Summer Research Conference "DNA palindromes: roles, consequences and implications of structurally ambivalent DNA", Saxtons River, VT, July 6–11, 2008.
- **Downing B.**, VanHulle K., Malkova A. "Deleterious pathways channeling repair of double-strand breaks into chromosomal rearrangements." National Conference on Undergraduate Research. Salisbury MD, April 10-12, 2008.
- **Downing B.**, VanHulle K., Malkova A. "Deleterious pathways channeling repair of double-strand breaks into chromosomal rearrangements." IUPUI Undergraduate Spring Research Conference. Indianapolis IN, March 28, 2008.
- Deem A., VanHulle K., **Downing B.**, Hull K., and Malkova A. "Deleterious pathways channeling repair of double-strand breaks into chromosomal rearrangements." FASEB Summer Research Conference. "Genetic recombination and genome rearrangements", Snow Mass CO, July 28-August 2, 2007.
- **Downing B.**, Malkova A. "Genetic control of the SSA-GCR pathway of double-strand repair." IUPUI Summer Undergraduate Research Poster Symposium, Indianapolis IN, July 26, 2007.
- **Downing B.**, Malkova A. "Genetic control of SSA-GCR pathway in yeast". IUPUI Undergraduate Summer Research Conference. Indianapolis IN, March 30, 2007.

- VanHulle K., Lemoine F. J., Narayanan V., **Downing B.**, Hull K., McCullough C., Bellinger M., Lobachev K., Petes T.D., Malkova A. "Inverted DNA repeats channel repair of distant double-strand breaks into chromatid fusions and chromosomal rearrangements". Gordon Research conference "Mutagenesis", Newport RI, August 1-5, 2006.
- McCullough C., VanHulle K., Lemoine F. J., Narayanan V., **Downing B.**, Hull K., Bellinger M., Lobachev K., Petes T.D., Malkova A. "Inverted DNA repeats channel repair of distant double-strand breaks into chromatid fusions and chromosomal rearrangements". IUPUI Undergraduate Summer Research Conference, Indianapolis, IN, July 2006.
- Deem A, VanHulle K., Lemoine F. J., Narayanan V., **Downing B.**, Hull K., McCullough C., Bellinger M., Lobachev K., Petes T. D., and Malkova A. Inverted DNA repeats channel repair of distant double-strand breaks into chromatid fusions and chromosomal rearrangements. SALK Institute Research Conference on DNA replication and genomic integrity, San Diego, CA, July 26-29, 2006.
- VanHulle K., Lemoine F. J., Narayanan V., **Downing B.**, Hull K., McCullough C., Bellinger M., Lobachev K., Petes T.D., Malkova A. "Inverted DNA repeats channel repair of distant double-strand breaks into chromatid fusions and chromosomal rearrangements". Yeast chromosome structure, replication, and segregation, Indian Wells CA, June 24-29, 2006.
- VanHulle K., Lemoine F. J., Narayanan V., **Downing B.**, Hull K., McCullough C., Bellinger M., Lobachev K., Petes T.D., Malkova A. "Inverted DNA repeats channel repair of distant double-strand breaks into chromatid fusions and chromosomal rearrangements". 8<sup>th</sup> Annual Midwest DNA Repair and Mutagenesis Symposium, Indianapolis IN, May 20-21, 2006.